

***FIELD LOAD TESTS OF OPEN –DECK
TIMBER TRESTLE RAILROAD BRIDGES***

Richard M. Gutkowski, Professor

Research Assistants:

Geoffrey Robinson
Abdalla Shigidi

Colorado State University

August 2001

ACKNOWLEDGEMENTS

The authors graciously acknowledge the additional financial support provided by the Association of American Railroads. Also, Dr. Duane Otter, Ms. Diana Oliva and other technical personnel of the Transportation Test Center, Inc. in Pueblo, Colo., were directly involved in the planning and conduct of tests on site. The Union Pacific Railroad provided access to two of the bridge sites and personnel to assist in the control of the test train and field load tests. Many graduate and undergraduate students from Colorado State University (CSU) participated in the conduct of the test set-ups and field load tests. Dr. Marvin Criswell, Professor of Civil Engineering at CSU, provided extensive guidance in the M.S. thesis work of Mr. Geoffrey Robinson, done as an outcome of this project. Ms. Laura Ludwig provided the extensive staff assistance needed to prepare the report itself.

DISCLAIMER

The contents of this report reflect the views of the authors, who are responsible for the facts and the accuracy of the information presented. This document is disseminated under the sponsorship of the Department of Transportation, University Transportation Centers Program, in the interest of information exchange. The U.S. Government assumes no liability for the contents or us thereof.

ABSTRACT

A field load test program was conducted to evaluate three open-deck timber railroad trestle bridges. The bridges included part of a 31-span bridge, a four-span bridge with skewed interior bents and a three-span bridge. Piles of the chords of the bridges were evaluated non-destructively for material properties using an ultrasonic stress wave device. The bridges were modeled using typical frame analysis techniques to predict response to loads. Deflection and strain measurements were recorded from the load testing. The responses of the bridges to various loads are compared to the predicted responses from several analytical modeling assumptions.

The diagnostic testing used loads applied statically by axles of a test train and ramp loads applied by a specially designed railroad test car. Rolling train loads were conducted using the axles of the test train. Displaced chord and ground reference deflections plus some strain measurements were recorded at selected locations.

The bridges performed within the expected range of behavior predicted by the analytical models. The chord systems of the bridges performed as beams semi-continuous over multiple supports. Two forms of support motion were observed; motion of the caps and gap closing between individual piles and the supporting caps. Load sharing among individual piles was examined empirically. No definable pattern for load sharing of the piles was identified.

TABLE OF CONTENTS

INTRODUCTION	12
In Situ Timber Railway Bridges	12
Goal and Objectives.....	14
Test Program Description	15
Project Background.....	15
DESCRIPTION OF TEST BRIDGES	19
General Description of Open Deck Timber Trestle Bridges.....	19
Bridge No. 32.35 (Fort Collins).....	20
Bridge No. 32.56 (Fort Collins).....	21
Bridge No. 101 (Pueblo)	22
ASSESSMENT OF MATERIAL PROPERTIES	25
Objective and Background	25
Selection and Testing of Timbers	27
Stiffness Evaluation Results	27
Analytical Modeling Approach.....	33
Pinned Single Span Beam Model	33
Continuous Beam Model.....	34
Semi-Continuous Beam Model.....	35
Extended Semi-Continuous Chord Model.....	37
Fixed End Beam Model	38
Load Application.....	38
FIELD LOAD TESTING	41
Bridge Loading Equipment	41
Load Test Methodology.....	42
Loadings Used.....	42
Instrumentation	46
RESULTS OF STATIC LOAD TESTS	51
Static Load Test Results – Bridge 32.35.....	51
Displacements Relative to the Displaced Chord.....	55
Measured Results	55
Comparison of Analytical and Measured Results.....	62
Deflections Relative to the Ground	65
Measured Results	65
Observations from the Static Load Testing	73
RAMP LOADING TEST RESULTS	75
Ramp Loading Tests	75
Bridge 101 Results.....	75
Linear Behavior of Transducer and Extensometer Measurements	78
Deflections Relative to the Displaced Chord.....	83
Displacements Relative to the Ground	93
Investigation of Support Motion and Gap Closing.....	98
LOAD DISTRIBUTION BETWEEN PILES	103
Empirical Formulation.....	103

ROLLING LOAD TESTS – BRIDGE 101	109
Conduct of the Tests	109
Test Results	109
CONCLUSIONS AND RECOMMENDATIONS	119
REFERENCES	121

LIST OF TABLES

Table 3-1	Predicted E value summaries for measurements for all members of Bridge 32.35 tested with the Sylva Test ultrasonic test device.....	19
Table 3-2	Predicted E value summaries for measurements for all members of Bridge 32.56 tested with the SylvaTest ultrasonic test device.....	20
Table 3-3	Predicted E value summaries for measurements for all members of Bridge 101 tested with the SylvaTest ultrasonic test device.....	20
Table 3-4	Predicted E value summaries for measurements for all bridge members tested with the SylvaTest ultrasonic test device.....	21
Table 5-1	Loads applied by train in Fort Collins, Colorado. TLB axle at 0 kip, 30 kip, 60 kip and 78 kip load levels.....	35
Table 5-2	Load spacing for axles of train used on Fort Collins locations on Union Pacific line....	36
Table 5-3	Loads applied by train in Pueblo, Colorado. TLV axle at 0 kip, 30 kip, 60 kip, and 78 kip load levels.....	37
Table 5-4	Load spacing for axles of train used on Pueblo locations.....	38
Table 5-5	Load positions selected for testing on Bridge 32.35, Bridge 32.56 and Bridge 101.....	39
Table 6-1	Displacement transducer data collected at mid-span of selected chord plys for loads 1-2@I, 1@J, 1-2@K, 1@L, 1-2@M, and 1@O. All displacements in inches referenced from the displaced chord.....	48
Table 6-2	Comparison of load test measurements to predicted deflection of mid-span chord members for Bridge 32.35 using three frame analysis models.....	55
Table 6-3	Displacement transducer data collected at mid-span of selected chord piles for loads 1-2@I, 1@J, 1-2@K, 1@L, 1-2@M, and 1@O. All displacements in inches referenced from the ground.....	58
Table 6-4	Comparison of displaced chord and ground referenced deflection measurements by both magnitude and percentage difference.....	64

Table 7-1	Summary of the number of load positions or train passes and associated number of data records for each bridge.....	67
Table 7-2	Deflection and strain data for Bridge 101, instrumentation position US1-2, 11@F ramp loading from the TLV load axle.....	72
Table 7-3	Summary of Deflection and Strain measurements on the east chord of Bridge 101 while experiencing a load of 78 kips during 11@F loading. Instrumentation data set US2-1.....	74
Table 7-4	Predicted deflection of mid-span chord members for Bridge 101 using four frame analysis models.....	83
Table 8-1	Comparison of percentage of load determined by deflection or strain. Variables for each ply used in computation have been included.....	96
Table 8-2	Comparison of percentage of load determined by deflection or strain for Span 2, Bridge 101. Variables for each ply used in computation have been included.....	98
Table 9-1	Record or displacement data for rolling train loads, instrumentation position US2-1, train moving forward slowly.....	103
Table 9-2	Displaced chord deflection of piles for Span 2, Bridge 101, West chord.....	107
Table 9-3	Deflection of west chord piles at mid-span of the center span of Bridge 101 for moving and similar static loads.....	108

LIST OF FIGURES

Figure 1-1	Illustrations of the Cooper E-40 and E-60 design loads.....	6
Figure 1-2	Location of bridges 21.35 and 32.56 on the Union Pacific Railroad	9
Figure 1-3	Location of Bridge 101 near Pueblo, Colorado.....	10
Figure 2-1	Typical elevation and plan views of open deck timber bridges showing major structural elements.....	11
Figure 2-2	Schematic of Bridge 32.56, four spans over irrigation ditch with skewed abutments...14	
Figure 3-1	Photo of the SylvaTest as used in obtaining stiffness measurements of piles.....	18
Figure 3-2a	Bridge No. 32.35, in Fort Collins, predicted E values of timbers. Spans 1-4 shown...22	
Figure 3-2b	Bridge No. 32.35, in Fort Collins, predicted E values of timbers. Spans 5-8 shown...23	
Figure 3-2c	Bridge No. 32.35, in Fort Collins, predicted E values of timbers. Spans 9-12 shown..23	
Figure 3-3	Bridge No. 32.35, in Fort Collins, predicted E values of timbers. Imperial units.....	24
Figure 3-4	Bridge No. 101, near Pueblo, predicted E values of timbers. Imperial units.....	24
Figure 4-1	Schematic representation of frame analysis models used to evaluate load test data for timber railroad.....	26
Figure 5-1	Schematic of the Association of American Railroads Track Loading Vehicle including axle loads.....	33
Figure 5-2	Schematic depiction of the locomotive, instrumentation car and Track Loading Vehicle used in the bridge testing.....	34
Figure 5-3	Photo of frame for displaced chord instrumentation installed on Bridge 32.35.....	40
Figure 5-4	Photo of displacement transducers installed to measure relative motion of piles to a cap on Bridge 101.....	41
Figure 5-5	Photo of an extensometer installed on a pile on Bridge 101.....	41
Figure 6-1	Electronic instrumentation positions for displacement transducers in Spans 4, 5, 6 and 7 on Bridge 32.35.....	43
Figure 6-2	Loads applied to Bridge 32.35 due to load position 1-2@I.....	44

Figure 6-3	Loads applied to Bridge 32.35 due to load position 1@J.....	45
Figure 6-4	Loads applied to Bridge 32.35 due to load position 1-2@K.....	45
Figure 6-5	Loads applied to Bridge 32.35 due to load position 1@L.....	46
Figure 6-6	Loads applied to Bridge 32.35 due to load position 1-2@M.....	46
Figure 6-7	Loads applied to Bridge 32.35 due to load position 1@O.....	47
Figure 6-8	Transducer deflection measurements referenced to the displaced chord for Bridge 32.35 for load 1-2@I.....	49
Figure 6-9	Transducer deflection measurements referenced to the displaced chord for Bridge 32.35 for load 1-2@J.....	49
Figure 6-10	Transducer deflection measurements referenced to the displaced chord for Bridge 32.35 for load 1-2@K.....	50
Figure 6-11	Transducer deflection measurements referenced to the displaced chord for Bridge 32.35 for load 1-2@L.....	50
Figure 6-12	Transducer deflection measurements referenced to the displaced chord for Bridge 32.35 for load 1-2@M.....	51
Figure 6-13	Transducer deflection measurements referenced to the displaced chord for Bridge 32.35 for load 1-2@O.....	51
Figure 6-14	Transducer deflection measurements referenced to the ground for Bridge 32.35 for load 1-2@I.....	59
Figure 6-15	Transducer deflection measurements referenced to the ground for Bridge 32.35 for load 1-2@J.....	59
Figure 6-16	Transducer deflection measurements referenced to the ground for Bridge 32.35 for load 1-2@K.....	60
Figure 6-17	Transducer deflection measurements referenced to the ground for Bridge 32.35 for load 1-2@L.....	60
Figure 6-18	Transducer deflection measurements referenced to the ground for Bridge 32.35 for	

load 1-2@M.....	61
Figure 6-19 Transducer deflection measurements referenced to the ground for Bridge 32.35 for load 1-2@O.....	61
Figure 7-1 Locations of displacement instrumentation shown on plan view of Bridge 101.....	68
Figure 7-2 Load positioning on Bridge 101 for 11@I.....	69
Figure 7-3 Load positioning on Bridge 101 for 11@F.....	69
Figure 7-4 Load positioning on Bridge 101 for 11@C.....	70
Figure 7-5 Extensometer and displacement transducer locations for test sequence US 1-2, Bridge 101.....	71
Figure 7-6 Load-deflection relationship for Bridge 101, US1-2, load 11@F, Piles 1 thru 4.....	73
Figure 7-7 Load-Strain relationship for Bridge 101, US1-2, load 11@F, eight extensometers.....	75
Figure 7-8 Transducer measurements for displacement referenced to the displaced chord and relative ply/cap motion for a 78 kip load at 11@I on Bridge 101.....	76
Figure 7-9 Transducer measurements for displacement referenced to the displaced chord and relative ply/cap motion for a 78 kip load at 11@F on Bridge 101.....	77
Figure 7-10 Transducer measurements for displacement referenced to the displaced chord and relative ply/cap motion for a 78 kip load at 11@C on Bridge 101.....	78
Figure 7-11 All electronic ground referenced data for Bridge 101, for 78 kip load at 11@I.....	86
Figure 7-12 All electronic ground referenced data for Bridge 101, for 78 kip load at 11@F.....	87
Figure 7-13 All electronic ground referenced data for Bridge 101, for 78 kip load at 11@C.....	88
Figure 7-14 Deflection measurements of Cap D referenced to the ground for 1, 30, and 78 kip loads applied by the TLV for load 11@F.....	92
Figure 7-15 Deflection measurements of Cap G referenced to the ground for 1, 30, and 78 kip loads applied by the TLV for load 11@F.....	92
Figure 7-16 Differential motion of Cap D from 0 to 78 kips by the TLV for the load 11@F.....	92
Figure 7-17 Differential motion of Cap G from 0 to 78 kips by the TLV for the load 11@F.....	92

Figure 7-18	Relative motion between Cap D and piles 1 to 8 for 0, 30, and 78 kip loads by 11@F.....	94
Figure 7-19	Relative motion between Cap G and piles 1 to 8 for 0, 30, and 78 kip loads by 11@F.....	94
Figure 8-1	Estimated percentages of load carried by each ply based on deflection or strain measured at mid-span, Span 6, Bridge 32.35.....	97
Figure 8-2	Estimated percentage of load carried by each ply based on deflection or strain measured at mid-span, Span 2, load 11@F for 78 kips, Bridge 101.....	98
Figure 9-1	Displaced chord referenced displacement record, Bridge 101, instrumentation position US2-1, train rolling forward slowly.....	104
Figure 9-2	Ground referenced displacement record, Bridge 101, instrumentation position US2-1, train rolling forward slowly.....	104
Figure 9-3	Deflections of chord piles of the west chord, mid-span of Span 2, Bridge 101 due to static train loads.....	108

EXECUTIVE SUMMARY

Nationally, the structural condition of short span railroad bridges is an important issue. Many have been in service for 50-100 years, particularly on short lines in sparsely populated areas. In some cases severe degradation has been occurring. During service life, single car loads have increased significantly and the frequency of dual cars has risen dramatically. Consequently, a 30 percent increase in design axle loads is being considered and the research is examining how adequately existing bridges sustain contemporary loads and if strengthening is needed.

The research reported here consisted of an examination of rehabilitation needs of existing open deck-timber trestle railroad bridges in the United States via a pilot field load test program. The study was done in cooperation with Transportation Technology Center, Inc. (TTCI), a subsidiary of the Association of American Railroads. The AAR's overall timber bridge research needs were determined by a team of invited experts who conducted a research needs workshop for the AAR on the topic. The TTCI was undertaking a larger comprehensive study of overall timber trestle bridge performance. The goal of the larger effort was to examine performance under present day train loads, as related to increasing the design load requirements in the applicable design code.

Reconnaissance visits were made to about 35 bridges sites in four states. Three sites were selected to examine structural response to realistic train loads. Bridge No. 32.35 was a right bridge approximately 465 feet long (31-spans at 15 ft). Bridge No. 32.56 (was a 4-span bridge and approximately 69 feet long). End abutments were perpendicular to the track and bridge centerline but intermediate bents were skewed at about 30 degrees. Bridge No. 101 was a 3-span bridge about 40 feet long, with spans about 13, 14 and 13 feet. A load test program consisting of 1) static loadings, 2) ramp loadings, 3) moving train loadings and 4) pilot cyclic dynamic loads was employed. Material properties of the timber were measured in the field by an ultrasonics based non-destructive evaluation technique.

A specialized loading train was used to apply ramp loads via a Track Loading Vehicle (TLV). Various multi-point static loadings were achieved by positioning the 12 axle train at different locations.

For Bridges 32.35, 32.56 and 101, the number of static load positions used were 76, 34 and 108; respectively. By positioning the loading bogey of the TLV at various locations, the isolated effect of a ramp type loading was simulated. This was done by first reading all instrumentation with the train in place, then incrementing the TLV bogey loading levels and then unloading. Data was recorded incrementally during the loading and unloading. The axle load levels used were 0, 30, 60 and 78 kips. The latter two correspond to the existing and anticipated new code design load levels for a single axle, respectively. Moving train loads consisted of roiling the entire test train across the bridges at controlled speeds. Dynamic loading consisted of applying sinusoidal loading via the TLV actuator and recording dynamic response. The moving train and dynamic loads were done outside the scope of the MPC project but some aspects are not included in this report.

Voluminous data were captured for the numerous static and ramp load positions and some key points are summarized. Few cases of upward displacement were observed, support motion was a likely factor. At some pile bents support motion was evident in the range of .05-.10" downward. Relative displacement between piles and caps was typically, below .06". Empirical calculation reflecting individual stringer material properties and span type showed a ply takes between 17 percent and 35 percent of chord loading. This changed moderately if support motion was removed. There was no evident pattern of load sharing among piles of a chord. This is attributed to variability in member properties, cap displacement, differential bearing conditions of individual piles and possible relative (track to tie, tie to chord, chord to cap) motion. The NDE data indicated that the wood material was stiffer and stronger than anticipated and this is partially attributed to long term drying effects.

Outcomes of the static and ramp load tests were examined by computer-based structural analysis. This included bounding an individual span response between fully fixed ends and fully pinned ends. A semi-continuous beam model was used to simulate the bridges and reasonably predict the deflection response.

Bridge 101 was selected for strengthening by the addition of a ply to each chord and retested under rolling train loads. A subsequent project was anticipated for that purpose.

CHAPTER 1

INTRODUCTION

In Situ Timber Railway Bridges

From the beginning of railway history in the United States, timber has been a major source of structural material for the railroads. Consequently railroads have a large number of timber trestle bridges in service. One study assigned the typical service life of timber trestles at 72 years with a normal range between 35 and 95 years (Byers 1996). Over the service life of these existing bridges, the maximum loads carried by railroad cars have increased significantly.

Railway bridges have been commonly analyzed by a series of loads referred to as a Cooper E loading (McCormac 1984). This load configuration is shown in Figure 1-1. Since introduction of the E-40 load, design loads increased progressively. In the 1960s, the maximum axle load was increased to 60,000 lbs (60 kips) per axle. Some railroad lines must now carry cars with 78,000 lbs loads per axle (Oommen and Sweeney 1996). To adapt to higher actual axle loads, those loads were increased proportionally using the E number to identify the load associated with the drive axles. For example, the Cooper E-60 load, also shown in Figure 1-1, simply has all loads increased by a 60/40 ratio.

The loads now applied to the older bridges are much higher than originally intended. For example, a bridge may have been designed a number of years ago for E-60 loads, but now may be expected to carry a higher load, such as an E-72 load. Older bridges must be inspected, analyzed and evaluated for adequacy to carry increased loads. This has become more critical as the railroad industry in North America is currently anticipating a 30 percent increase in its maximum design loading.

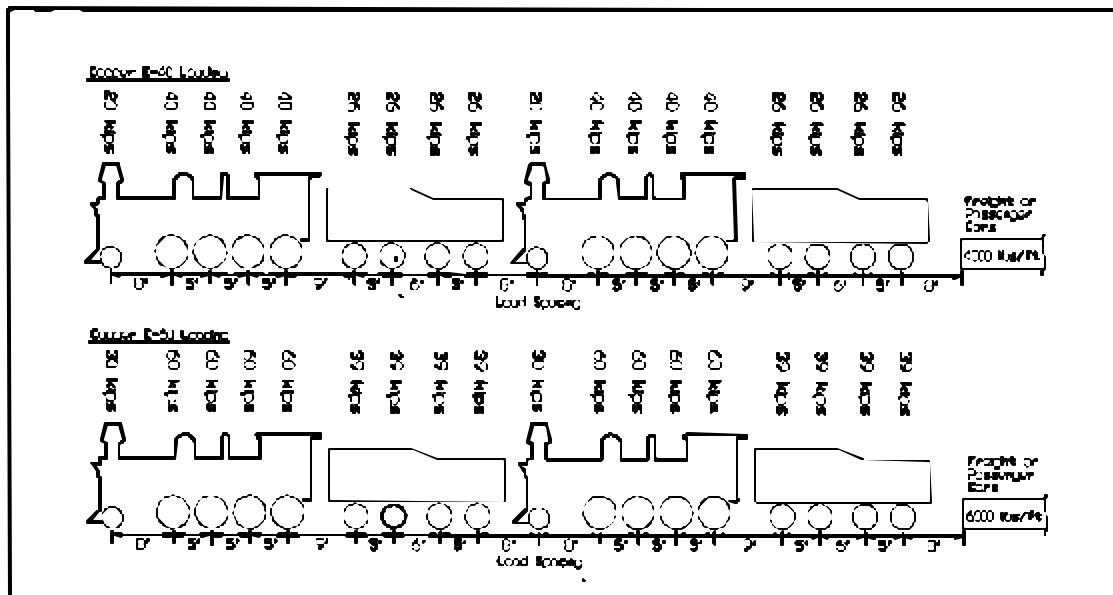


Figure 1-1. Illustrations of the Cooper E-40 and E-60 design loads.

This change could result in some additional bridges needing to be rehabilitated or replaced. One option that could offset upgrading costs would be to evaluate effectiveness of the in situ structures by use of improved assessment techniques. Most of these timber bridges were designed using methods presented in the American Railroad Engineering Association manual (American Railroad Engineering Association Manual 1995). This design method incorporates typical assumptions of material properties, standard bridge forms and applied loads. Design or evaluation of performance relies on the assumptions made to represent material properties, loads applied, distribution of loads to the structure and load paths through the structure. Increased knowledge of these issues improves the understanding of how a particular structure will perform when resisting applied loads.

Since structural members of the existing bridges already are in place, the material properties are “what they are,” not the tabulated code values. If actual values can be readily determined, an analysis of the structure using measured material properties instead of a low end assumption could lead to increased allowable capacity of the structure. Also, the Cooper E-type loadings do not resemble typical loads applied to railroad bridges today. Via computers, advanced structural analysis has become a practical tool

in evaluating bridge design. Bridges can easily be evaluated for actual axle load patterns and weights of typical traffic.

Experimentally investigating the response of a bridge to actual loads can be a useful tool in defining field performance of the bridge. This can be done by a diagnostic load test. Comparison of the analytical model performance with measured performance allows a benchmark by which to refine the analytical modeling assumptions.

Load testing can provide improved knowledge of load distribution and load paths through bridge structures. Axle loads are applied through contact between wheels and the rails and then to the ties and chords. The proportion of the loading transmitted to each stringer in a chord is different.

In-situ timber trestle bridges also have the complication of imperfect connections between members, gaps between members, non-parallel bearing surfaces, etc. As a bridge ages, connections wear and loosen, repairs or modification may be made and support settlements may occur. Thus, the load distribution between stringers can change significantly.

Goal and Objectives

This report presents the results of a program of research investigating the field performance of three existing open-deck timber trestle railroad bridges. The goal of this research was to develop an improved understanding of load paths through such bridge structures.

Three objectives were established for this research study:

1. Field studies of selected timber trestle railroad bridges by conducting controlled load tests to examine load paths;
2. Determination of material properties of the primary structural components, as needed in analytical modeling;
3. Analytical modeling of the bridges to predict their structural performance

Test Program Description

The primary load testing involved static positioning of a three-car test train along each bridge. Static loading allowed deflections and stress to be measured at selected locations for specific, known loads. The service loading of railroad bridges is dynamic in nature. Exploratory dynamic testing was included in the overall program of study to observe whether differences between static and dynamic response of the bridge exist or not. By comparing the responses dynamic impact effects could be observed.

Project Background

The Association of American Railroads (AAR) is in a process of evaluating the capacity of railway bridges to accommodate the need for increased design axle loads. A jointly funded project to load test three bridges was initiated in March 1995. The scope of the project included diagnostic load testing of each structure using static loads, incremental loads and limited speed rolling loads. The AAR provided and operated a special train car, referred to as the Track Loading Vehicle (TLV), designed to apply loads to the railway track. Colorado State University (CSU) researchers planned the instrumentation, loading and data acquisition methods, and assessed the results of the load tests.

Initially, site evaluation and reconnaissance visits were made to approximately 30 potential bridges, located in Colorado, western Kansas, and northwest Oklahoma. Three bridges were selected for testing and the tests were conducted in July and August of 1995. Two of the selected bridges were in Fort Collins, Colo. They were a 31-span bridge over the Poudre River (Bridge No. 32.35) and a 4-span, skewed bridge over an irrigation ditch (Bridge No. 32.56) approximately one-fourth mile north of the Poudre River crossing. Both were on a local Union Pacific line. Figure 1-2 provides a map locating the bridges.

Bridge 32.35 was selected because it was a long multi-span bridge, which allowed a wide range of loading positions with repetitive members, plus it offered sufficient distance for study of dynamic response to a moving train. Bridge 32.56 was of interest because it has larger piles and somewhat longer

spans than other bridges of this chord configuration. It also has a skewed geometry of the intermediate supports. This geometry was of interest due to the consequent unsymmetrical behavior under train loads. Both bridges were of spaced (defined subsequently) chord construction.

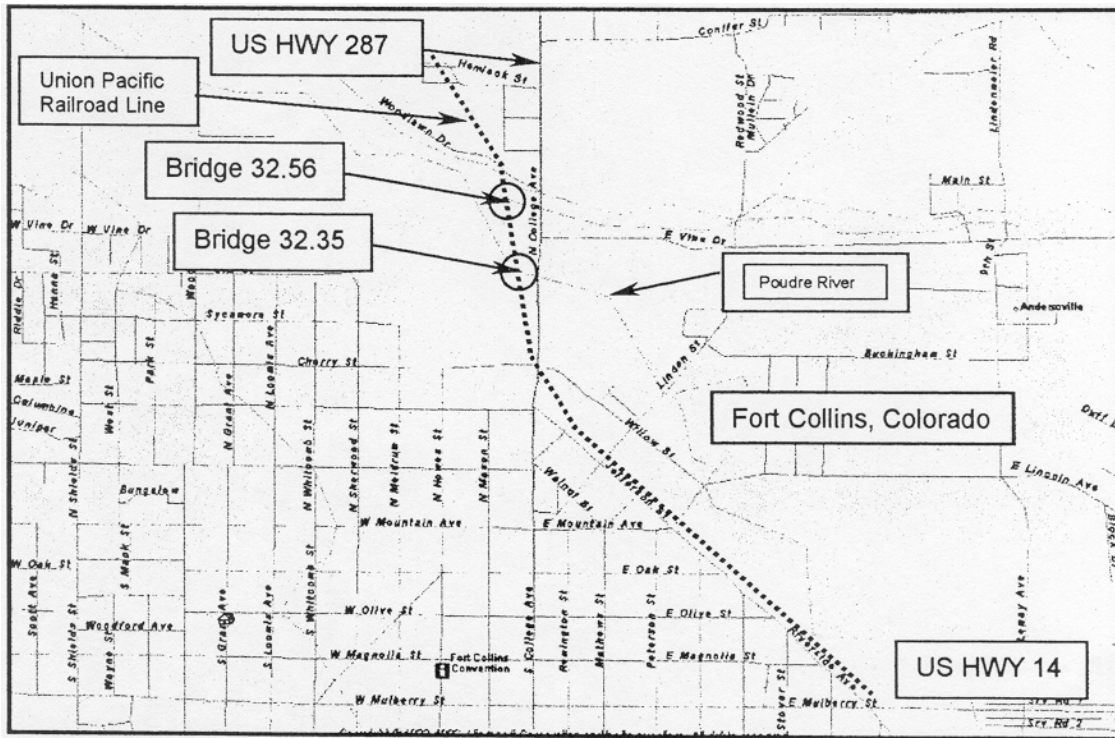


Figure 1-2. Location of Bridges 32.35 and 32.56 on the Union Pacific Railroad in Fort Collins, Colorado.

The third bridge (Bridge No. 101) located near Pueblo, Colo., was on an access track into the Transportation Technology Center (TTC) of the AAR. Figure 1-3 is a map showing the location of the bridge. It was a 3-span bridge composed of packed (defined subsequently) chord construction. This bridge also provides the fewest spans possible for use of the half-lapped chord system.

The three bridges are described in detail in Chapter 3. All three were of lapped chord stringer configuration. The bridges varied slightly in geometry and minor connection details due to site requirements.

The detailed experimental findings of the overall test program are available in an AAR technical report (Gutkowski, et al. 1998 and Gutkowski, et al. 1999). Some preliminary results were presented at a

various conferences and published in accompanying technical papers (Gutkowski, et al. 1997, Gutkowski, et al. 1998, Gutkowski, et al. 1999, Gutkowski et al. 2000, and Gutkowski, et al. 2001). This MPC report is a condensed version of the AAR report and findings of a M.S. thesis based on the study (Robinson et al. 1998).

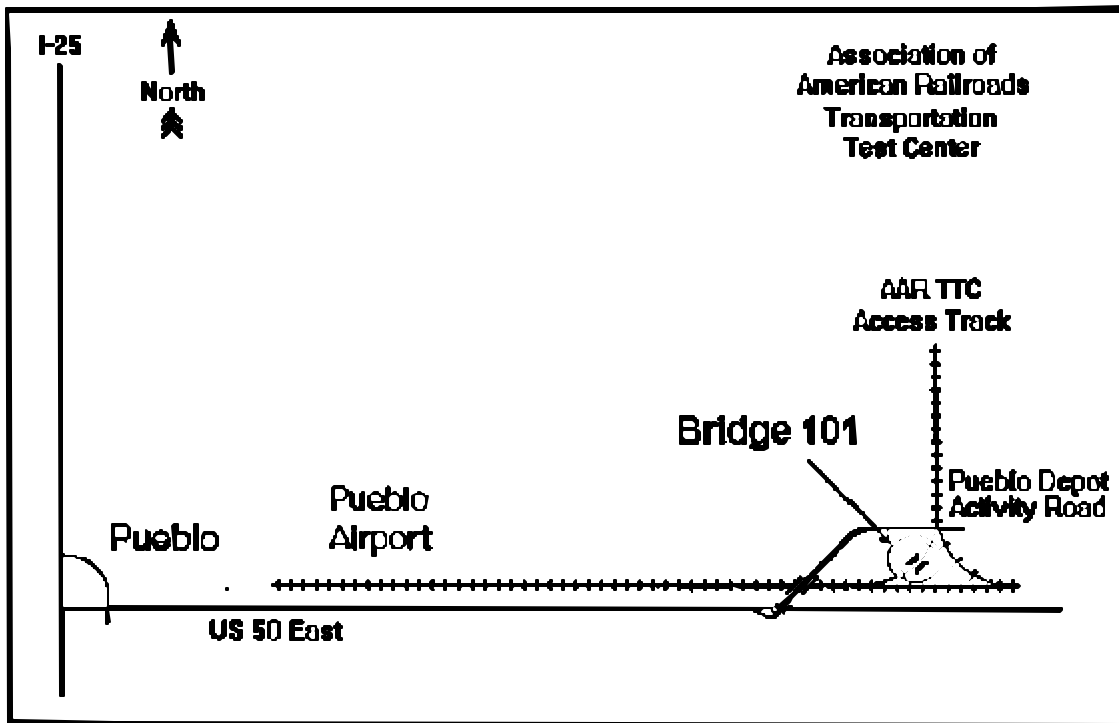


Figure 1-3. Location of Bridge 101 near Pueblo, Colorado

CHAPTER 2

DESCRIPTION OF TEST BRIDGES

General Description of Open Deck Timber Trestle Bridges

The AREA Manual for Railway Engineering (American Railway Engineering Association 1995) design manual defines the current specifications for standard railroad bridges. Bridges studied in this project have the configuration of the open deck timber trestle, illustrated in Figure 2-1. The configuration shown is repeatable for any number of spans.

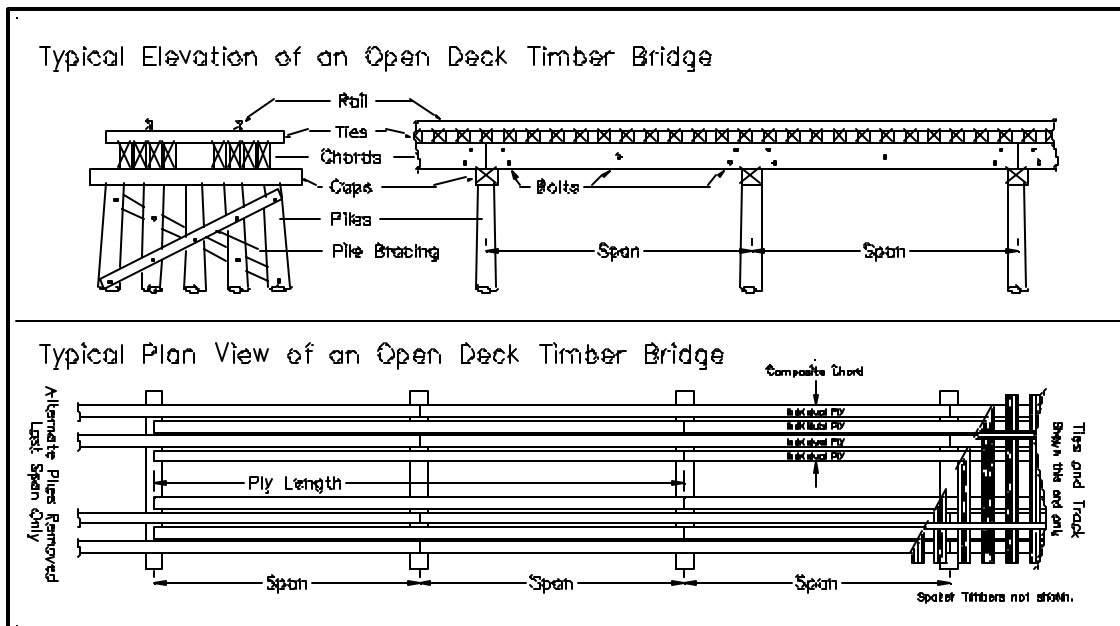


Figure 2-1. Typical elevation and plan views of open deck timber bridges showing major structural elements.

Each of the bridges are described in more specific detail in the following sections. Some general construction aspects are described in the following paragraphs.

The primary structural elements are two longitudinal chords consisting of sets of three or four heavy timber stringers, termed “piles” herein. The chords extend semi-continuously for the entire length of the bridge. The chords support wood cross ties, which in turn support the steel rails. The chords are then supported by bents made up of caps atop timber piles. The chords are arranged such that each ply

within a chord is continuous over two spans. Adjacent piles are offset longitudinally, or “staggered,” forming a partially continuous chord for the entire length of the bridge.

Individual ply dimensions observed ranged from approximately six to nine inches wide and from about 16 to 20 inches deep. They ranged from about 24 to 36 feet in length over two spans. Near the bents, the piles are intra-connected with a pair of rods on each side of the cap. Some bridges, typically those with longer spans, include a single rod through the chord at mid-span. The chords are either “spaced ” or “packed.” Spaced chord piles are laterally separated, having a clear distance of 1.5 to 2.5 inches between vertical faces. Spacing was set by spacers over rods connecting the groups of piles. Packed chords have no intentional spacing between piles. However, natural gaps, about 0.2 to 0.3 inches wide, were observed between the piles.

Cap members were supported on sets of either five or six piles. The piles were driven into the soil beneath the bridge. Each set of piles was laterally braced. Piles at the ends of the bridge were battered to form a short retaining wall against the railroad bed. The term “battered” means the addition of planks to the embankment side on the piles forming a wall to hold back the soil. Piles at mid-span typically had X-bracing added for resistance to lateral loads.

Bridge No. 32.35 (Fort Collins)

The bridge is on a Union Pacific line crossing the Poudre River in Fort Collins, Colo. The bridge spans the river and a bike path just west of U. S. Highway 287. It is approximately 465 feet long, contains 31-spans and is of open-deck timber railway bridge construction (as depicted in Fig. 2-1) with spaced chords. All spans are approximately 15 feet in length. As the bridge crosses the river channel, the channel flows under the middle third of the bridge. The outer thirds are within an observable flood plain. The piles of greatest height in the river channel extend approximately 15 feet above the water level. In the flood plain regions, the piles extend only about 4 to 12 feet above ground.

The sizes of bridge components are:

Track:	90 lbs/yd
Spacers:	7.75 inches wide by 4.5 inches deep
Ties:	7.75 inches wide by 7.75 inches deep with four-inch gaps
Chords:	Four piles each side, piles spaced two inches apart, chords spaced 20 inches apart
Piles:	7.75 inches by 16.75 inches by 30 feet long each continuous over two spans, four piles each end span are single span and only 15 feet in length
Caps:	13.5 inches by 11 inches deep by 12 feet long
Piles:	Five per cap - 12 inch minimum diameter at top
X-bracing:	4" x 8" timber each side of piles

All bridge components were attached with connectors typical to railway bridge construction. The caps were drive-spiked to the piles. It appeared that chords also were drive-spiked to the caps. The longitudinal members of the chords were through-bolted near the caps. Every third tie was through-bolted to the outside member of each chord and each tie end was drive spiked to the spacer timber.

Bridge No. 32.56 (Fort Collins)

This is a 4-span bridge crossing an irrigation ditch just north of Bridge 32.35 over the Poudre River in Fort Collins, Colo., on the same Union Pacific line. Figure 2-2 provides a schematic of the plan view. It is approximately 69 feet long. It has open-deck construction with spaced chords. The end abutments are perpendicular to the track and bridge while the intermediate bents are skewed at approximately 30 degrees from perpendicular so they are parallel with the ditch channel. The main spans are approximately 18.5 feet in length along the centerline. Because of the angle between the abutments and interior pile bents, the length of spans at the end of the bridge ranged from between approximately 12.5 feet to 18.5 feet.

The sizes of bridge components are:

- Track: 90 lbs/yd – slightly curved (3-4 inch chord off-set at center of bridge)
- Spacers: 7.75 inches wide by 4.5 inches deep
- Ties: 7.75 inches wide by 7.75 inches with 4-inch gaps
- Chords: Three piles each side, piles spaced 3.5 inches apart
Chords spaced 25.5 inches apart
- Piles: 9.75 inches wide by 19.75 inches deep by 38 feet long over interior spans
Two piles each end are single span
- Caps: 14 inches wide by 13.5 inches deep by 14 feet long
- Piles: Five per cap - 12 inch minimum diameter at top
- X-bracing: 4" x 8" timber each side of piles

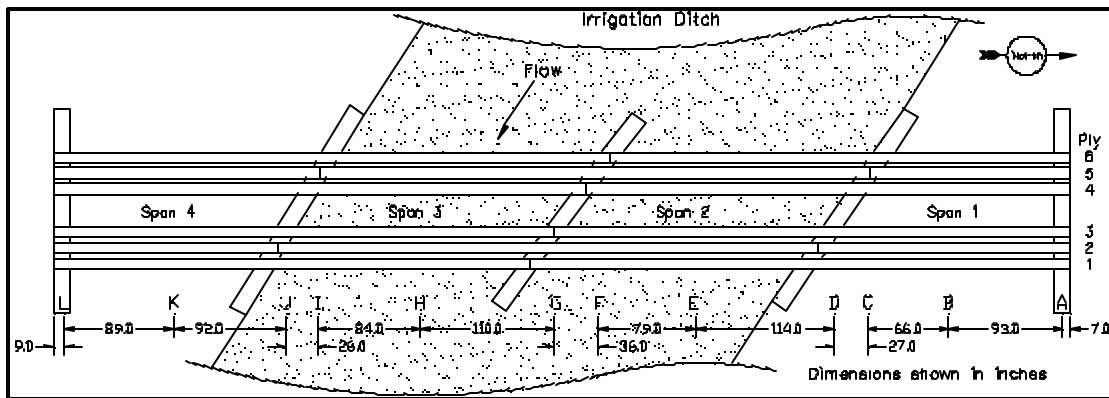


Figure 2-2. Schematic of Bridge 32.56, four spans over irrigation ditch with skewed abutments

Figure 3-6 shows configuration of the piles and the variation in the ply member lengths at the end spans. The ply lengths are typically 38 feet over two spans, except for members of end spans. End span ply lengths ranged from 38 feet (over two full spans) to less than 14 feet (single span, short end chord). Near the supports and at mid-spans the three chord members are bolted together.

Bridge No. 101 (Pueblo)

The third bridge is a three span bridge located on the West Y, Avondale Junction on the Army Munitions Depot Access to the TTC near Pueblo, Colo. The bridge is of the type depicted in Fig. 2-1.

The bridge is approximately 40 feet in length with individual spans of approximately 13, 14, and 13 feet.

It has packed chords. A walkway is attached on each side of the bridge at tie level.

The sizes of bridge components are:

Track:	120 lbs/yd – slightly curved (1 inch chord off-set at center of bridge)
Spacers:	Eight inches wide by four inches deep
Ties:	8.75 inches square with 8-inch gaps
Chords:	Four piles each side, packed (nominal gap of 0.25 inch), chord spacing 34 inches
Piles:	6.5 inches by 15.5 inches deep and 28 foot long if two span Four piles each end are single span
Caps:	13.5 inches by 15.25 inches deep by 14 feet long
Piles:	Six per cap – 12 inch minimum diameter at top
X-bracing:	4" x 8" timber each side of piles

The individual chord lengths are approximately 14 feet (if the ply is single span at the end of the bridge) and 28 feet (if the ply is continuous over two spans). Near the supports, all four of the piles in each chord are bolted together. There were no mid-span bolts between piles. The walkway structures cantilever out over the ends of the caps. They are attached to the ends of each cap by a strap. A number of minor repairs had been made in recent years including shims, seals, plates on caps, several pile replacements, straps between piles and chords, replacement and treatment of ties.

CHAPTER 3

ASSESSMENT OF MATERIAL PROPERTIES

Objective and Background

Accurate knowledge of the material properties of individual components of a structure is essential to either predict or verify performance characteristics. Conventionally, the designer uses material properties, specified by codes or handbooks. In reality, the timber material will have significant variability. Once a structure is in existence, structural components can be evaluated individually to form a basis for a more accurate assessment.

One objective of this project was to quantify the material stiffness of members in the test bridges. From a structural load test viewpoint, Young's Modulus (modulus of elasticity), E , of individual members in a structure is of primary interest. Assessment of E provides information needed in analytically predicting deflection. Measured deflections of the bridge during load tests then can be compared to the predicted deflections.

Wood material in the bridges was visually identified as being Douglas-fir species, treated to a high retention level with an oil-based preservative treatment. The treatment was thought to be Pentachlorophenol, commonly used in timber railroad structures. Relatively few defects, such as knots or high slope of grain, existed. Drying defects, such as checks along the grain, were observed and would be typical of such large members that were installed green and dried in situ.

A non-destructive assessment technique was used to evaluate the E values. A proven ultrasonic instrument, SylvaTest (Sandoz 1996), was used for the evaluation. Figure 3-1 shows the general setup used for measuring individual ply E values with the instrument in operation. The technique was based on measurement of the propagation speed of 30 kHz ultrasonic waves between two piezo-electric transducers. The speed of propagation of the wave is used in a model. The model predicts stiffness and bending strength, adjusted for both moisture content and temperature, of either rectangular or round timber materials.

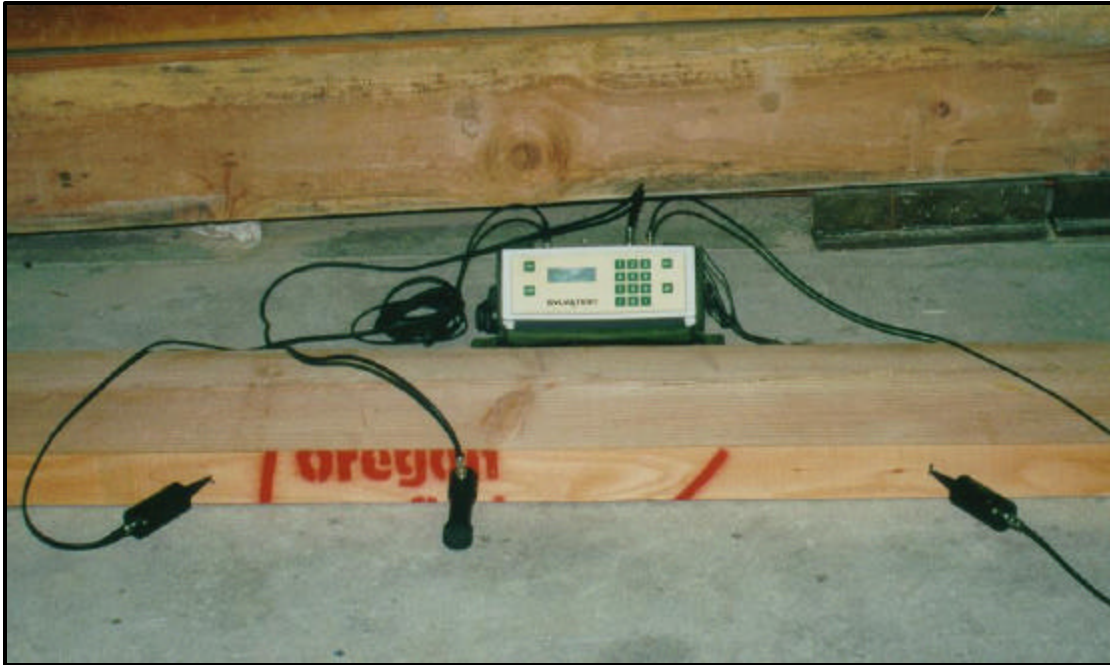


Figure 3-1. Photo of the SylvaTest as used in obtaining stiffness measurements of piles

While the SylvaTest instrument did give a speed of propagation value for all measurements, it limited its numeric prediction of stiffness between an upper and a lower limit. An estimate of stiffness of those members outside the boundaries set by the instrument was needed to quantify the existing material property population. The relationship between propagation wave speed and predicted Young's modulus for members of the three bridges is described by the linear relationship given:

$$E = 766.2 \cdot C_0 - 2.26 \times 10^6 \quad (1)$$

Where C_0 is the wave speed propagation of the 30 kHz impulse wave in m/s and E is modulus of elasticity in psi. Equation 1 is a statistical fit obtained by linear regression of the data obtained in the limits of the SylvaTest instrument on the three bridges. This relationship then was used to predict stiffness of those timbers outside the range of the SylvaTest instrument.

Selection and Testing of Timbers

For Bridge No. 101, the 3-span bridge near Pueblo, all longitudinal piles, caps, and intermediate piles were tested. The piles located under the abutment caps were not exposed and could not be evaluated. On Bridge No. 32.56, the 4-span bridge in Fort Collins, all longitudinal piles and caps were tested. For Bridge No. 32.35, the 31-span bridge in Fort Collins, all longitudinal piles of the north 12 spans and 14 cap timbers (associated with the north 13 spans) were tested.

The data were collected between Dec. 20 and Dec. 26, 1995. The weather conditions during testing were typical for Colorado in December.

Stiffness Evaluation Results

Ultrasonic measurements were made for a total of 199 locations on timbers in the three bridges of the test program. Summaries of the measured modulus of elasticity predictions, are presented in Tables 3-1 through 3-4.

Table 3-1. Predicted E value summaries for measurements for all members of Bridge 32.35 tested with the SylvaTest ultrasonic test device.

Bridge No. 32.35 Members Tested	Population Descriptor	Measured E (psi)	Lower Limit Extrapolated E (psi)	Combined Population E (psi)
Ply Locations	N	94	18	112
	Mean	2.05×10^6	1.63×10^6	2.04×10^6
	Minimum	1.77×10^6	1.13×10^6	1.13×10^6
	Maximum	2.15×10^6	1.77×10^6	2.49×10^6
	St.Dev.	1.21×10^5	1.48×10^5	2.53×10^5
Cap Locations	COV	.059	.091	.124
	N	13	1	14
	Mean	2.04×10^6	1.16×10^6	1.98×10^6
	Minimum	1.83×10^6		1.16×10^6
	Maximum	2.15×10^6		2.18×10^6
St.Dev.	1.02×10^5		2.55×10^5	
COV	.050		.129	

Table 3-2. Predicted E value summaries for measurements for all members of Bridge 32.56 tested with the SylvaTest ultrasonic test device.

Bridge No. 32.56 Members Tested	Population Descriptor	Measured E (psi)	Lower Limit Extrapolated E (psi)	Combined Population E (psi)
Ply Locations	N	23	1	24
	Mean	2.01×10^6	1.69×10^6	2.01×10^6
	Minimum	1.89×10^6		1.69×10^6
	Maximum	2.15×10^6		2.29×10^6
	St.Dev.	8.77×10^4		1.31×10^5
	COV	.044		.065
Cap Locations	N	3	2	5
	Mean	2.06×10^6	9.99×10^5	1.65×10^6
	Minimum	1.97×10^6	8.92×10^5	8.92×10^5
	Maximum	2.15×10^6	1.11×10^6	2.23×10^6
	St.Dev.	8.70×10^4	1.53×10^5	6.07×10^5
	COV	.042	.153	.368

Table 3-3. Predicted E value summaries for measurements for all members of Bridge 101 tested with the SylvaTest ultrasonic test device.

Bridge No. 101 Members Tested	Population Descriptor	Measured E (psi)	Lower Limit Extrapolated E (psi)	Combined Population E (psi)
Ply Locations	N	20	4	24
	Mean	2.06×10^6	1.66×10^6	2.06×10^6
	Minimum	1.80×10^6	1.59×10^6	1.59×10^6
	Maximum	2.15×10^6	1.77×10^6	2.46×10^6
	St.Dev.	1.15×10^5	8.46×10^4	2.55×10^5
	COV	.056	.051	.124
Cap Locations	N	2	6	8
	Mean	1.87×10^6	1.43×10^6	1.54×10^6
	Minimum	1.83×10^6	9.59×10^5	9.59×10^5
	Maximum	1.91×10^6	1.74×10^6	1.91×10^6
	St.Dev.	6.15×10^4	2.91×10^5	3.20×10^5
	COV	.033	.203	.208
Piles	N	7	5	12
	Mean	1.92×10^6	1.51×10^6	1.75×10^6
	Minimum	1.77×10^6	1.24×10^6	1.24×10^6
	Maximum	2.15×10^6	1.73×10^6	2.19×10^6
	St.Dev.	1.44×10^5	1.91×10^5	2.67×10^5
	COV	.075	.126	.152

Table 3-4. Predicted E value summaries for measurements for all bridge members tested with the SylvaTest ultrasonic test device.

All Members Tested	Population Descriptor	Measured E (psi)	Lower Limit Extrapolated E (psi)	Combined Population E (psi)
Ply Locations	N	137	23	160
	Mean	2.05 x10 ⁶	1.60 x10 ⁶	2.04 x10 ⁶
	Minimum	1.77 x10 ⁶	1.13 x10 ⁶	1.13 x10 ⁶
	Maximum	2.15 x10 ⁶	1.77 x10 ⁶	2.49 x10 ⁶
	St.Dev.	1.16 x10 ⁵	1.35 x10 ⁵	2.38 x10 ⁵
	COV	.057	.084	.117
Cap Locations	N	18	9	27
	Mean	2.02 x10 ⁶	1.31 x10 ⁶	1.78 x10 ⁶
	Minimum	1.83 x10 ⁶	8.92 x10 ⁵	8.92 x10 ⁵
	Maximum	2.15 x10 ⁶	1.74 x10 ⁶	2.23 x10 ⁶
	St.Dev.	1.08 x10 ⁵	3.06 x10 ⁵	3.93 x10 ⁵
	COV	.053	.234	.221
Piles	N	7	5	12
	Mean	1.92 x10 ⁶	1.51 x10 ⁶	1.75 x10 ⁶
	Minimum	1.77 x10 ⁶	1.24 x10 ⁶	1.24 x10 ⁶
	Maximum	2.15 x10 ⁶	1.73 x10 ⁶	2.19 x10 ⁶
	St.Dev.	1.44 x10 ⁵	1.91 x10 ⁵	2.67 x10 ⁵
	COV	.075	.126	.152

Of the 199 locations on structural members of the bridges, the instrument was able to directly provide an E value at 162 locations. For the other 37 locations, ultrasonic wavespeed was recorded, but the instrument did not provide an E value. These wave speeds were below the device lower limit. Of the 162 directed measurements, 39 were at the instrument’s truncated upper limit. For these 39, wave speeds above 19,267 ft/s were recorded, but the prediction of E remained at 2.14x10⁶ psi. The remaining predictions, 123 measurements, were based on wave speeds within the model limits. In Tables 3-2 to 3-5 these measurements as recorded from the device are presented in the “Measured E” columns.

The stiffness of the remaining 37 locations, though not directly provided by the instrument, were predicted using the recorded wave speed in Equation 1. These values are presented in the tables under the “Lower Limit Extrapolated E” column heading.

The final column of each table presents summary values combining the original measured stiffness values with those values predicted by Equation 1 substituted when the wave speed was either

above or below the instrument limits of stiffness prediction. This provided stiffness values for all 199 timbers, referred to as the “Combined Population E.”

Each of the first three tables presents a summary of stiffness values for members in an individual bridge. The fourth table presents the results of measurements at all three bridges combined.

Figures 3-2 to 3-4 present stiffness predictions for the individual members of the three bridges studied. The figures are plan views of the bridge spans tested. This provides some visual representation of how the stiffness varies throughout each bridge.

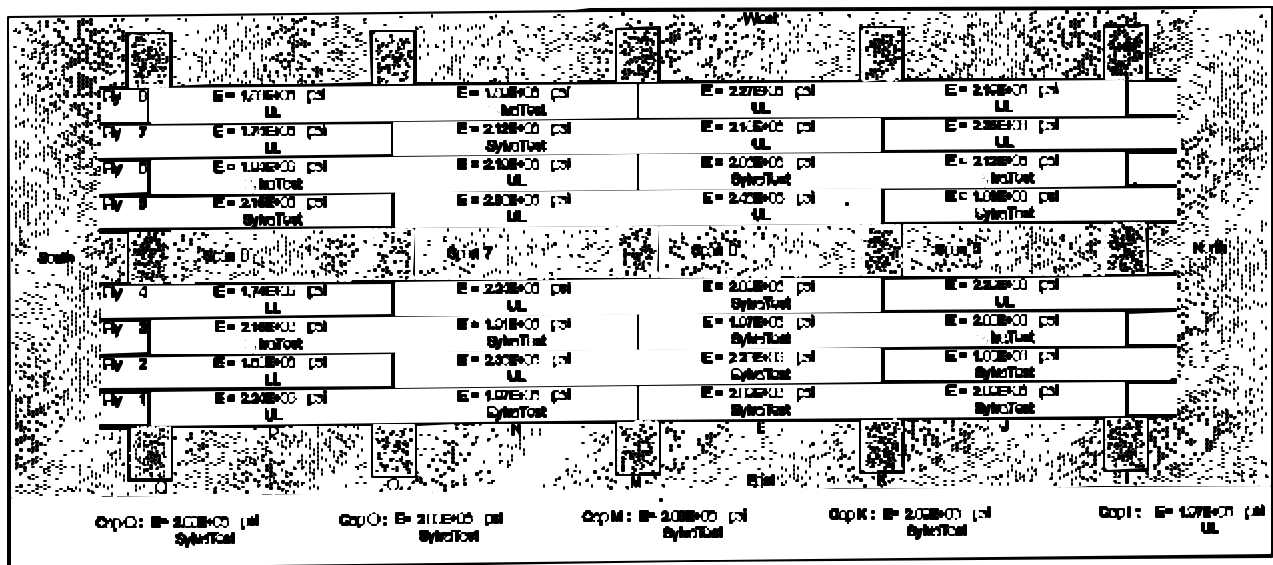


Figure 3-2(a). Bridge No. 32.35, in Fort Collins, predicted E values of timbers showing the location of members in the bridge. Spans 1 through 4 shown. Stiffness values have been converted from SI units to accepted imperial units.

Sylva Test – Indicates stiffness prediction made by Sylva Test Instrument.

LL – Indicates wavespeed measurement below 17,600 ft/s, no prediction by instrument.

Prediction made using Equation 1.

UL – Indicates wavespeed measurement above 15,934 ft/s, Sylva Test prediction capped at 2.14×10^6 psi.

Prediction made using Equation 1.

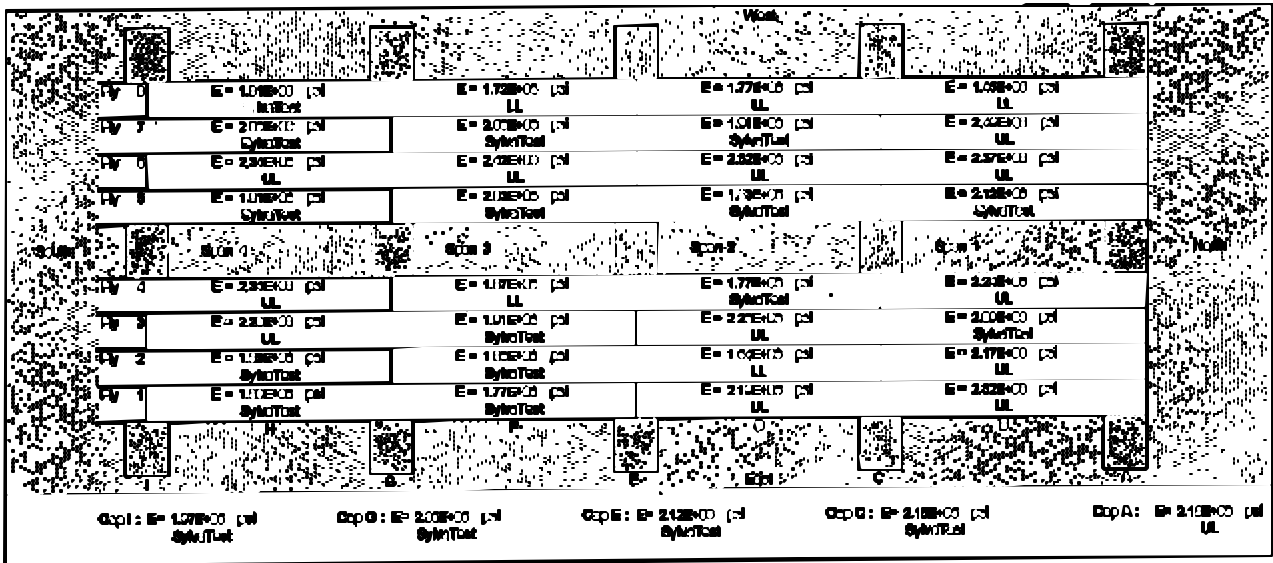


Figure 3-2(b). Bridge No. 32.35, in Fort Collins, predicted E values of timbers showing the location of members in the bridge. Spans 5 through 8 shown. Stiffness values have been converted from SI units to accepted imperial units.

Sylva Test – Indicates stiffness prediction made by Sylva Test Instrument.

LL – Indicates wavespeed measurement below 17,600 ft/s, no prediction by instrument.

Prediction made using Equation 1.

UL – Indicates wavespeed measurement above 15,934 ft/s, Sylva Test prediction capped at 2.14×10^6 psi.

Prediction made using Equation 1.

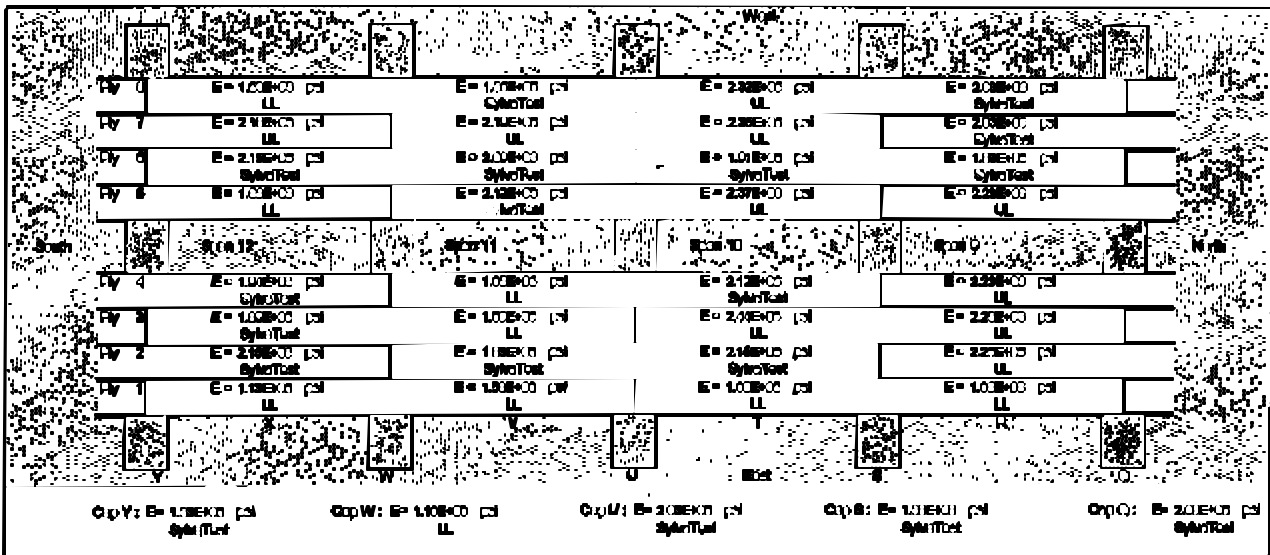


Figure 3-2(c). Bridge No. 32.35, in Fort Collins, predicted E values of timbers showing the location of members in the bridge. Spans 9 through 12 shown. Stiffness values have been converted from SI units to accepted imperial units.

Sylva Test – Indicates stiffness prediction made by Sylva Test Instrument.

LL – Indicates wavespeed measurement below 17,600 ft/s, no prediction by instrument.

Prediction made using Equation 1.

UL – Indicates wavespeed measurement above 15,934 ft/s, Sylva Test prediction capped at 2.14×10^6 psi.

Prediction made using Equation 1.

		West							
South	Ply 0	E = 1.07E+03 SylvaTest	E = 1.02E+03 SylvaTest	E = 1.13E+03 UL	E = 1.22E+03 UL				
	Ply 8	E = 1.03E+03 SylvaTest	E = 2.11E+03 SylvaTest	E = 1.02E+03 LL	E = 1.19E+03 UL				
	Ply 4	E = 2.17E+03 SylvaTest	E = 1.02E+03 SylvaTest	E = 1.02E+03 SylvaTest	E = 2.11E+03 SylvaTest				
	Section 4 Section 3 Section 2 Section 1 North								
South	Ply 9	E = 1.07E+03 SylvaTest	E = 2.11E+03 SylvaTest	E = 2.11E+03 SylvaTest	E = 1.02E+03 SylvaTest				
	Ply 2	E = 1.07E+03 SylvaTest	E = 2.11E+03 SylvaTest	E = 1.02E+03 SylvaTest	E = 1.02E+03 SylvaTest				
	Ply 1	E = 2.11E+03 SylvaTest	E = 2.11E+03 SylvaTest	E = 1.02E+03 SylvaTest	E = 1.02E+03 SylvaTest				
	East								
Cap L: E = 1.02E+03 SylvaTest		Cap J: E = 1.11E+03 LL		Cap G: E = 2.11E+03 UL		Cap D: E = 2.11E+03 SylvaTest		Cap A: E = 1.02E+03 LL	

Figure 3-3. Bridge No. 32.56, in Fort Collins, predicted E values of timbers showing the location of members in the bridge. Stiffness values have been converted from SI units to accepted imperial units.

Sylva Test – Indicates stiffness prediction made by Sylva Test Instrument.

LL – Indicates wavespeed measurement below 17,600 ft/s, no prediction by instrument.

UL – Indicates wavespeed measurement above 15,934 ft/s, Sylva Test prediction capped at 2.14×10^6 psi.

Both LL & UL predictions made using Equation 1.

		Span Average - West Girder					
		E = 2.02E+03 SylvaTest	E = 2.11E+03 SylvaTest	E = 2.02E+03 SylvaTest			
South	Ply 0	E = 1.01E+03 SylvaTest	E = 2.11E+03 UL	E = 2.22E+03 UL			
	Ply 7	E = 2.11E+03 UL	E = 2.11E+03 UL	E = 1.02E+03 SylvaTest			
	Ply 6	E = 2.11E+03 SylvaTest	E = 2.21E+03 UL	E = 2.11E+03 SylvaTest			
	Ply 5	E = 1.02E+03 SylvaTest	E = 1.02E+03 LL	E = 2.02E+03 SylvaTest			
South	Section 4 Section 3 Section 2 Section 1 North						
	Ply 4	E = 1.02E+03 SylvaTest	E = 1.02E+03 LL	E = 1.02E+03 SylvaTest			
	Ply 3	E = 2.11E+03 UL	E = 2.11E+03 UL	E = 2.11E+03 UL			
	Ply 2	E = 2.11E+03 UL	E = 2.11E+03 UL	E = 1.02E+03 SylvaTest			
Ply 1	E = 2.11E+03 UL	E = 1.77E+03 LL	E = 1.02E+03 LL				
		Span Average - East Girder					
		E = 2.11E+03 SylvaTest	E = 2.02E+03 SylvaTest	E = 1.02E+03 SylvaTest			
Cap A: E = 1.02E+03 LL		Cap D: E = 1.11E+03 LL		Cap G: E = 1.01E+03 SylvaTest		Cap J: E = 1.74E+03 LL	

Figure 3-4. Bridge No. 101, near Pueblo, predicted E values of timbers showing the location of members in the bridge. Stiffness values have been converted from SI units to accepted imperial units.

Sylva Test – Indicates stiffness prediction made by Sylva Test Instrument.

LL – Indicates wavespeed measurement below 17,600 ft/s, no prediction by instrument.

UL – Indicates wavespeed measurement above 15,934 ft/s, Sylva Test prediction capped at 2.14×10^6 psi.

Both LL & UL predictions made using Equation 1.

CHAPTER 4

ANALYTICAL MODELING APPROACH

In advance of the field testing, the static loadings to be used were approximately determined using ordinary influence diagrams. After testing, computer modeling was done using a two-dimensional matrix stiffness method. The modeling was done using the GS-USA Frame software (Rajan 1998). Each of the analytic models used is detailed in the following paragraphs.

Pinned Single Span Beam Model

The pinned single span model is the most simplistic model for the bridges considered. It assumes that the chords of each span resist applied loads as a single span, pinned end member. The following modeling assumptions were made.

1. Each span acts as a separate member, simply supported by caps at either end of the span. The entire reaction of any applied loads in that span must be completely reacted by the adjoining supports at the ends of the span. The loads and resulting behavior of that span have no influence on any other spans. Caps supporting loads on adjacent spans would support the combined load applied by the two spans.
2. The properties of all individual piles in both chords of any one span were combined into a single chord member. The members maintained the individual member depth, but were increased in width to the sum of the individual member widths. The assigned modulus of elasticity values represented average values measured for the individual chords of the spans.

The general single span beam model configuration used for Bridge 101 and Bridge 32.35 is shown in Figure 4-1 a). For modeling purposes, a node was used at mid-span, which allowed stresses and deflection at mid-span to be determined. Loads were applied to nodes or to members. The configuration consisted of each element having two nodes with three degrees of freedom each (horizontal, vertical, and rotational motion). Each consecutive pair of elements represented one beam over one span. Support

nodes were fixed in the Y-axis direction (vertical fixity). Connectivity was such that elements were hinged at supports and rigidly intra-connected at mid-span.

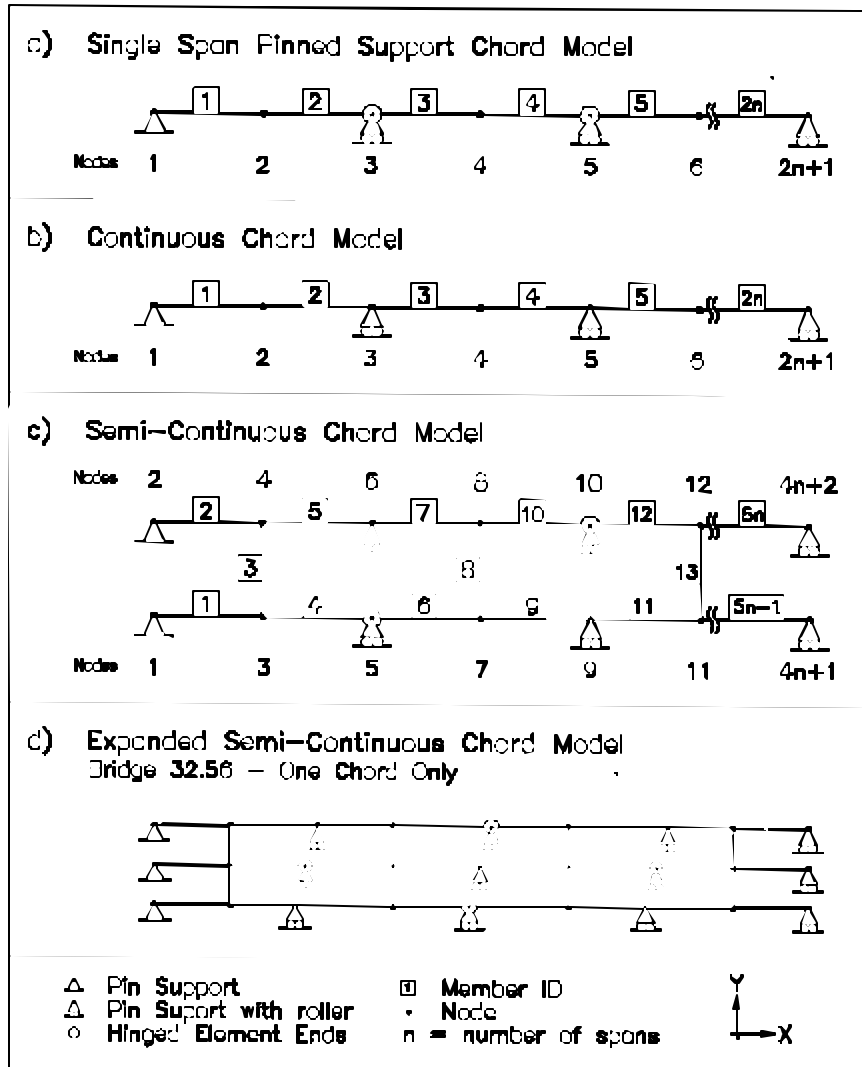


Figure 4-1. Schematic representation of frame analysis models used to evaluate load test data for timber railroad bridge.

Continuous Beam Model

This model simplifies the structure to a continuous multi-span member. The following assumptions were made. (Primary changes from previous model are underlined.)

1. One member extends continuously over all supports for the entire length of the bridge. This member was divided into elements with nodes at supports and mid-span locations.

2. The properties of all individual piles in both chords of any one span were combined into a single chord member. The members maintained the individual member depth, but were increased in width to the sum of the individual member widths. The assigned stiffness properties represented average values measured for the individual chords of the spans.
3. No provision was made for support movement. The assumption was made that the caps and pile systems had no influence on the chord behavior.
4. No provision was made to account for non-perfect member contact with the supports.

The continuous beam model configuration used for Bridge 101 and Bridge 32.35 is shown in Figure 4-1 b). The primary difference from modeling the beam as a series of single spans is that instead of hinges at each support, the member is fully continuous to the adjacent beam spans.

Semi-Continuous Beam Model

It was surmised that field performance of the bridge chords would not correspond to either truly single span or fully continuous chord modeling. This is due to the use of discontinuous one-span and two-span piles. Actual behavior is further affected by the bolts that connect the piles together at the ends and mid-span. All the bridges tested had bolts close to the support. Two of them, Bridges 32.35 and 32.56, included bolts at the mid-point of each span. Thus, a third model (“semi-continuous beam” model) was developed to provide a better representation of the real bridge structures.

The semi-continuous beam model treats the piles of the bridge chords as two separate chords, each representing a part of the lapped chord geometry, which are then linked together at mid-span to transfer load between the two chord components. A depiction of the general semi-continuous beam model configuration suitable for modeling Bridge 32.35 is shown in Figure 4-1 c).

For modeling the lapped chord configuration, two chord sub-systems were used. Each sub-system represented half of the piles in both chords. Each sub-system was effectively a series of beams continuous over two spans. The two systems are offset along the length of the bridge by one span length such that each system is continuous over only one of the span supports. In the case of Bridges 32.35 and

101, the properties of each system consisted of one beam representing four piles, two from either of the chords. From a modeling perspective, each system is separate and continuous over two span intervals with simple supports.

On all three bridges, there were two tie rods through all piles of a chord, located a few inches from the caps. On Bridge 32.35 and 32.56, there also were single tie rods at mid-span. To simplify the analysis, it was decided to include the mid-span tie rod in the model and ignore the effects of the tie rods near the caps.

The bolt connection was modeled as a pin connected axial member between the two chord sub-systems of the model. A dummy element with high EA but negligible EI properties was used to connect the mid-span nodes of each system for each span. This element would transfer shear, but not moment between the two sub-systems.

As with the previous models, the semi-continuous beam elements were standard frame elements with three degrees of freedom at either end. Several assumptions were made for this model. (Significant changes from previous models are underlined.)

1. The chord piles were represented by two independent beam sub-systems. For each sub-system, the beam is continuous over two adjacent spans, hinged at every other support. The hinging pattern is alternated between the two systems.
2. Dummy elements of near infinity axial stiffness and near zero bending stiffness were used to connect members at mid-span, representing the mid-span bolts. The stiffness magnitudes selected were sufficient to force the same deflection of the systems to five significant figures.
3. While the bolts at mid-span were represented in the model, the bolts near the caps were ignored.
4. The properties of all individual piles represented by either sub-system for any span were combined into a single system member. The members maintained the individual member depth, but were increased in width to the sum of the individual member widths. The assigned stiffness properties represented average values measured for the individual chords associated with each sub-system and spans.

5. No provision was made for support movement.
6. No provision was made to model connector behavior.
7. No provision was made to account for non-perfect member contact.
8. Load was applied equally to the two systems at axle load points.
9. No attempt was made to emulate the forced deflection of the piles by the tie and rail system.

The semi-continuous model was used to predict deflections for Bridge 32.35. It also was modified to predict the response of Bridge 101, which did not have the mid-span bolts. This model was not used for Bridge 32.56 because of its skewed geometry.

Extended Semi-Continuous Chord Model

During development of the semi-continuous chord model, it became apparent that this approach could be extended from two systems to individual representation of multiple piles and chords. For example if there were a total of eight timbers across the width of a bridge, it could be represented by eight systems. Each system would be representative of a single timber ply. Two advantages immediately were obvious.

First, this approach allowed modeling of Bridge 32.56. The previous models could not adequately represent this bridge since the intermediate pile supports were not perpendicular to the chords. When loads were applied to chords, each ply was loaded at a different location within the span. Further, each of the piles in the end span was of different length. By individually modeling each ply, any reasonable geometry could be addressed.

The second advantage was that this extended model allowed assignment of individual stiffness properties to each ply of each span. Doing that allows the model to distribute load resistance appropriately between members of varying stiffness.

One of the limitations of this model is that the load share applied to individual piles of a chord is not known. In the real structure, the load from the axles is applied to the rail, which spreads the load to several ties, which in turn bear on the piles. The rail spreads the load longitudinally on the ply, the ties

spread the load laterally among piles of the chords. While the rail, ties and chord piles form a grid system, the potential gaps between any individual members makes defining the load distribution to individual piles a complex problem in itself. Because of this issue, an assumption was made to simplify the load pattern to equally distributed point loads among each ply directly below the axle load. Work is in progress to overcome this limitation.

The general extended semi-continuous beam model configuration is illustrated in Figure 5-1 d) for only one chord of three lapped piles. The major assumptions of the model were the same as the semi-continuous model, except:

1. The chord piles were each represented individually by a beam system. For each system, except for some piles of the end spans, the beam is continuous over two adjacent spans, hinged at every other support. The hinging pattern is alternated between the two systems.
2. The stiffness properties of all individual piles were assigned as determined by the non-destructive analysis.
3. Load was applied equally among all piles under the applied axle loads.

Fixed End Beam Model

This model assumes that each end of the chord at either end of the span is fixed. It is similar to the pinned single span model except the elements are not allowed to rotate at the supports. Further, like the pinned single span model, the only loads causing effects to the beam in the span are loads in the span itself. As with the single span and continuous beam models, the chord system is represented as one member representing the sum of the eight individual members.

Load Application

All the modeling in this study was done representing only the chords of the system, to have an expedient means by which to estimate the expected field test results. The effects of load distribution by the rail and ties affect the predicted performance of each bridge. However, for the pinned, single span

beam, continuous beam, and fixed, single span beam models, the entire axle load was applied at the longitudinal position of the axle. For the semi-continuous beam models, the load was distributed equally as multiple point loads on each element.

The general matter of longitudinal load distribution is unknown, but approximately examined for sensitivity. As an example, consider a 15-foot single span with simply supported ends with a load at mid-span. Two load cases were evaluated. One load case modeled the load as a single point load at mid-span. The other modeled the load as equally distributed over a 36-inch length centered at mid-span. The effect of using the spread uniform load produced 2 percent less deflection when compared to a single point load. The uniform load also produced 9 percent less stress than the point load. Where the effect on stress appears significant and must be addressed in further modeling to define load paths, the 2 percent improvement in deflection seems minor when checking general correctness of measured deflections.

CHAPTER 5

FIELD LOAD TESTING

Bridge Loading Equipment

The TLV used in the load tests is a specialized train car fitted with hydraulic loading axle capability by which controlled concentrated loading can be applied to railroad tracks. The TLV loading axle allows loads to be applied to the rail simultaneously in three orthogonal directions. This bridge testing involved only vertical loading. In this mode of loading the actuators and axle serve to lift the TLV at its mid-span such as to transfer part of its weight to the track at that location. Figure 5-1 is a schematic of the test vehicle used to apply ramp loads to the bridges. Loads were applied and held at discrete intervals while displacements and strain were measured. Static loads also were applied by the train – composed of a locomotive, the instrumentation car and the TLV. The train itself was used for applying desired static loading by simply positioning it along the bridge. The entire train also was used for applying rolling loads.

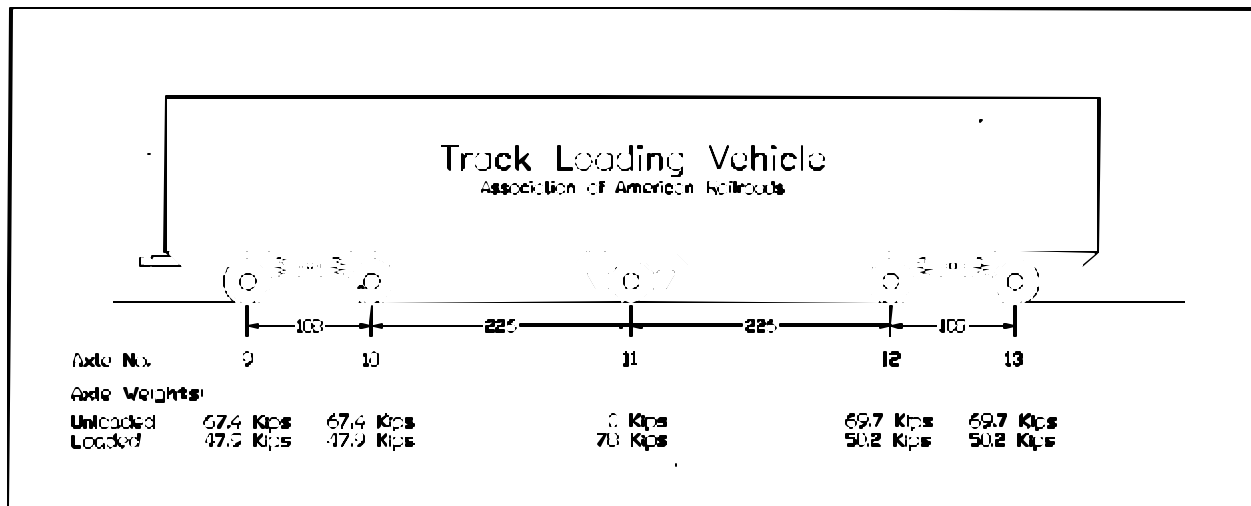


Figure 5-1. Schematic of the Association of American Railroads Track Loading Vehicle Including Axle Loads

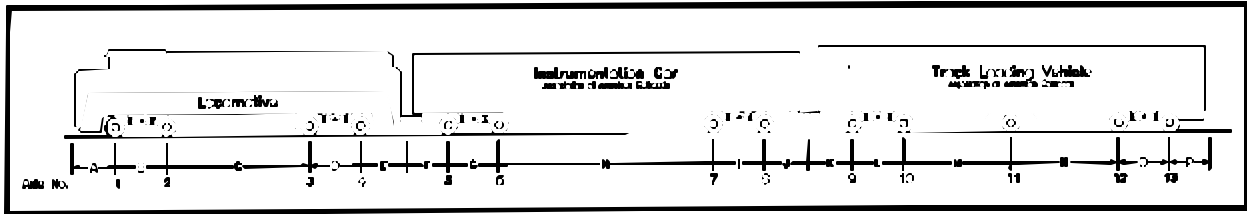


Figure 5-2. Schematic depiction of the locomotive, instrumentation car and Track Loading Vehicle used in the bridge testing. Axle loads and spacing presented in Tables 5-1 and 5-2 for the Fort Collins sites and in Tables 5-3 and 5-4 for the Pueblo site.

For the testing of bridges in Fort Collins, a four-axle engine was provided by the Union Pacific Railroad. Figure 5-2 is a schematic drawing of the test train used in Pueblo showing its axle spacing. The axle spacing and weights are listed in Tables 5-1 to 5-4 and correspond to the dimensions shown in Figure 5-2.

Load Test Methodology

Loadings Used

Static loading cases were achieved by positioning the three-car train at specific locations with reference to the bridge being tested. For a given loading sequence, the train was positioned just off the bridge and instrumentation measurements were taken (instrumentation was “zeroed”). Then the train was moved to a predetermined position and measurements (electronic data and optical back-up data) were taken again. After that, the process of locating the train and taking measurements was repeated for all positions of interest.

Each load was identified by specifying a particular position of an appropriate axle of the train system. The axles of the train were numbered from 1 to 13 starting at the first axle of the locomotive. Sequential letters were used to identify locations on the bridge being tested. Typical locations were directly above supports and mid-span of chords. Table 5-5 presents load positions for the bridges. “Positioning” of an axle implies specifying at what location (point) along the bridge the axle was to be placed to achieve the desired position of the overall train. For example, if axle 3 was to be positioned at a

location B, the identifier used was “3@B”. In many cases, it was desirable to position two axles as being centered about a point on the bridge. For example, the identifier “3-4@C” was used to indicate axles 3 and 4 were centered at point C.

Table 5-1. Loads applied by train in Fort Collins, Colo. TLB axle at 0 kip, 30 kip, 60 kip and 78 kip load levels.

Axle weights - 0 kips applied at TLV center axle				
	Truck	Weight (kips)	Axle	Weight (kips)
Locomotive	Front	135.00	1 & 2	67.500
	Rear	135.00	3 & 4	67.500
Test Car	Front	67.35	5 & 6	33.675
	Rear	64.95	7 & 8	32.475
TLV Car	Front	134.80	9 & 10	67.400
	Center	0.00	11	0.000
	Rear	139.35	12 & 13	69.675
TLV axle weights - 30 kips applied at TLV center axle				
	Truck	Weight (kips)	Axle	Weight (kips)
TLV Car	Front	119.80	9 & 10	59.900
	Center	30.00	11	30.000
	Rear	124.35	12 & 13	62.175
TLV axle weights - 60 kips applied at TLV center axle				
	Truck	Weight (kips)	Axle	Weight (kips)
TLV Car	Front	104.80	9 & 10	52.400
	Center	60.00	11	60.000
	Rear	109.35	12 & 13	54.675
TLV axle weights - 78 kips applied at TLV center axle				
	Truck	Weight (kips)	Axle	Weight (kips)
TLV Car	Front	95.80	9 & 10	47.900
	Center	78.00	11	78.000
	Rear	100.35	12 & 13	50.175

Axle Identification matches Figure 5-2 configuration.

Table 5-2. Load spacing for axles of train used on Fort Collins locations on Union Pacific line

	Points of Interest on Figure 13		Dimension Reference	Spacing (inches)	Load Reference from 1st Axle		
					(axle)	(inches)	(feet)
Locomotive	Hitch	1st axle	A	97			
	1st axle	2nd axle	B	108	1	0	0.0
	2nd axle	3rd axle	C	300	2	108	9.0
	3rd axle	4th axle	D	108	3	408	34.0
	4th axle	Hitch	E	97	4	516	43.0
Test Car	Hitch	1st axle	F	111			
	1st axle	2nd axle	G	102	5	724	60.3
	2nd axle	3rd axle	H	610	6	826	68.8
	3rd axle	4th axle	I	102	7	1436	119.7
	4th axle	Hitch	J	111	8	1538	128.2
TLV Car	Hitch	1st axle	K	90			
	1st axle	2nd axle	L	108	9	1739	144.9
	2nd axle	Load axle	M	226	10	1847	153.9
	Load axle	3rd axle	N	226	11	2073	172.8
	3rd axle	4th axle	O	108	12	2299	191.6
	4th axle	Hitch	P	90	13	2407	200.6

Axle and reference identification matches Figure 5-2 configuration.

Ramp loading was achieved by use of the TLV loading axle. Various critical positions were predetermined, and the TLV axle then was positioned at these locations. Initial measurements were first taken for no load applied by the axle, then at specific applied load increments achieved by controlling the TLV actuator. Typical load levels at the load axle location were 0, 30, 60 and 78 kips and the reverse.

Rolling train loads involved recording electronic data while a train was passing over the bridge. For each bridge, the deflection of several primary members at selected locations was recorded while local rail traffic crossed the bridge. On the first bridge, Bridge 32.35, the local traffic encountered included a pair of six-axle Union Pacific locomotives pulling a local ballast train and the three-car test train. On the second and third bridges, a moving load applied by the locomotive plus the IC and TLV cars was used for obtaining deflection information. To estimate the velocity of the train crossing the bridge, a stopwatch was used to measure time of travel of a position on the train as it crossed the length of the bridge.

Table 5-3. Loads applied by train in Pueblo, Colo. TLV axle at 0 kip, 30 kip, 60 kip, and 78 kip load levels.

Axle weights - 0 kips applied at TLV center axle				
	Truck	Weight (kips)	Axle	Weight (kips)
Locomotive	Front	120.20	1 & 2	60.100
	Rear	122.20	3 & 4	61.100
Test Car	Front	67.35	5 & 6	33.675
	Rear	64.95	7 & 8	32.475
TLV Car	Front	134.80	9 & 10	67.400
	Center	0.00	11	0.000
	Rear	139.35	12 & 13	69.675
TLV axle weights - 30 kips applied at TLV center axle				
	Truck	Weight (kips)	Axle	Weight (kips)
TLV Car	Front	119.80	9 & 10	59.900
	Center	30.00	11	30.000
	Rear	124.35	12 & 13	62.175
TLV axle weights - 60 kips applied at TLV center axle				
	Truck	Weight (kips)	Axle	Weight (kips)
TLV Car	Front	104.80	9 & 10	52.400
	Center	60.00	11	60.000
	Rear	109.35	12 & 13	54.675
TLV axle weights - 78 kips applied at TLV center axle				
	Truck	Weight (kips)	Axle	Weight (kips)
TLV Car	Front	95.80	9 & 10	47.900
	Center	78.00	11	78.000
	Rear	100.35	12 & 13	50.175

Axle Identification matches Figure 5-3 configuration.

Table 5-4. Load spacing for axles of train used on Pueblo locations

	Points of Interest on Figure 13		Dimension Reference	Spacing (inches)	Load Reference from 1st Axle		
					(axle)	(inches)	(feet)
Locomotive	Hitch	1st axle	A	97			
	1st axle	2nd axle	B	108	1	0	0.0
	2nd axle	3rd axle	C	264	2	108	9.0
	3rd axle	4th axle	D	108	3	372	31.0
	4th axle	Hitch	E	97	4	480	40.0
Test Car	Hitch	1st axle	F	111			
	1st axle	2nd axle	G	102	5	688	57.3
	2nd axle	3rd axle	H	610	6	790	65.8
	3rd axle	4th axle	I	102	7	1400	116.7
	4th axle	Hitch	J	111	8	1502	125.2
TLV Car	Hitch	1st axle	K	90			
	1st axle	2nd axle	L	108	9	1703	141.9
	2nd axle	Load axle	M	226	10	1811	150.9
	Load axle	3rd axle	N	226	11	2037	169.8
	3rd axle	4th axle	O	108	12	2263	188.6
	4th axle	Hitch	P	90	13	2371	197.6

Axle and reference identification matches Figure 5-3 configuration.

Instrumentation

Instrumentation of the bridges was comprised of a combination of displacement transducers, extensometers, optical surveying equipment (for back up) and accelerometers. Linearly variable displacement transducers (LVDTs) were used to measure deflection of the bridge system at various locations. The transducers were installed in several different ways.

For comparison of chord deflection to simple modeling, ignoring support motion issues, it was necessary to measure deflection with reference to the displaced chord. The displaced chord is a straight line connecting the mid-depth of the deflected chord over its supports. This removes differential support motion from the measurements. To measure this deflection, a support frame was suspended under a chord of one span on the bridge. The support was attached to the chord’s outer piles at its neutral axis

Table 5-5. Load positions selected for testing on Bridge 32.35, Bridge 32.56 and Bridge 101.

Selected Load Positions					
Static Loads			Ramp Loads		
Bridge 32.35	Bridge 32.56	Bridge 101	Bridge 32.35	Bridge 32.56	Bridge 101
1@B	1@A	1@J	11@J	11@B	11@J-
1@C	2@A-	1@I	11@K	11@E	11@I
1@D	2@A	2@J-	11@L	11@H	11@G+
1@E	1-2@B	1@H	11@M	11@K	11@G
1@F	1@D	1@G+	11@N		11@G-
1-2@F	1-2@D	1@G-			11@F
1@G	2@D	1-2@G			11@D+
1-2@G	1-2@E	1@F			11@D
1@H	1@G	2@G			11@D-
1-2@H	1-2@G	2@G-			11@C
1@I	3-4@B	1@E			11@A+
1-2@I	1-2@H	1@D+			11@A
1@J	1-2@I	1@D-			
1-2@J	1@J	1-2@D			
1@K	1-2@K	1@C			
1@L	1@L	2@D			
1-2@L	3-4@E	2@D-			
1-2@M	3@G	1@B			
1@N	3-4@G	1@A+			
1-2@N	3-4@K	9@J			
4@I		9@J-			
1@O		10@J-			
1-2@O		9@I			
1@P		9@H			
1-2@P		9@G+			
1@Q		9@G-			
4@L		9-10@G			
3-4@M		9@F			
3@N		9@E			
3-4@N		6@E			
5@K		5-6@E			
7-8@I		5@E			
8@I		4@G			
9-10@I					
10@I					
12-13@I					
12-13@J					

over the supports. The frame is shown in Figure 5-3 under a span of Bridge 32.35 as transducers are being attached.

There also was interest in monitoring deflection referenced to the ground, which would include any support motion and gap closing between chord piles, caps and piles. For monitoring the relative motion between the piles and the caps, the transducers were mounted directly on the caps. Figure 5-4 shows a group of transducers positioned for monitoring relative motion between caps and piles on Bridge 101. For monitoring the absolute cap motion, the transducers were supported directly from the ground.



Figure 5-3. Photo of frame for displaced chord instrumentation being installed on Bridge 32.35. Frame is suspended under the bridge chord.

Clip extensometers were used to measure longitudinal deformation in selected members. Figure 5-5 shows an extensometer in use on Bridge 101.

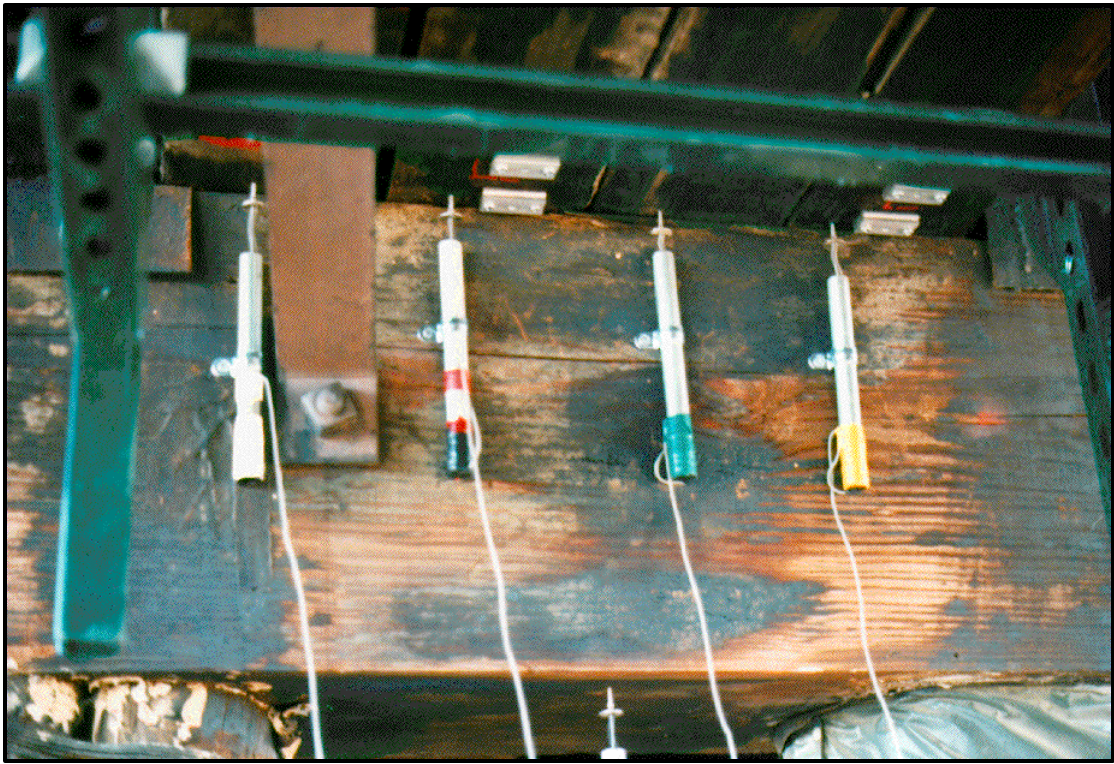


Figure 5-4. Photo of displacement transducers installed to measure relative motion of piles to a cap on Bridge 101.

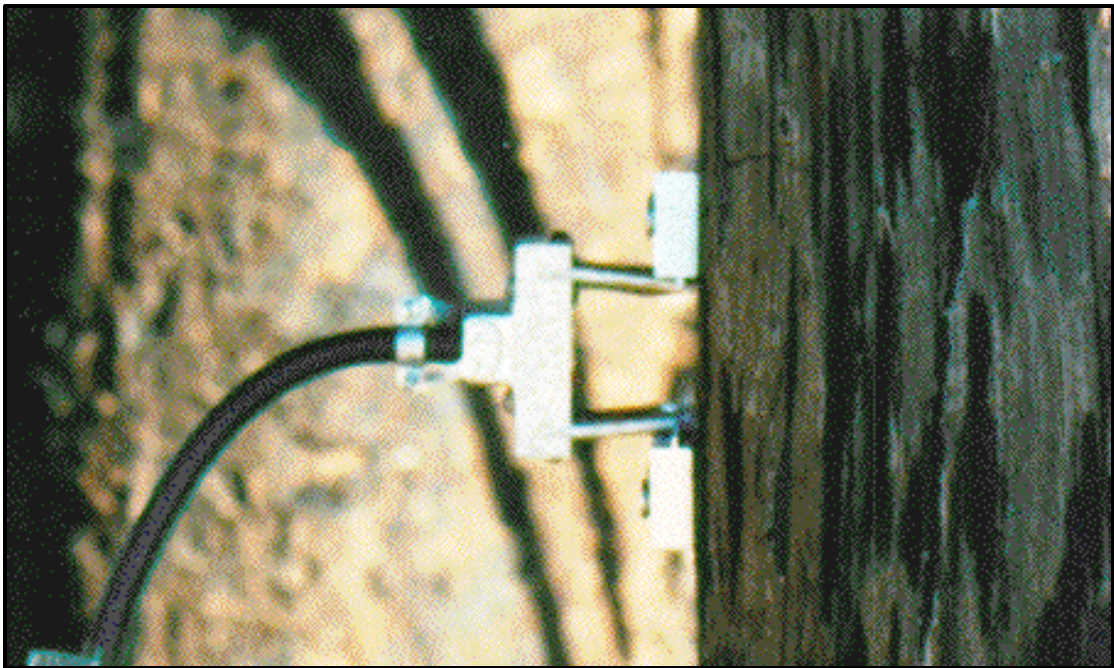


Figure 5-5. Photo of an extensometer installed on a pile on Bridge 101.

The LVDT and extensometer output voltages were monitored by a Hewlett Packard 3852A Data Acquisition Unit that recorded all channels. Data was either collected by single scan of all channels triggered by command, as in the case of static and ramp testing, or by continuous scanning of the channels as used in the rolling vehicle tests. For monitoring the rolling loads, each channel was sampled approximately once every 1.3 seconds. Although rather slow, this sampling rate was the fastest the data acquisition unit and measurement devices could sample the channels set up for the tests.

CHAPTER 6

RESULTS OF STATIC LOAD TESTS

Static Load Test Results – Bridge 32.35

Static loading, was a major emphasis of the test program for Bridge 32.35. Six static load cases from Bridge 32.35 were selected to demonstrate the behavior of the bridge.

Figure 6-1 shows the positions of electronic instrumentation in the four spans monitored in Bridge 32.35. All eight piles of Spans 5 and 6 were instrumented with transducers to measure deflection with reference to the displaced chord. Selected piles in Spans 4, 5, 6 and 7 were instrumented with transducers to measure deflection referenced from the ground. All transducers were as close to mid-span as possible. Although the figure shows all transducer instrumentation locations, only six transducers were in use at any one time.

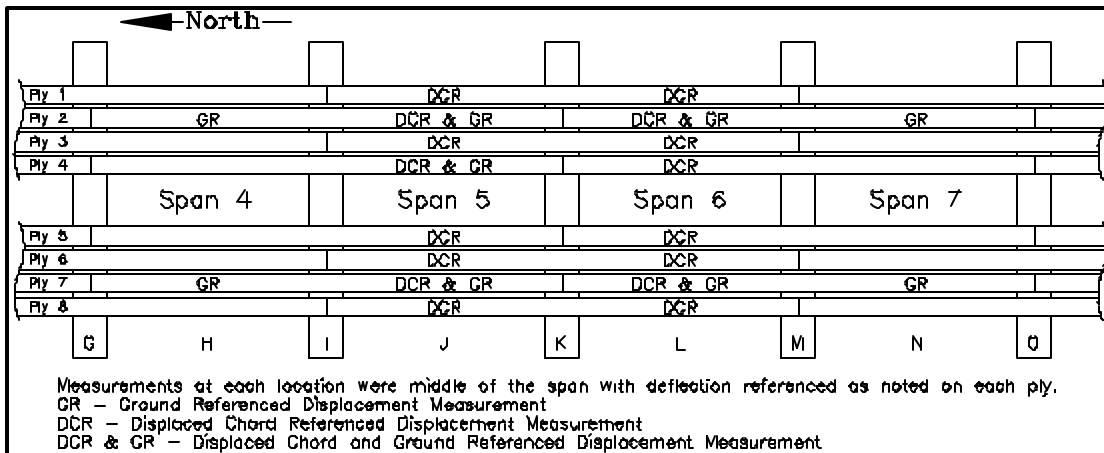


Figure 6-1. Electronic instrumentation positions for displacement transducers in Spans 4, 5, 6 and 7 on Bridge 32.35.

Several static load positions were selected to illustrate the displacement response of Bridge 32.35 as the test train progressed southward across the instrumented spans. These load positions (identified as 1-2@I, 1@J, 1-2@K, 1@L, 1-2@M and 1@O) are illustrated in Figs. 6-2 to 6-7.

Load positions 1-2@I, 1-2@K and 1-2@M (Figures 6-2, 6-4 and 6-6; respectively) center the lead axles of the locomotive over pile bents I, K and M respectively. Load positions 1@J and 1@L (Figures 6-3 and 6-5; respectively) center the lead axle of the locomotive at mid-span in Span 5 and Span 6, respectively. These positions apply a heavy single axle load, 67.4 kips, at a mid-span location. The second axle of the locomotive also applies a 67.4 kip load near the adjacent north bent. Figure 6-7 illustrates the load position 1@O, which centers the lead axle of the locomotive over the bent between Spans 7 and 8. Axle 2 is near mid-span of Span 7. Axles 3 and 4 are close to mid-span of Span 5. Axle 6 is near mid-span of Span 3. Spans 4 and 6 have no loads applied to them.

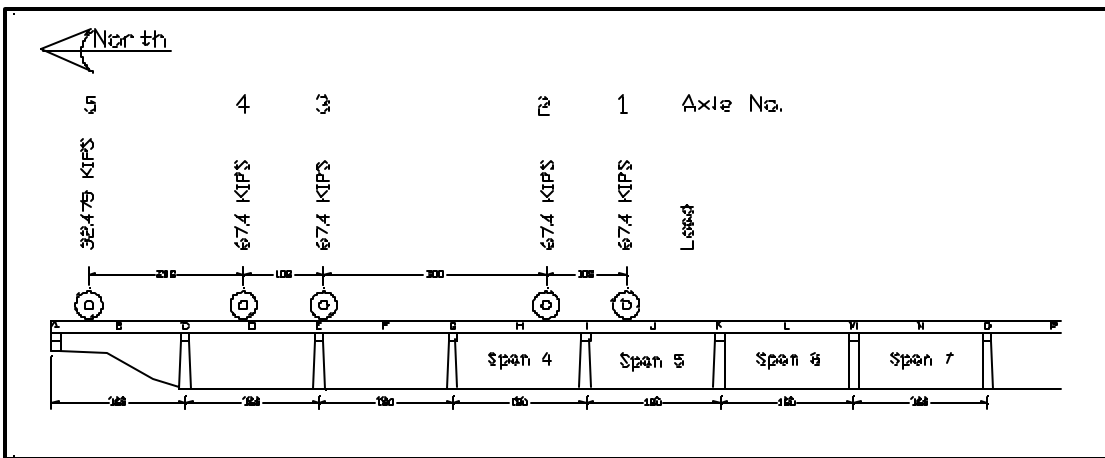


Figure 6-2. Loads applied to Bridge 32.35 due to load position 1-2@I. Dimensions are in inches.

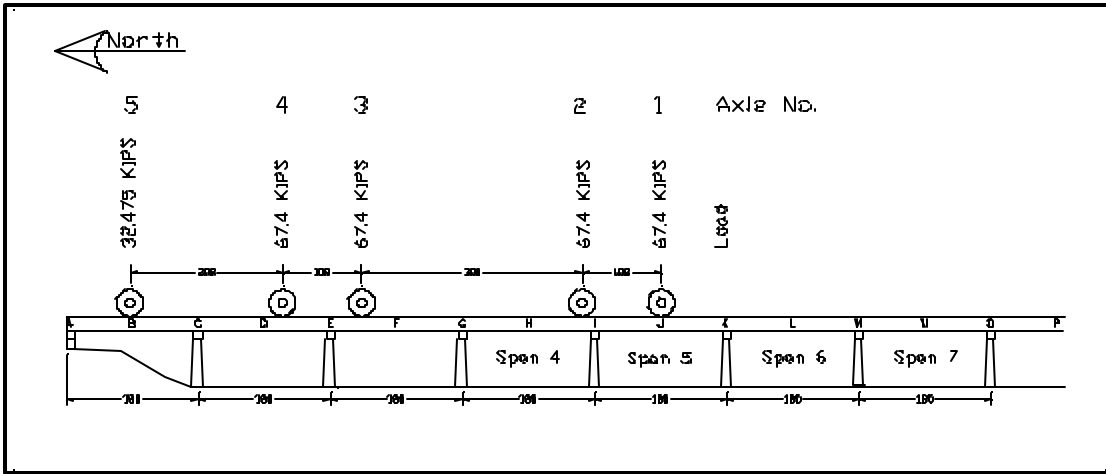


Figure 6-3. Loads applied to Bridge 32.35 due to load position 1@J. Dimensions are in inches.

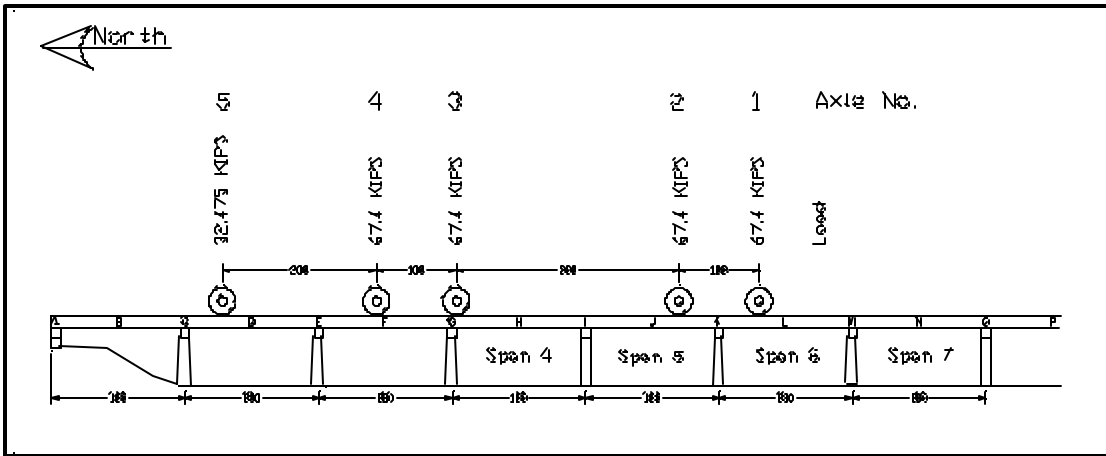


Figure 6-4. Loads applied to Bridge 32.35 due to load position 1-2@K. Dimensions are in inches.

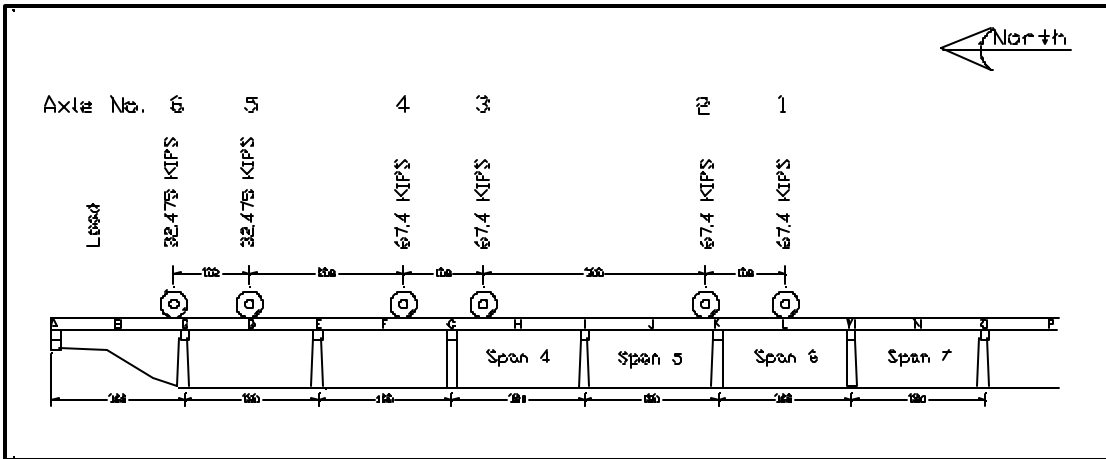


Figure 6-5. Loads applied to Bridge 32.35 due to load position 1@L. Dimensions are in inches.

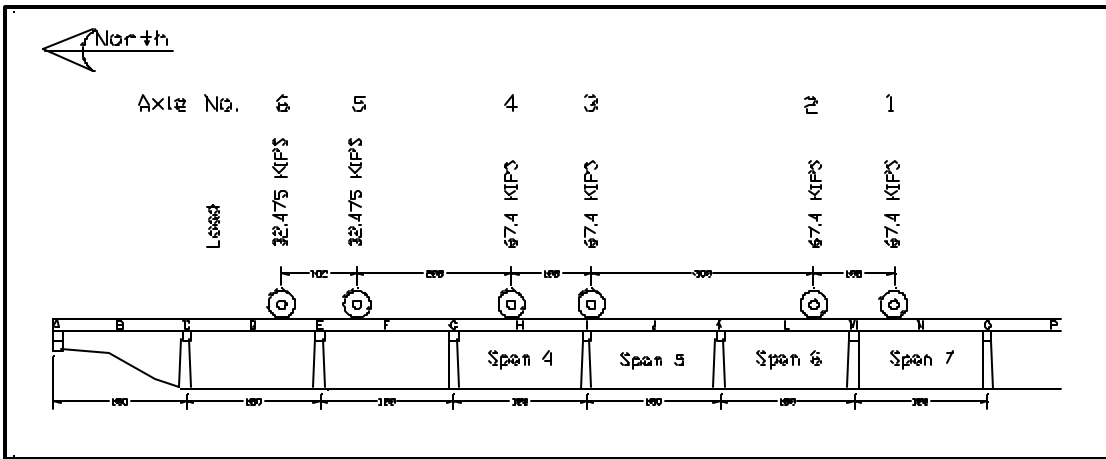


Figure 6-6. Loads applied to Bridge 32.35 due to load position 1-2@M. Dimensions are in inches.

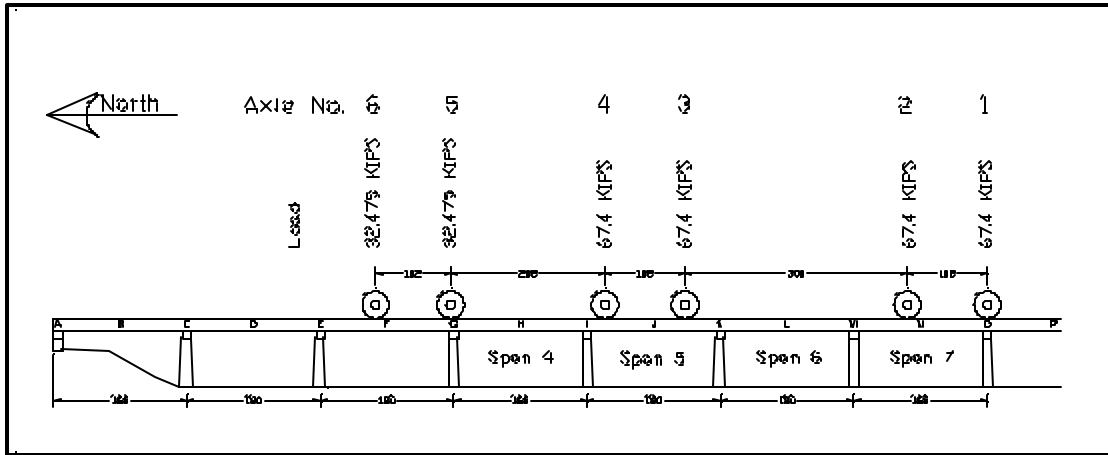


Figure 6-7. Loads applied to Bridge 32.35 due to load position 1@O. Dimensions are in inches.

Displacements Relative to the Displaced Chord

Measured Results

The displacement data presented in this section are referenced to the “displaced chord.” Data for each of the six load conditions are presented in Table 6-1 and displayed in six illustrations Figures 6-8 through 6-13. Each figure presents displacement of the piles at the mid-spans of Spans 5 and 6 recorded for the corresponding load cases. LDVT 5 (used to measure displacement of Ply 4) failed to perform adequately and its data was not included. The displacements are relative to the initial “no load” measurement taken just before the load sequence was initiated. The horizontal axis of each graph represents a portion of the bridge (Spans 3 to 7) located from 450 to 1360 inches, measured from the north end. Downward displacement is considered positive and shown downward in the figure.

Figure 6-8 presents displacement data for load position 1-2@I. Both Spans 4 and 5 have a 67.4 kip load applied 54 inches from the center of the cap. It was expected that the bridge would be to have downward deflection in both Spans 4 and 5 some upward displacement in Span 6. The data support this expectation. On average, the piles of Span 5 experienced downward displacement of approximately 0.1 inches while those of Span 6 experienced an upward displacement of 0.006 inches.

Table 6-1. Displacement transducer data collected at mid-span of selected chord plies for loads 1-2@I, 1@J, 1-2@K, 1@L, 1-2@M, and 1@O. All displacements in inches referenced from the displaced chord.

Distance from north end of bridge	Span 5	Span 6
	Mid-Span	Mid-Span
	(inches)	(inches)
	810	990
Load 1-2@I		
Ply 1	0.1025	-0.0178
Ply 2	0.1131	0.0327
Ply 3	0.0977	-0.0127
Ply 4		
Ply 5		-0.0077
Ply 6		-0.0222
Ply 7		-0.0154
Ply 8		-0.0019
Mean	0.104	-0.006
Load 1@J		
Ply 1	0.1322	-0.0305
Ply 2	0.1415	0.0264
Ply 3	0.1088	-0.0161
Ply 4		
Ply 5	0.1013	-0.0137
Ply 6	0.0661	-0.0308
Ply 7	0.0678	-0.0202
Ply 8	0.0495	-0.0075
Mean	0.095	-0.013
Load 1-2@K		
Ply 1		0.05
Ply 2		0.1742
Ply 3		0.065
Ply 4		
Ply 5		0.025
Ply 6		0.039
Ply 7		0.063
Ply 8		0.095
Mean		0.073
Load 1@L		
Ply 1	0.0475	0.0865
Ply 2	0.0405	0.2768
Ply 3	0.0223	0.0964
Ply 4		
Ply 5	0.0077	0.0608
Ply 6	0.01	0.089
Ply 7	-0.0089	0.1084
Ply 8	-0.0701	0.1628
Mean	0.007	0.126
Load 1-2@M		
Ply 1	0.038	0.0677
Ply 2	0.0161	0.2139
Ply 3	0.0434	0.0745
Ply 4		
Ply 5		0.0249
Ply 6		0.056
Ply 7		0.0649
Ply 8		0.0931
Mean	0.033	0.085
Load 1@O		
Ply 1	0.1674	
Ply 2	0.1681	
Ply 3	0.1459	
Ply 4		
Ply 5	0.1367	
Ply 6	0.1234	
Ply 7	0.0779	
Ply 8	0.0206	
Mean	0.12	

Note: Ply 4 - No data records due to possible malfunction of LVDT 5 - Ply 4 data suspect.

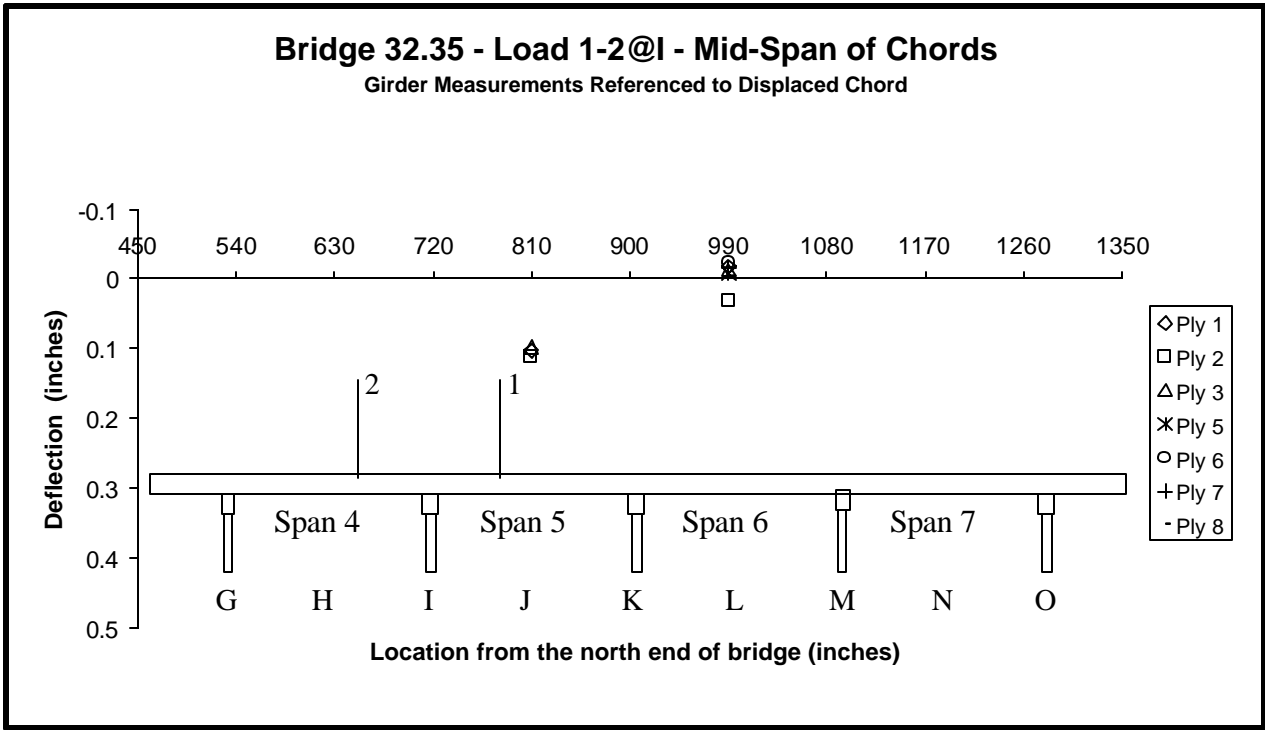


Figure 6-8. Transducer deflection measurements referenced to the displaced chord for Bridge 32.35 for load 1-2@I.

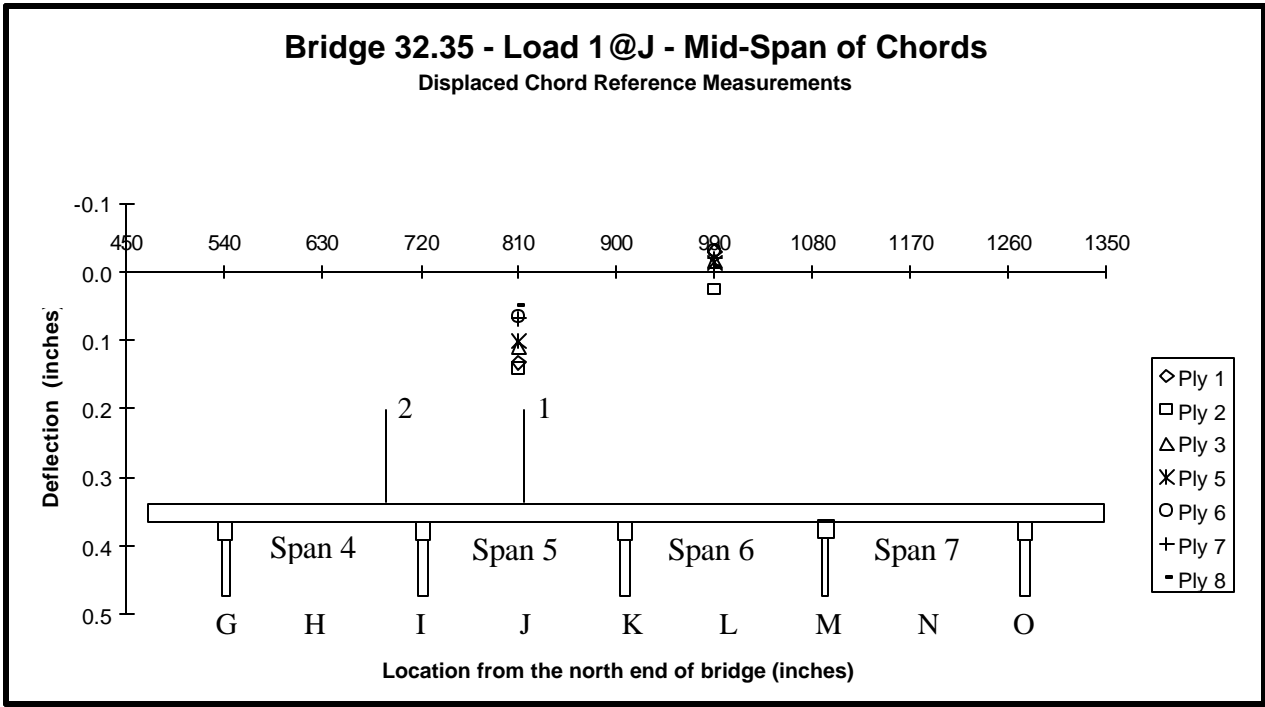


Figure 6-9. Transducer deflection measurements referenced to the displaced chord for Bridge 32.35 for load 1-2@J.

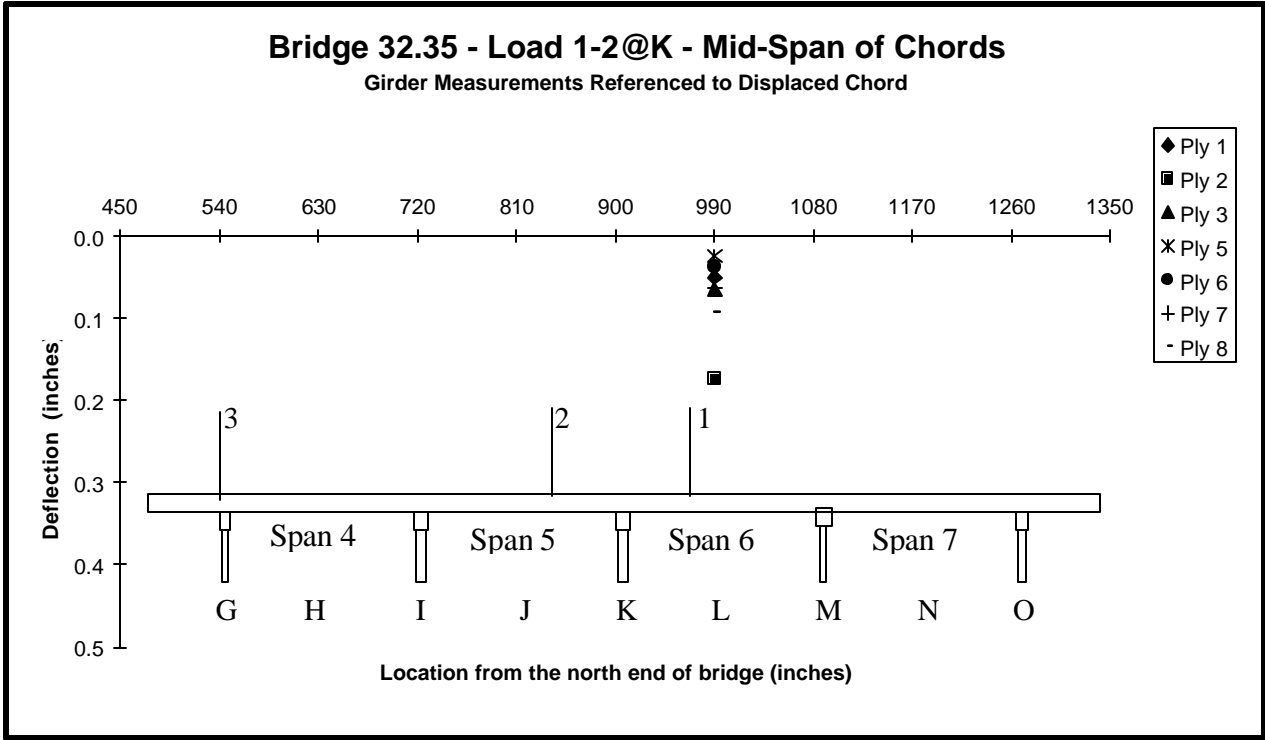


Figure 6-10. Transducer deflection measurements referenced to the displaced chord for Bridge 32.35 for load 1-2@K.

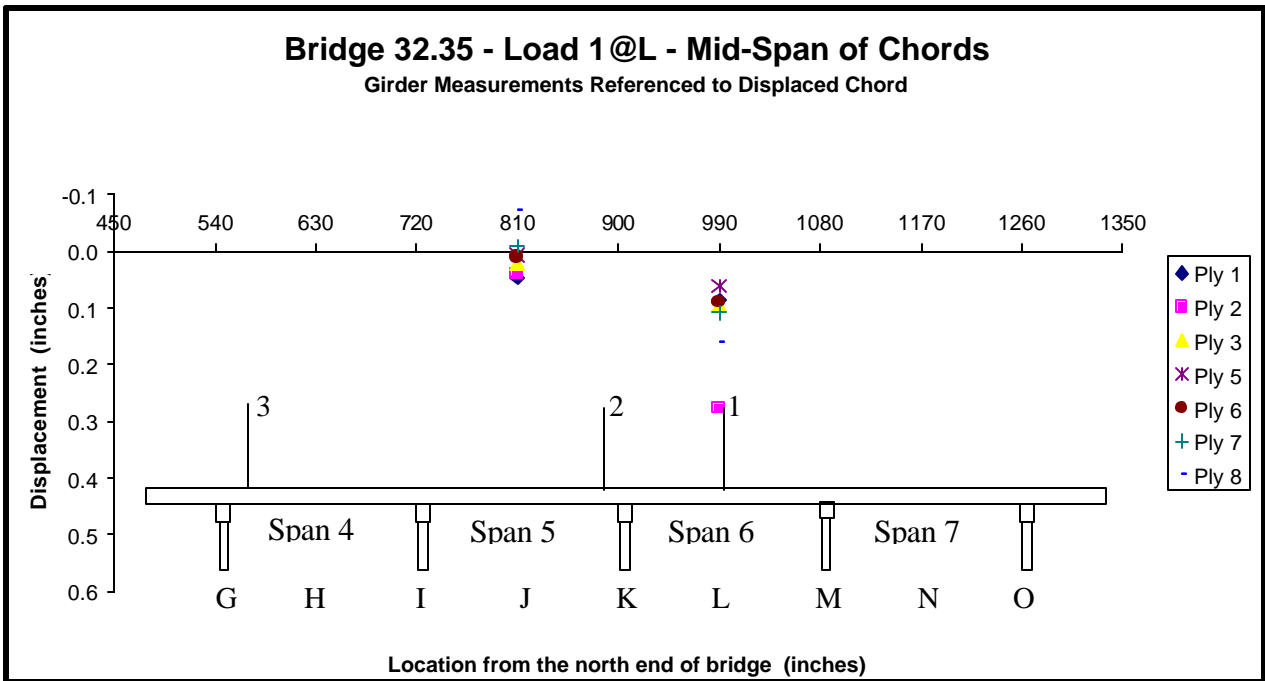


Figure 6-11. Transducer deflection measurements referenced to the displaced chord for Bridge 32.35 for load 1-2@L.

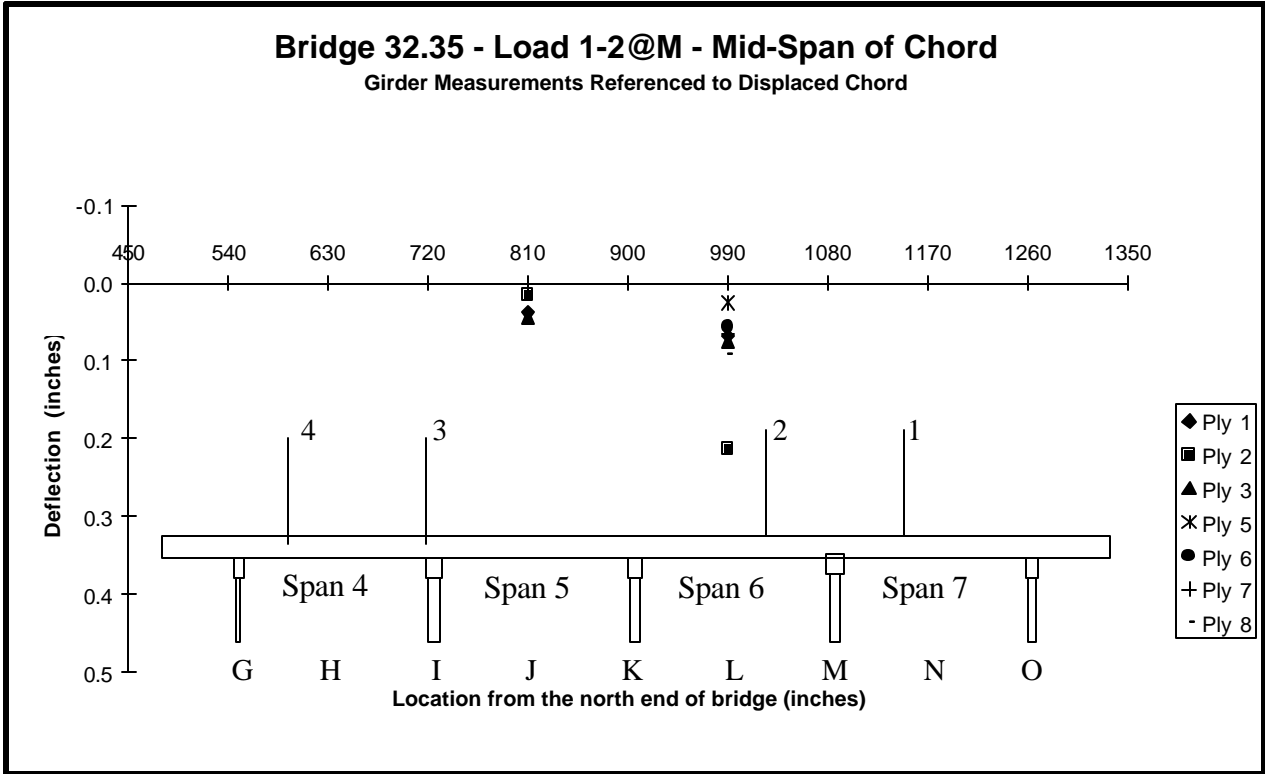


Figure 6-12. Transducer deflection measurements referenced to the displaced chord for Bridge 32.35 for load 1-2@M.

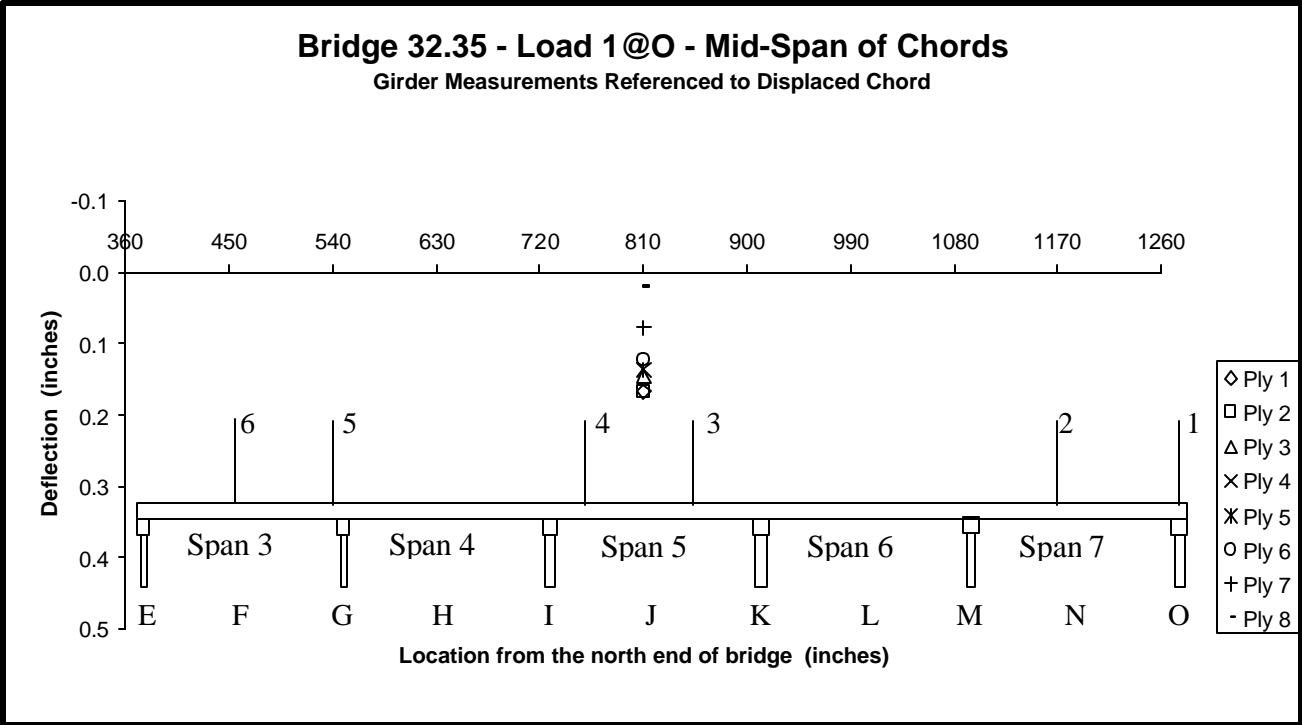


Figure 6-13. Transducer deflection measurements referenced to the displaced chord for Bridge 32.35 for load 1-2@O.

The individual ply displacements in Span 5 were of a consistent magnitude. The displacement recorded in Span 6 was 0.0327 inches downward. All other displacement measurements in Span 6 were upward, with a minimum of 0.0019 inches and a maximum of 0.0222 inches. The mean of all measurements in Span 6 was 0.006 inches upward.

The next load case in the sequence is 1@J. Deflection effects were expected to be near maximum since the effects of that 67.4 kip load are not countered by any nearby loads. The load from the second axle falls close to the adjacent support and Axles 3 and 4 are several spans away. Figure 6-9 presents the measured displacements of piles. It was expected that Span 5 would experience downward displacement and Span 6 would experience some uplift. The data verified this behavior. In Span 5, the mean displacement was 0.095 inches downward. In Span 6 the mean was 0.013 inches upward.

For Span 5 and load 1@J, the relationship between deflection and relative E was examined. The deflections were 0.1322, 0.1415, 0.1088, 0.1013, 0.0661, 0.0678 and 0.0495 (all inches) for Piles 1, 2, 3, 5, 6, 7 and 8, with corresponding E values of 2.09×10^6 , 1.80×10^6 , 2.00×10^6 , 1.83×10^6 , 2.12×10^6 , 2.35×10^6 and 2.19×10^6 (all psi), respectively. There is a general relationship apparent, which suggests the piles with the higher stiffness values tend to deflect less.

Load case 1-2@K is similar to 1-2@I except that the train has progressed a full span length along the bridge so the front truck of the locomotive is centered over the cap at K. Figure 6-10 presents the data for this load case. Only data for Span 6 exists. The mean mid-span displacement was 0.073 inches, downward. As expected, this was similar in magnitude to the displacement Span 5 due to load 1-2@I, which was a similar loading. The only anomaly was that Ply 2 displaced about twice that of the other piles. The measured stiffness values of the piles are listed in Span 6 of Figure 3-2(b). There is no noticeable relationship between E value and the relatively high displacement measured for Ply 2. There was no other information available to assess what caused this ply to displace more than the others.

The next sequential load case is 1@L. This load case is similar to 1@J and again displacement effects were expected to be near maximum in Span 6. Furthermore, the load on Span 5 from Axle 2 was close to the cap between Spans 5 and 6. While this may cause some downward displacement effects, the

effects from the first axle on Span 6 would be more significant in creating some upward motion. Figure 6-11 presents displacements of piles for this load condition. The displacement data indicate almost no displacement for Span 5, a mean of 0.007 inches downward. For Span 6, a mean displacement of 0.126 inches downward was observed. In Span 5, five of the seven monitored piles were observed to have small displacements downward while the two east most piles had small upward displacements. Since the magnitude of displacement is small for all piles, this could be the net effect of the load on Span 5 causing downward deflection and, the load on Span 6 causing uplift. Ply 2 exhibited a significant magnitude of displacement above its neighboring piles.

Load case 1-2@M is similar to 1-2@I and 1-2@K. The difference was the train had moved a full span length along the bridge past 1-2@K so the front truck of the locomotive was centered over the cap at M. Figure 6-12 presents the data from this load case. Data exists for Piles 1-4 of Span 5 and all piles in Span 6. The deflection was downward in Spans 4, 6 and 7. The deflection in Span 6 had a mean magnitude of 0.085 inches downward for Piles 1, 2, 3, 5, 6, 7 and 8. The downward displacement in this span was similar to the magnitude of responses of Span 5 as a result of 1-2@I and of Span 6 due to 1-2@K. The mean downward displacements in Span 5 under load 1-2@I and in Span 6 under load [1-2@K](#) were 0.104 inches and 0.073 inches, respectively. No loads were on Span 5, thus it was expected that the continuity would cause upward motion as an effect of the loads in Spans 4, 6, and 7. For load 1-2@M, Span 5 did not show the expected upward motion, but rather a slight downward displacement mean of 0.033 inches. The lack of upward motion may be the effect a gap closing between one or more piles.

The last load case of the sequence presented is 1@O. The first axle of the locomotive was positioned over the support at O, i.e. at the cap between Spans 7 and 8. Axle loads also were on Spans 3, 5 and 7. Only the responses of the piles in Span 5 were recorded. Figure 6-13 presents the displacements of the individual piles. The mean response was 0.120 inches downward. The deflection of individual piles exhibits much the same pattern as for load case 1@J. The primary difference (within Span 5) between loadings 1@J and 1@O was that 1@J had one 67.4 kip load mid-span while 1@O had two 67.4

kip loads near the quarter span locations. While load 1@O produced more deflection, the relative behavior of the piles appears similar.

Of the six load cases considered, load case 1@O appears to apply the greatest load effect to Span 5 and load case 1@L appears to apply the greatest load effect to Span 6. Deflection results are consistent with this. Load case 1@O produced the greatest deflections in the piles in Span 5 with a mean displacement of 0.120 inches. Load case 1@L produced the greatest deflections in Span 6 with a mean displacement of 0.126 inches for a 15-foot span. The latter value corresponds to $L/1429$.

Comparison of Analytical and Measured Results

As described in Chapter 5, several analytical factors were used to assist in evaluating whether or not the test data were reasonable. The models used were single span, continuous and semi-continuous models. The beam cross-sectional properties were summed for all eight piles. For the single span and the continuous model, the average E for each span of the bridge was used. For the semi-continuous model, the E values of piles with matching support and continuity conditions were averaged.

Deflection predictions from three of the models were used to evaluate the results of load cases, 1@J, 1-2@K, 1@L and 1@O. The responses for loadings 1-2@I and 1-2@M were considered to be similar to 1-2@K thus these are not presented directly, but the data was used to augment the 1-2@K data. Table 6-2 presents a comparison of the measured displacements to those calculated by the analytical models. Values are listed for Spans 3 to 7. The field test results listed are mean mid-span displacement measurements for all piles in a given span and were referenced to the displaced chord.

Load case 1@J (see Fig. 6-3) positioned the first axle of the locomotive mid-span of span 5 and this is the primary of load position interest. The continuous, semi-continuous and single span models predicted 0.0739, 0.1001 and 0.1661(all inches), respectively, all downward.

The continuous model predicted the lowest magnitude of displacement, 0.0739 inches, in Span 5. The predicted displacements in Span 6 and Span 7 were 0.0254 inches upward and 0.0068 inches

downward respectively. Spans 3 and 4 were loaded near supports. The model predicts 0.0270 inches downward for Span 3 and 0.0154 inches upward for Span 4.

The semi-continuous model predicted 0.1001 inches of deflection in Span 5. In Spans 6 and 7, where no loads were applied, the calculated deflection was 0.0204 inches upward in Span 6 and 0.0042 inches downward in Span 7. These predictions were similar to the continuous model, just smaller magnitudes. In Span 4, the calculated deflection was 0.0009 inches upward. In Span 3, the calculated displacement was 0.0463 inches downward, an increase from the prediction by the continuous model.

Table 6-2. Comparison of load test measurements to predicted deflection of mid-span chord members for Bridge 32.35 using three frame analysis models.

Models	Predicted Mid-span Deflection				
	Span 3 (inches)	Span 4 (inches)	Span 5 (inches)	Span 6 (inches)	Span 7 (inches)
1@J					
Continuous Model	0.0270	-0.0154	0.0739	-0.0254	0.0068
Semi-continuous Model	0.0463	-0.0009	0.1001	-0.0204	0.0042
Single Span Model	0.1079	0.0492	0.1661	0.0000	0.0000
Mean Field Test Data			0.0953	-0.0132	
1-2@K					
Continuous Model	0.0773	-0.0294	0.0403	0.0340	-0.0103
Semi-continuous Model	0.1001	-0.0207	0.0642	0.0612	-0.0103
Single Span Model	0.1619	0.0166	0.1316	0.1316	0.0000
Mean Field Test Data				0.0730	
Mean Field Test Data*		0.0330	0.0850	0.0885	-0.0060
1@L					
Continuous Model	0.0368	0.0258	-0.0151	0.0738	-0.0253
Semi-continuous Model	0.0676	0.0458	-0.0008	0.1001	-0.0204
Single Span Model	0.1500	0.1079	0.0492	0.1661	0.0000
Mean Field Test Data			0.0070	0.1260	
1@O					
Continuous Model	0.0533	-0.0523	0.0991	-0.0684	0.0910
Semi-continuous Model	0.0609	-0.0398	0.1223	-0.0523	0.1087
Single Span Model	0.0847	0.0000	0.1852	0.0000	0.1568
Mean Field Test Data			0.1200		

* - Data combined from 1-2@I, 1-2@K and 1-2@M to illustrate possible responses in spans 4 and 7.

The single span model gave calculated displacements for Spans 3, 4, and 5 of 0.1079, 0.0492 and 0.1661 (all inches) downward respectively. The loads on Spans 3, 4, and 5 were each 67.4 kips, thus the difference in deflections are strictly a function of load position and mean E of each span. Spans 6 and 7 were not loaded thus there were no displacements.

As with other loadings, the models only provide a range of expected performance. For load 1@J, the field measurements were a downward displacement of 0.0953 inches at mid-span of Span 5 and an upward displacement of 0.0132 inches at mid-span of Span 6. The field results were less than the maximum predicted displacement, (single span model) of 0.1661 inches downward for Span 5 and zero for Span 6. The measured value also was greater than the predicted displacements of 0.0739 inches downward for Span 5 and 0.0254 inches upward for Span 6 from the fully continuous model. As expected, the test data were between rational extremes. The remaining model, the semi-continuous model, was formulated to attempt a representation of the half-lapped chord behavior. The comparable predicted displacements of the semi-continuous model were 0.1001 inches downward in Span 5 and 0.0204 inches upward in Span 6. The measured displacement of 0.0953 inches in Span 5 was slightly less than the 0.1001 inches predicted by the semi-continuous model. The measured displacement of 0.0132 inches upward in Span 6 also was slightly less than the 0.0204 inches predicted by the semi-continuous model.

Load position 1-2@K (see Fig. 6-4) included significant loads in Spans 3, 5 and 6. The predicted mid-span displacement values of Span 5 for the continuous, semi-continuous and single span models were 0.0340, 0.0612 and 0.1316 (all inches) downward, respectively. The measured displacement was 0.0730 inches downward. The measured value is within the extremes of the continuous and single span models and compares reasonably to the semi-continuous model prediction of 0.0612 inches.

Load position 1@L (see Fig. 6-5) applied significant loads to Spans 3, 4 and 6. The predicted mid-span displacement values of Span 5 for the continuous, semi-continuous and single span models were 0.0151, 0.0008, upward and 0.0492 (all inches) downward, respectively. The measured displacement was 0.0070 inches downward. The measured value is within the extremes of the continuous and single span

models and compares closest to the semi-continuous model prediction. The predicted mid-span displacement values of Span 6 for the continuous, semi-continuous and single span models were 0.0738, 0.1001 and 0.1661 (all inches) downward, respectively. The measured displacement of 0.1260 inches downward was slightly more than the semi-continuous model and within the extremes of the other two models.

Load position 1@O (see Fig. 6-7) included significant loads in Spans 3, 5, and 7. The predicted mid-span displacement values of Span 5 for the continuous, semi-continuous and single span models were 0.0991, 0.1223 and 0.1852 (all inches) downward, respectively. The measured displacement of 0.1200 inches downward compares closely to the semi-continuous model prediction and is in the limits of the other two models.

In the preceding cases, the mid span test data fell within the expected range of predictions made by the models and compared favorably to the semi-continuous model predictions. This outcome indicates that displacements measured for Bridge 32.35 are reasonable values.

Deflections Relative to the Ground

Measured Results

Ground referenced chord displacement data collected on Bridge 32.35 are presented here. The primary data were measured with displacement transducers placed between the ground and mid-span of various chord piles. As a back up, selective optical measurements of the displacement of the outer piles were also recorded, but are not addressed in this report. Details can be found in the thesis of Robinson (Robinson et al. 1998). The ply displacement data were collected to provide a representation of the performance of the bridge and for comparison to the ply displacements measured relative to the displaced chord. The main interest was to evaluate if the substructure introduced significant motion into the overall displacement of the bridge.

Ground referenced displacement data for six load cases (shown earlier in Figs. 6-2 to 6-7), as recorded from the transducers, are listed in Table 6-3. The load positions are the same as used in Table 6-

2 in which displacements measured relative to the displaced chord were tabulated. The loadings and mid span displacements measured relative to the ground for Spans 4 through 7 are presented in graphical form in Figures 6-14 to 6-19. Because of limited instrumentation, it was decided to measure the response of Piles 2 and 7, one ply in from the outer piles of the chords.

Table 6-3. Displacement transducer data collected at mid-span of selected chord piles for loads 1-2@I, 1@J, 1-2@K, 1@L, 1-2@M, and 1@O. All displacements in inches referenced from the ground.

Distance from north end of bridge	Span 4	Span 5	Span 6	Span 7
	Mid-Span (inches)	Mid-Span (inches)	Mid-Span (inches)	Mid-Span (inches)
	630	810	990	1170
Load 1-2@I				
Ply 2	0.1653	0.1292	0.0287	-0.0154
Ply 7		0.1146		-0.0062
Mean	0.165	0.122	0.029	-0.011
Load 1@J				
Ply 2	0.0911	0.1935	0.0275	-0.0211
Ply 4		0.1954		
Ply 7		0.1582	0.0223	-0.0075
Mean	0.091	0.182	0.025	-0.014
Load 1-2@K				
Ply 2		0.1657		-0.0362
Ply 7		0.1314		0.0045
Mean		0.149		-0.016
Load 1@L				
Ply 2	0.1021	0.0882	0.2555	-0.0397
Ply 4		0.1355		
Ply 7		0.079	0.2808	0.0127
Mean	0.102	0.101	0.268	-0.013
Load 1-2@M				
Ply 2	0.2163	0.0349	0.2098	0.0827
Ply 7		0.0448		0.1751
Mean	0.2160	0.0400	0.2100	0.1290
Load 1@O				
Ply 2	0.0545		0.0576	
Ply 4		0.2428		
Ply 7			0.0626	
Mean	0.0540	0.2430	0.0600	

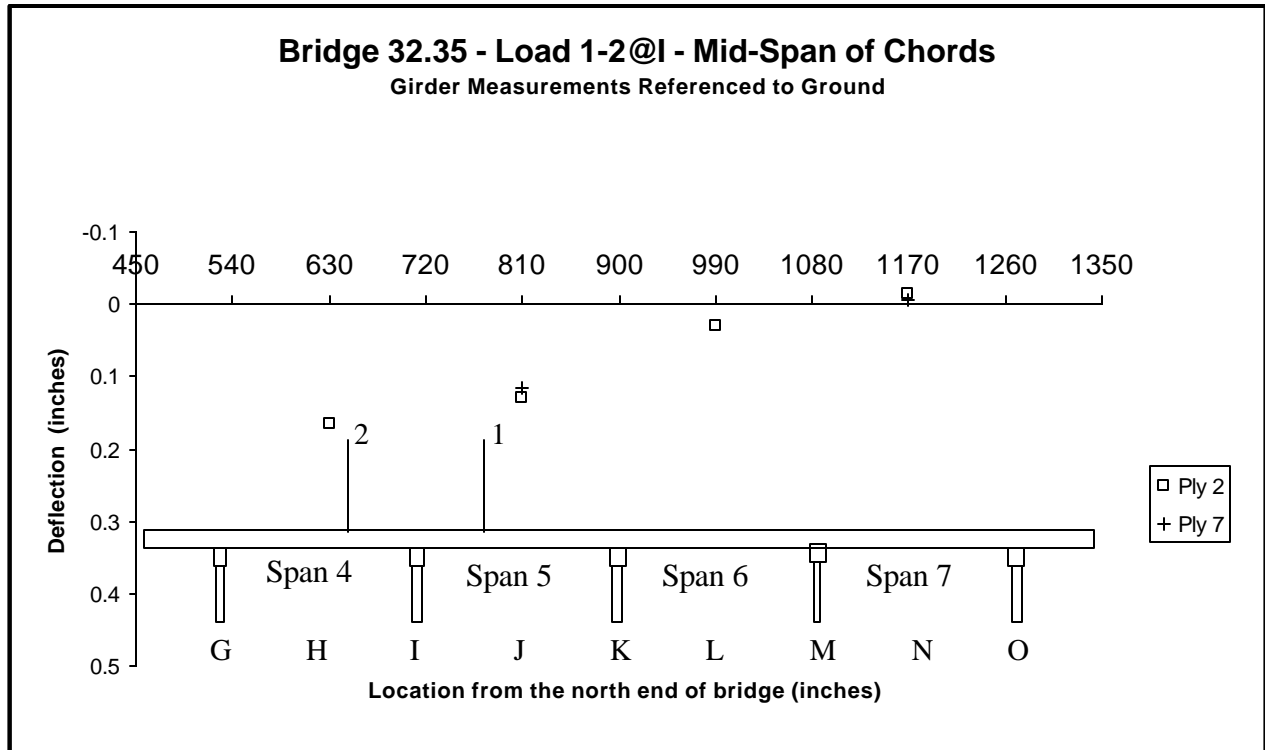


Figure 6-14. Transducer deflection measurements referenced to the ground for Bridge 32.35 for load 1-2@I.

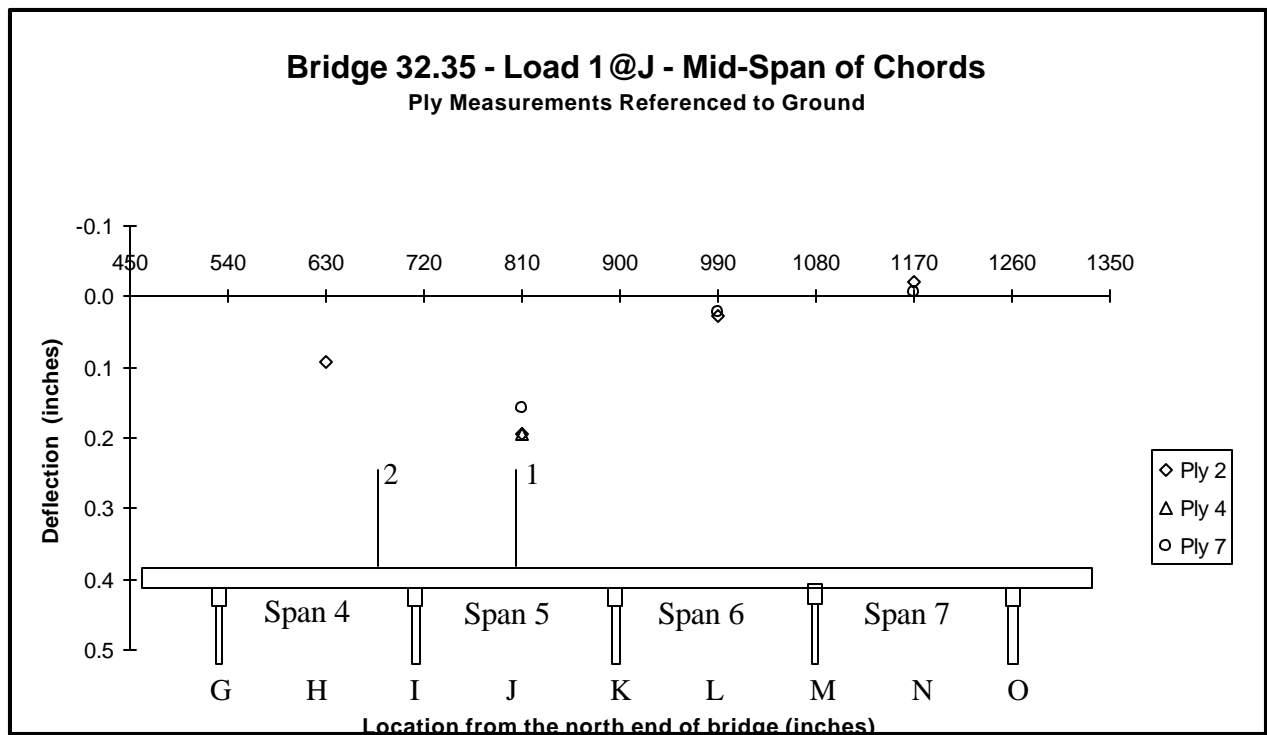


Figure 6-15. Transducer deflection measurements referenced to the ground for Bridge 32.35 for load 1-2@J.

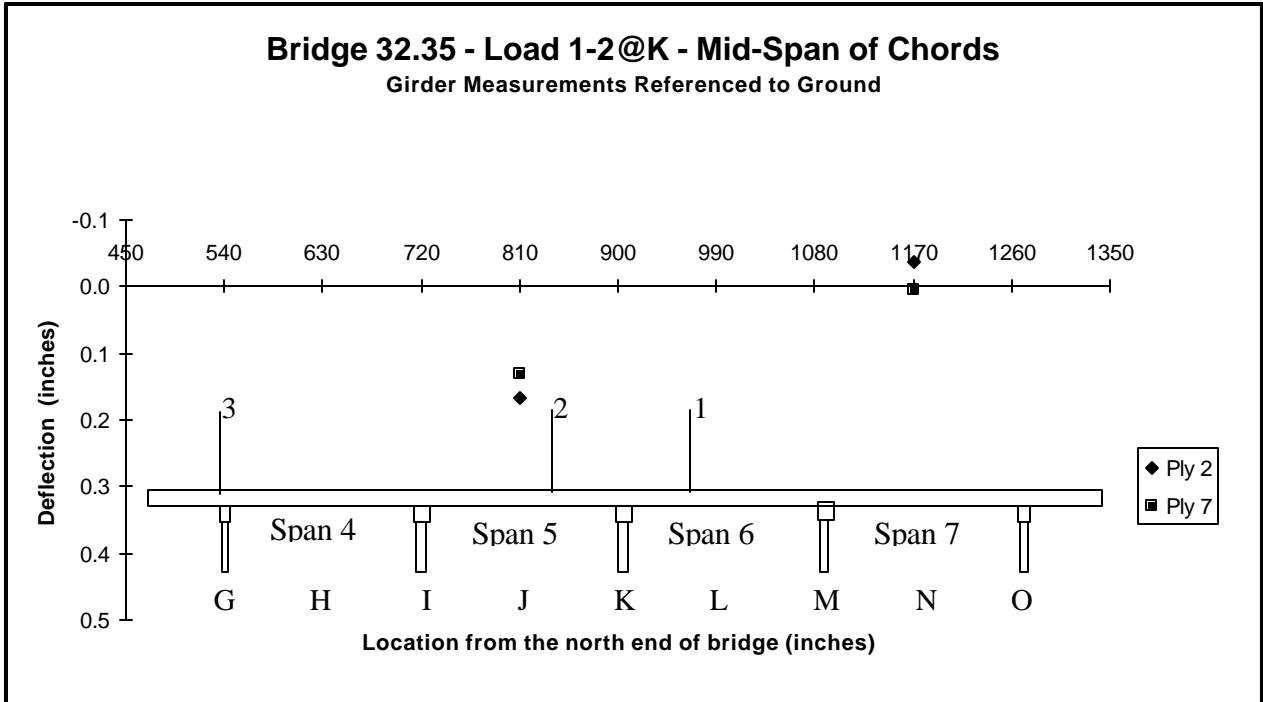


Figure 6-16. Transducer deflection measurements referenced to the ground for Bridge 32.35 for load 1-2@K.

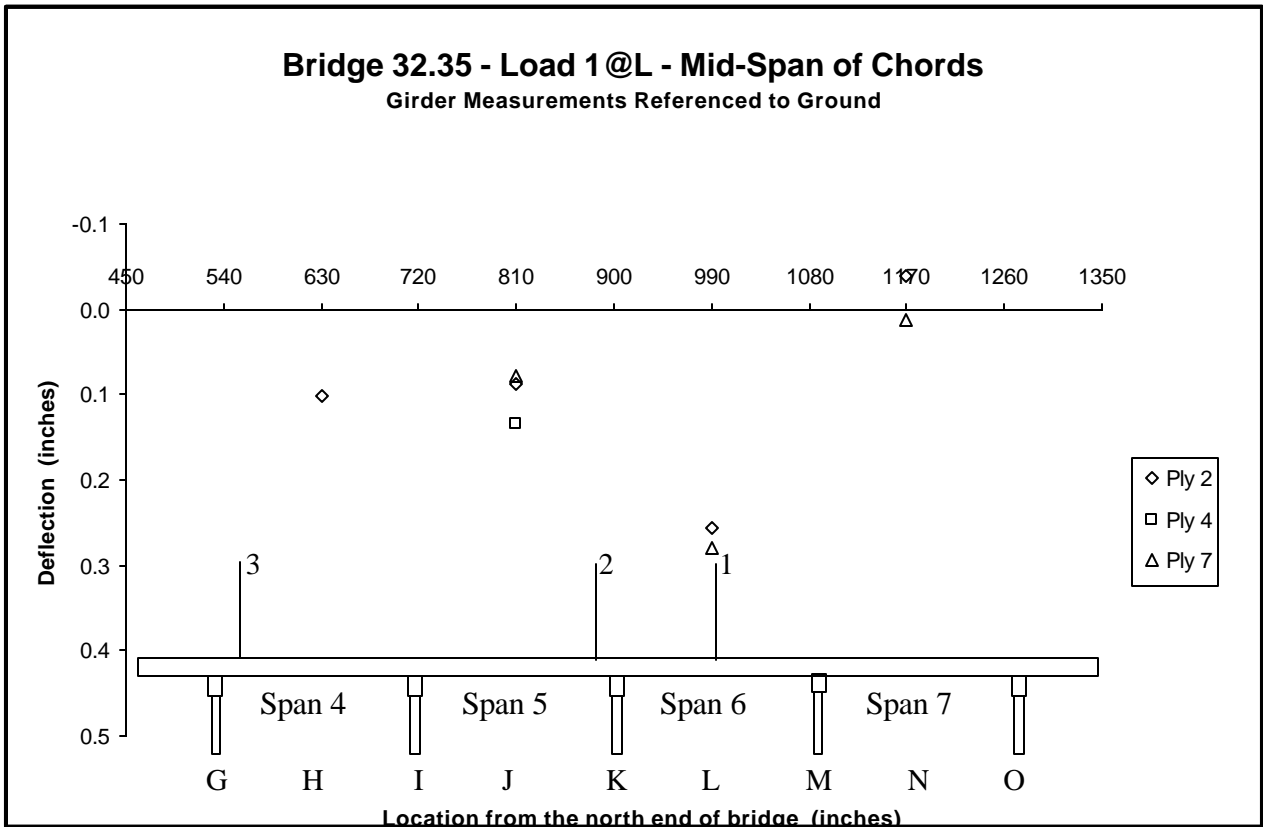


Figure 6-17. Transducer deflection measurements referenced to the ground for Bridge 32.35 for load 1-2@L.

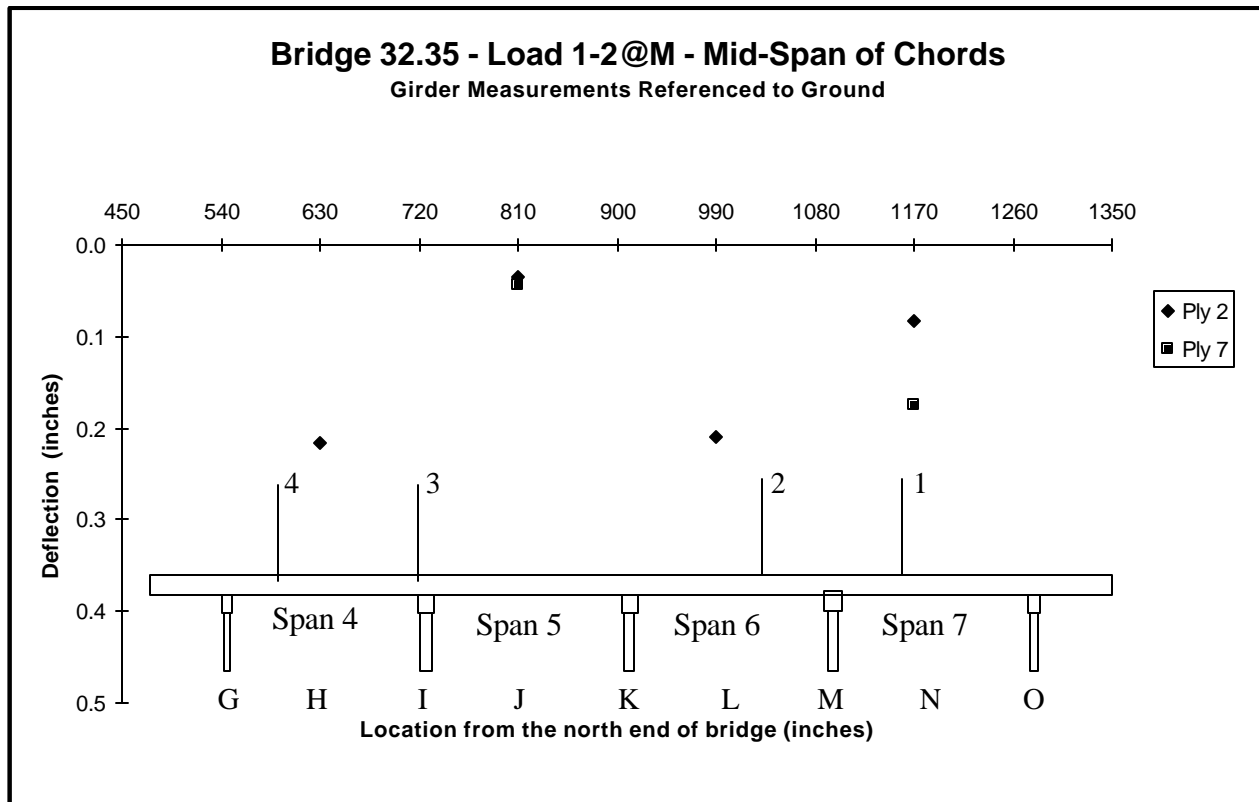


Figure 6-18. Transducer deflection measurements referenced to the ground for Bridge 32.35 for load 1-2@M.

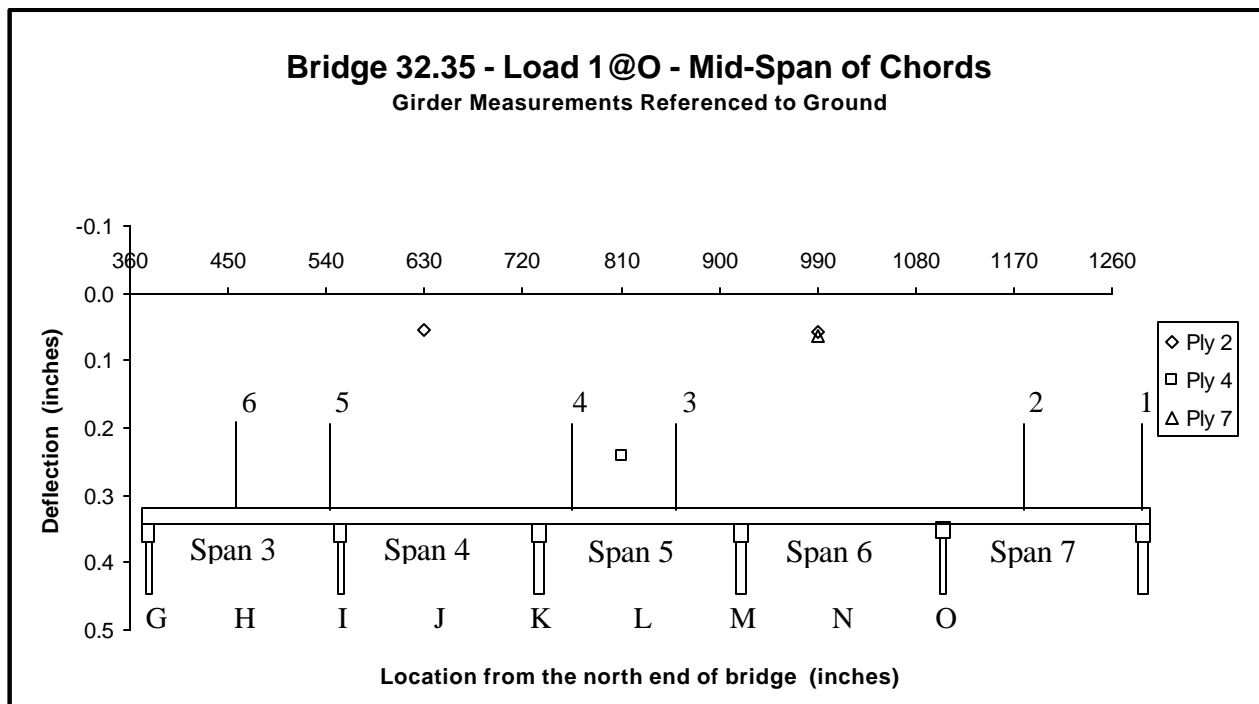


Figure 6-19. Transducer deflection measurements referenced to the ground for Bridge 32.35 for load 1-2@O.

The first load position presented is 1-2@I (see Fig. 6-14). The mean mid span displacements for Spans 4 through 7 were 0.165 inches, 0.122 inches, 0.029 inches, all downward, and 0.011 inches upward respectively. Displacement downward was expected in Spans 4 and 5 due to the loads on those spans. Uplift was expected in Span 6 because of the load in Span 5. The test data indicate Spans 4 and 5 displaced as expected. Span 6 had a downward displacement that was not expected, while Span 7 experienced a slight uplift. The net downward displacement of the mid-span location of Span 6 may have been caused by support motion in one or both supporting piers.

The next load position examined is [1@J](#) (see Fig. 6-15). Mean measured displacements for Spans 4 through 7 were 0.091 inches, 0.182 inches, 0.025 inches, all downward, and 0.014 inches upward, respectively. Downward displacement was expected in Spans 4 and 5 due to the loads on those spans, except less displacement was expected in Span 4 versus Span 5 due to the load shift. Uplift was expected in Span 6 because of the load in Span 5. The test data support expectations for Spans 4 and 5. Uplift was measured in Span 7 with little displacement measured in Span 6. From Table 6-3, the mean displacements for Spans 5 and 6 referenced to the ground were 0.182 inches and 0.025 inches, respectively, both downward. From Table 6-2, the corresponding mean displacements referenced to the displaced chord were 0.095 inches downward and 0.013 inches upward, respectively. The mean ground reference data exhibited greater magnitudes downward than the data referenced to the displaced chord, indicating the presence of support motion.

For load position 1-2@K (see Fig. 6-16) the mean displacements for Spans 5 and 7 for the piles monitored were 0.149 inches downward and 0.016 inches upward, respectively. Because of the load applied to Span 5, its downward displacement was expected. No ground referenced data existed for Spans 4 and 6. Span 7 had a mean displacement upward of 0.016 inches resulting from a 0.036 inches displacement upward in Ply 2 and a displacement downward of 0.005 inches by Ply 7. Considering the probable presence of support motion and gap closing, the small downward displacement measurement of Ply 7 seems probable.

For load position 1@L (see Fig. 6-17) the mean displacements for Spans 4 through 7 were 0.102 inches, 0.101 inches, 0.268 inches, all downward, and 0.013 inches upward, respectively. The displacements seem appropriate in direction assuming some amount of support movement occurred.

For load position 1-2@M (see Fig. 6-18) the mean displacements for Spans 4 through 7 were 0.216, 0.040, 0.210 and 0.129 inches respectively, all downward. Spans 4, 6, and 7 all have similar loads, thus the deflection magnitude appears consistent with the positioning of the loads and assuming some continuity. Because Span 5 had no load and loads existed on spans either side, uplift was expected. The small downward measured displacement again points toward the presence of support movement.

For load 1@O (see Fig. 6-19) the data indicate downward deflection at mid-span of Span 5, as expected, and slight displacements downward in Spans 4 and 6. Assuming even partial continuity, the absence of uplift in spans 4 and 6 suggests support motion occurred in at least two of the three supports of the spans instrumented.

Four of the load cases had measurement locations that matched for the data measured relative to displaced chord and relative to the ground. Two of the load cases did not have comparable data locations because several load positions were included in one sequence, but bypassed in another. Comparable data were available for Piles 2 and 7 of Spans 5 and 6. The individual displacements referenced to displaced chord and ground reference, plus the magnitude and percentage of increase from data referenced to the displaced chord are presented in Table 6-4. As an example, consider the displacement of Ply 2 for load case 1@J. The displacements relative to the displaced chord were 0.1415 and 0.0264 inches for Spans 5 and 6, respectively. The ground referenced displacements for the same spans were 0.1935 and 0.0275 inches, respectively. Span 5 had an increase of 0.0520 inches, or 36.8 percent, due to effects of the support system. Span 6 had an increase of 0.0011 inches, or 4.1 percent.

Table 6-4. Comparison of displaced chord and ground referenced deflection measurements by both magnitude and percentage difference.

	Displaced Chord		Ground Reference		Amount Increase from Displaced Chord		% Increase from Displaced Chord	
	Span 5 Mid-Span	Span 6 Mid-Span	Span 5 Mid-Span	Span 6 Mid-Span	Span 5 Mid-Span	Span 6 Mid-Span	Span 5 Mid-Span	Span 6 Mid-Span
Distance from north End of bridge	(ins.) 810	(ins.) 990	(ins.) 810	(ins.) 990	(ins.) 810	(ins.) 990	(ins.) 810	(ins.) 990
Load 1-2@I								
Ply 2	0.1131	0.0327	0.1292	0.0287	0.0161	-0.0040	14.3	-12.2
Load 1@J								
Ply 2	0.1415	0.0264	0.1935	0.0275	0.0520	0.0011	36.8	4.1
Ply 7	0.0678	-0.0202	0.1582	0.0223	0.0904	0.0425	133.4	-210.5
Load 1@L								
Ply 2	0.0405	0.2768	0.0882	0.2555	0.0478	-0.0213	118.1	-7.7
Ply 7	-0.0089	0.1084	0.0790	0.2808	0.0879	0.1725	-986.3	159.1
Load 1-2@M								
Ply 2	0.0161	0.2139	0.0349	0.2098	0.0188	-0.0041	116.5	-1.9
				Ply 2	Minimum	0.0161	-0.0213	
					Mean	0.0337	-0.0071	
					Maximum	0.0520	0.0011	
				Ply 7	Minimum	0.0879	0.0425	
					Mean	0.0892	0.1075	
					Maximum	0.0904	0.1725	

By considering the other data in Table 6-4, it is evident that, although being small in magnitude, effects of the support system can be significant in terms of the percentage of total deflection. In some cases the direction of movement was actually reversed. In the last two columns of Table 6-4, indication of percent increase from the displaced chord is often a large percentage and even negative in some instances. The cases of large percentage changes are associated with small deflections.

The negative percentage values indicate that the perceived direction of motion changed when the displacement reference changed from the displaced chord to the ground. For example, in Table 6-4, for Load 1@L considering Ply 7 in Span 5, the deflection referenced to the displaced chord indicated 0.0089 inches upward while the deflection referenced to the ground indicated 0.0790 inches downward. The

ground-referenced measurement indicates an additional 0.0879 inches downward compared to the displaced chord-referenced measurement. The percent increase was shown as -986 percent, negative because the change was opposite the original deflections and a large percentage because the additional increase downward was quite large in comparison to the original displacement referenced to the displaced chord. An interpretation of this is that while Ply 7 experienced a small uplift of 0.0089 inches in Span 5 due to load 1@L, the ply also experienced support motion resulting in a downward motion of 0.0879 inches. The combined effect of these two displacements, if viewed from a ground referenced observation, would be perceived as a downward motion of 0.0790 inches. This illustrates that the support motion did have an effect on this observed deflection.

Another assessment of this data can be made by identification of the load conditions causing the maximum apparent downward support motions. The maximums for Ply 2 of each span both occurred due to the load case 1@J. The maximums for Ply 7 occurred due to 1@J in Span 5 and 1@L in Span 6. Load case 1@J heavily loads Span 5, while 1@L heavily loads Span 6. The support in common for these two load cases is the support at K, possibly indicating that there was some particularly significant motion in that support.

Observations from the Static Load Testing

The deflection measurements from the static load testing program quantified the deflection response of selected members of the bridge to applied loads. The deflection data measured were referenced either to the displaced chord or to the ground or both. Deflection relative to the displaced chord provided response information comparable to structural modeling without effects of the support conditions. These data placed Bridge 32.35 closest to the modeling assumption of the semi-continuous chord model. These data also confirm that each of the piles in a single chord, or in a single span, respond differently to load, indicating that the piles are each carrying different load shares. The ground reference data provided information concerning the overall behavior of the bridge. By comparing the ground-referenced data to the displaced chord data, it is clear that there is motion in the supports of Bridge 32.35.

CHAPTER 7

RAMP LOADING TEST RESULTS

Ramp Loading Tests

Ramp loading tests were performed on each of the three bridges as summarized in Table 7-1. Using the loading axle of the TLV car, a controlled ramp loading could be applied at selected positions on each bridge. The primary difference compared to the static loads is that at the zero load, the bridge is already in some initial load condition due to the weight of the train itself. To present the information in a usable form, the initial strain and deflection conditions were assigned zero values. Selected results of the ramp loading tests for Bridge 101 and Bridge 32.56 are described in the following sections.

Table 7-1. Summary of the number of load positions or train passes and associated number of data records for each bridge.

Test Type		Bridge 32.35	Bridge 32.56	Bridge 101
Static	Positions:	76	34	108
	Data sets:	122	68	201
	Records:	1952	1088	3216
Ramp	Positions:	11	10	42
	Data sets:	116	84	307
	Records:	1856	1344	4912
Rolling	Positions:	4	2	2
	Data sets:	600	200	150
	Records:	1960	3200	2400

Bridge 101 Results

Three loadings were selected to illustrate the results of the ramp loading tests conducted on Bridge 101. These are positions 11@I, 11@F and 11@C, which are a sequence of positions as the TLV was moved from north to south across the bridge. In each case, the load was applied at mid-span of the particular span involved.

Figure 7-1 shows the instrumentation positions for ply deflection measurement. Because of limited clearance in the two end spans, data referenced to the displaced chord could only be taken in the

center span. The piles of both approach spans were instrumented for displacement referenced to the ground. Relative motion was measured between the piles and interior caps. The displacement of the caps relative to the ground was also measured.

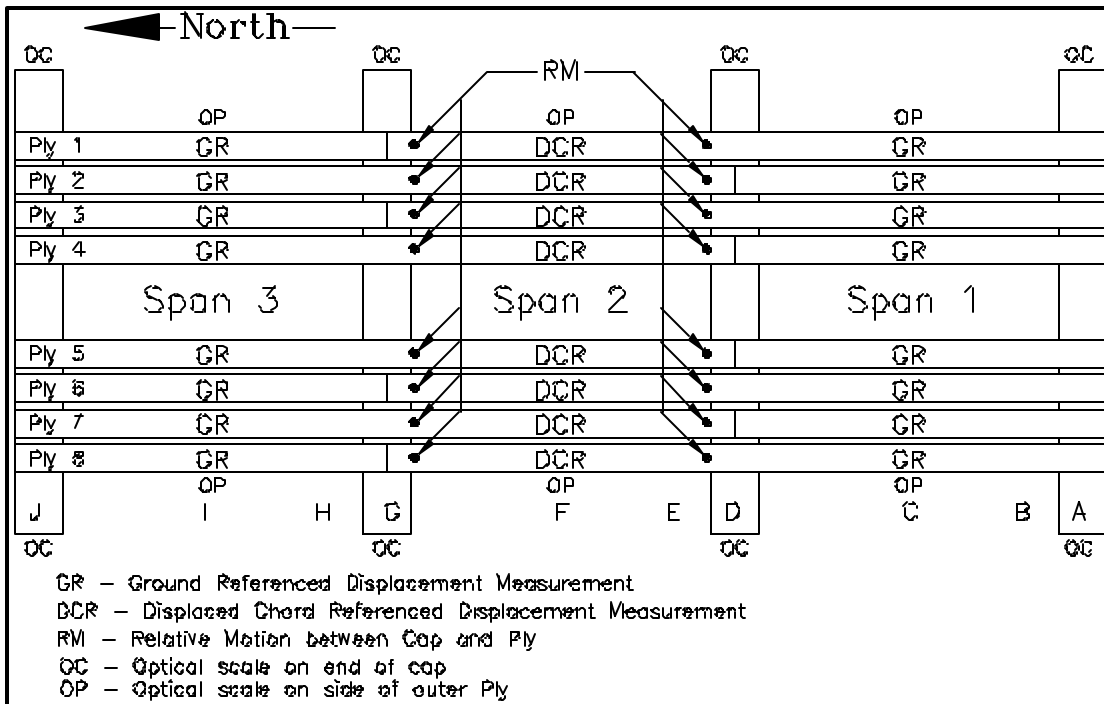


Figure 7-1. Locations of displacement instrumentation shown on plan view of Bridge 101.

The loadings 11@I, 11@F and 11@C are illustrated in Figures 7-2, 7-3 and 7-4, respectively. As the test load is applied by the TLV axle (lifting the car), the loads of the four other axles of the TLV are reduced. It was assumed that equal shares of load were removed from each of the four axles as load was applied to the loading axle. For this bridge, when the TLV load axle had no load, axles 9 and 10 were each applying 67.4 kips and axles 12 and 13 were each applying 69.675 kips. At the maximum load level for the test axle, 78 kips, axles 9 and 10 were each applying 47.9 kips and axles 12 and 13 were each applying 50.175 kips. The TLV axle loads for intermediate loadings were presented earlier in Table 5-3. Recognizing that the bridge had an existing load condition at the 0 kip load, data reflects the difference in displacement that occurred between the 0 to 78 kips load levels.

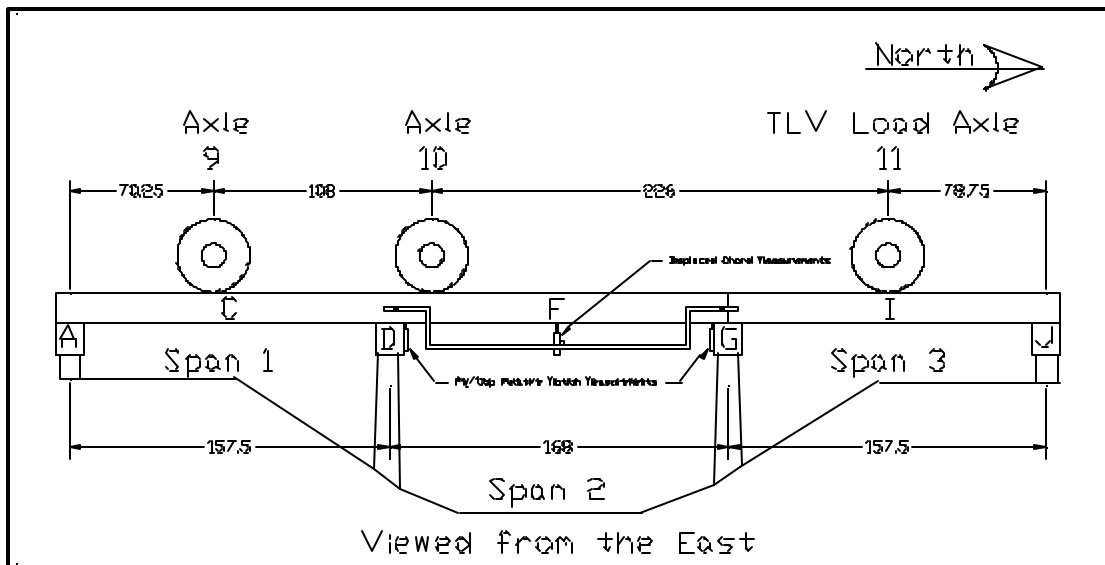


Figure 7-2. Load positioning on Bridge 101 for 11@I. Dimensions are in inches.

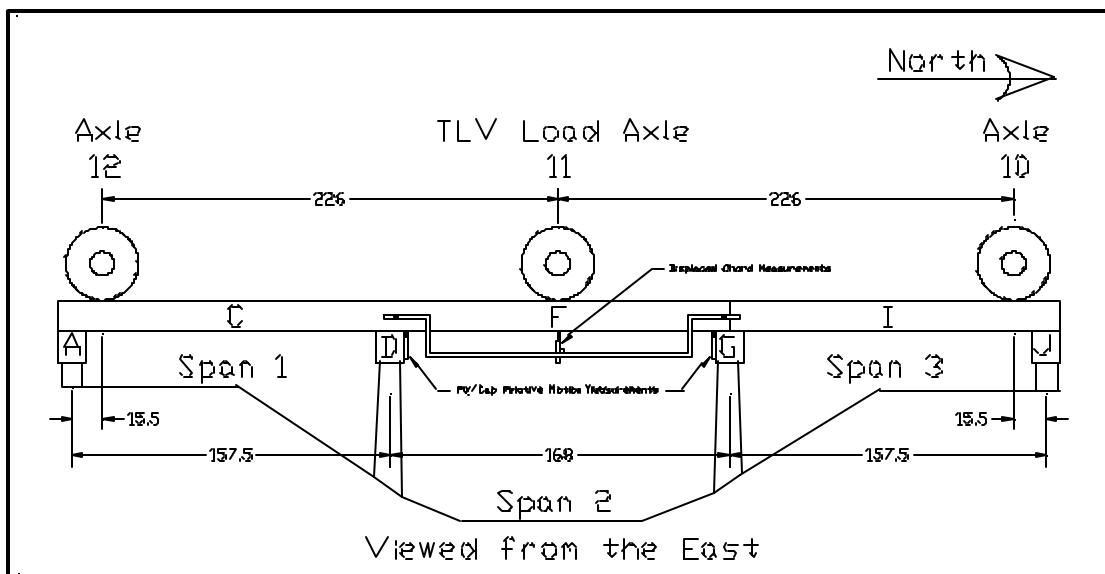


Figure 7-3. Load positioning on Bridge 101 for 11@F. Dimensions are in inches.

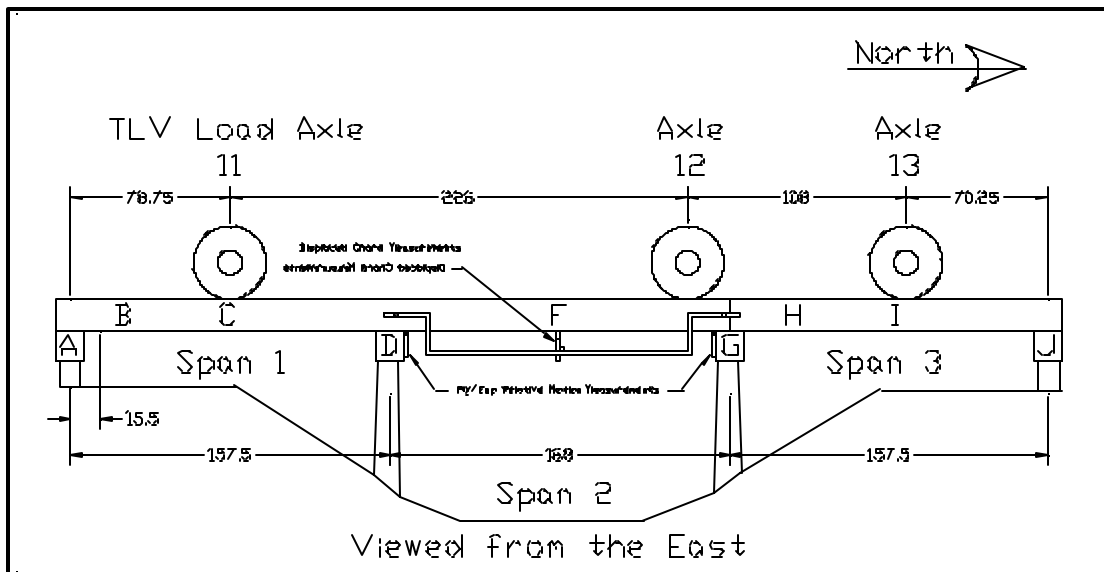


Figure 7-4. Load positioning on Bridge 101 for 11@C. Dimensions are in inches.

Linear Behavior of Transducer and Extensometer Measurements

A plan view of instrumentation positioning is given in Figure 7-5. The numerical measured data are provided in Table 7-2 and shown graphically in several subsequent figures. Deflection data were taken at 0, 30, 60, 78, 60, 30, and 0 kips load levels, as applied by the TLV load axle as a ramp load. The values in Table 7-2 are measured relative to the displaced chord. The data are adjusted so the deflection and stress values are relative to the initial readings taken for the set. These initial values were for the TLV load axle at zero. Some initial loads from the TLV axles 10 and 12 acted near the abutments of the outer spans.

Data for load location [11@F](#) from one of several load sequences (coded US1-2 in the reports (Gutkowski et al 1998 and Gutkowski et al 1999) and M.S. thesis (Robinson 1998)) were used to illustrate the linearity of behavior. From the data in Table 7-2, it is evident that the recorded deflections and strain varied slightly between the loading and unloading phases. For example, consider LVDT 3. The deflection value at the initial 0 kip level was assigned zero, but at the final 0 kip level, there was a slight residual deflection of 0.0004 inches. In fact, there is some difference at each load level. While increasing the load from zero to 30, 60 and 72 kips the measured deflections were 0.0723, 0.1387, and

0.1785 inches, respectively. While decreasing the load from 72 kips to 60, 30 and zero kips the corresponding deflection measurements were 0.1467, 0.0816, and 0.0004 inches, respectively.

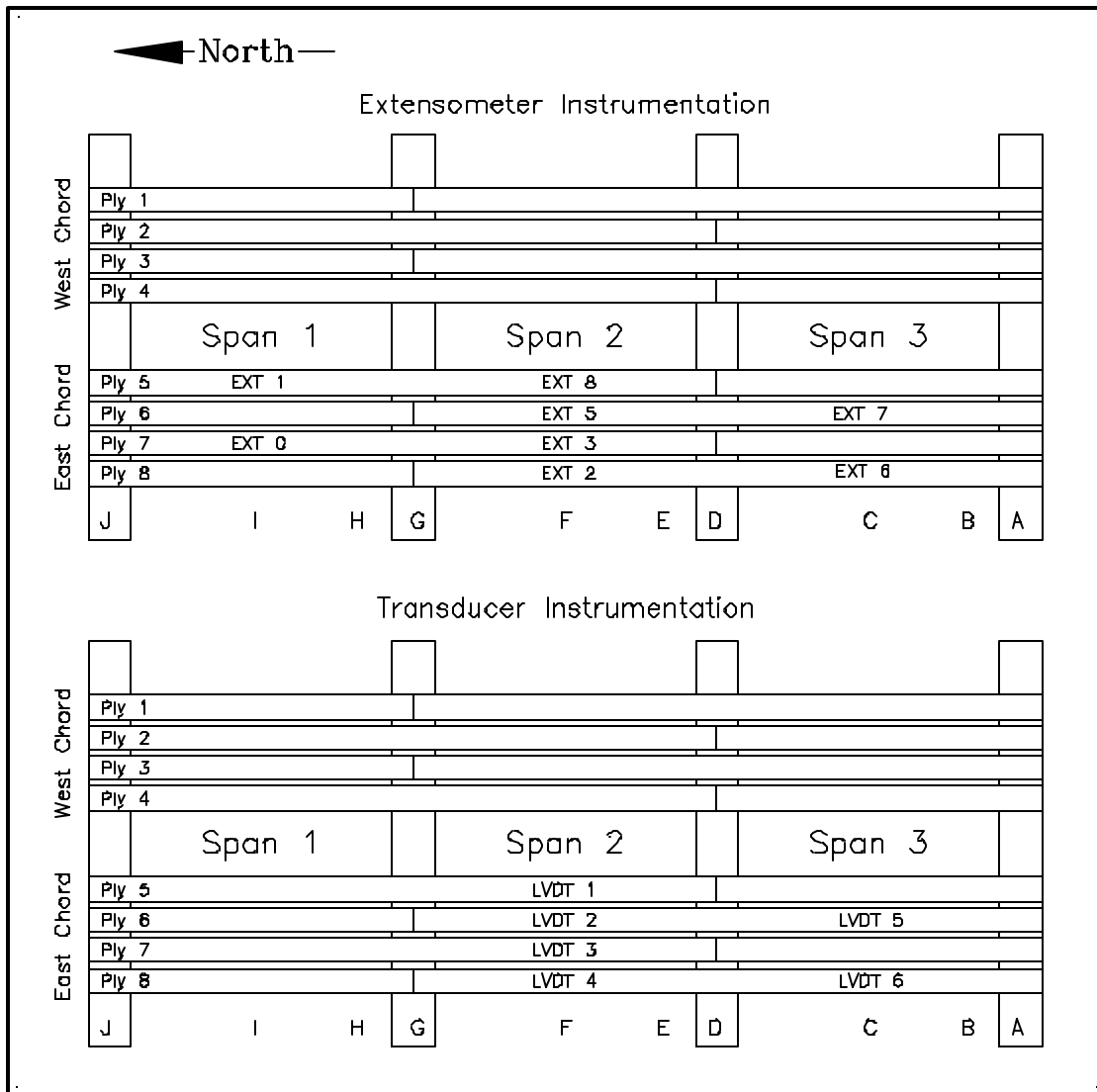


Figure 7-5. Extensometer and displacement transducer locations for test sequence US1-2, Bridge 101.

The increases were 0.0004, 0.0093, and 0.008 inches for the 0, 30 and 60 kips load levels, respectively. The presence of residual deflection after loading is typical and characteristic of timber structures. Gaps, connector looseness and material yield all contribute to the deflection, creep and recovery behavior of a timber structure.

Table 7-2. Deflection and strain data for Bridge 101, Instrumentation Position US1-2, 11@F ramp loading from the TLV load axle.

Deflection										
Load	Time	LVDT	LVDT	LVDT	LVDT	LVDT	LVDT			
(kips)	(sec)	1	2	3	4	5	6			
		(inches)	(inches)	(inches)	(inches)	(inches)	(inches)			
0	0	0.0000	0.0000	0.0000	0.0000	0.0000	0.0000			
30	102	0.0893	0.0322	0.0723	0.0492	0.0135	0.0260			
60	121	0.1562	0.0830	0.1387	0.1038	0.0112	0.0253			
78	148	0.1946	0.1166	0.1785	0.1397	0.0194	0.0196			
60	187	0.1622	0.0874	0.1467	0.1099	0.0275	0.0269			
30	207	0.0981	0.0327	0.0816	0.0566	0.0303	0.0345			
0	260	-0.0025	-0.0069	0.0004	0.0000	0.0106	0.0165			
Strain										
Load	Time	EXT	EXT	EXT	EXT	EXT	EXT	EXT	EXT	EXT
(kips)	(sec)	0	1	2	3	5	6	7	8	9
		(in/inx10 ⁶)	(in/inx10 ⁶)	(in/inx10 ⁶)	(in/inx10 ⁶)	(in/inx10 ⁶)	(in/inx10 ⁶)	(in/inx10 ⁶)	(in/inx10 ⁶)	(in/inx10 ⁶)
0	0	0.0	0.0	0.0	0.0	0.0	0.0	0.0	0.0	0.0
30	102	-19.0	-69.8	146.7	324.4	119.2	-37.4	-22.3	381.3	151.6
60	121	-39.1	-127.0	327.6	570.7	310.1	-88.2	-57.3	634.2	214.6
78	148	-52.5	-161.0	446.5	707.2	429.1	-120.0	-80.5	773.8	237.6
60	187	-38.3	-136.6	342.6	593.3	315.1	-84.7	-54.6	653.8	221.7
30	207	-18.1	-88.3	164.3	354.9	112.7	-32.4	-16.1	407.1	176.6
0	260	-8.7	-23.7	8.6	23.3	-13.1	1.2	3.6	17.9	46.6

Figure 7-6 shows the plotted load-deflection relationship for each of the four piles of the east chord at mid-span. These deflections were referenced to the displaced chord measurements. Several observations are apparent.

First, the load-deflection relationship generally is linear in all four piles. As the applied load was increased to 0, 30, 60, and 78 kips and then decreased to 60, 30, and 0 kips incrementally, the deflection change for each chord ply generally was proportional to the load. The deflection of the piles also indicates that alternating pairs exhibit similar behavior. This effect could be due to the continuity of the pairs of chord piles over the adjacent spans. On the bridge, Piles 1 and 3 are continuous over the middle and north spans of the bridge. From Figure 7-6, these piles had the least magnitudes of deflection for each load level measured. Further, the loads were of similar magnitude. Piles 2 and 4 were continuous over the middle and south spans of the bridge. These chord members also exhibited similar behavior, but at slightly higher magnitudes of deflection compared to piles 1 and 3. In this bridge there were no tie rods through the piles of a chord at the mid-spans.

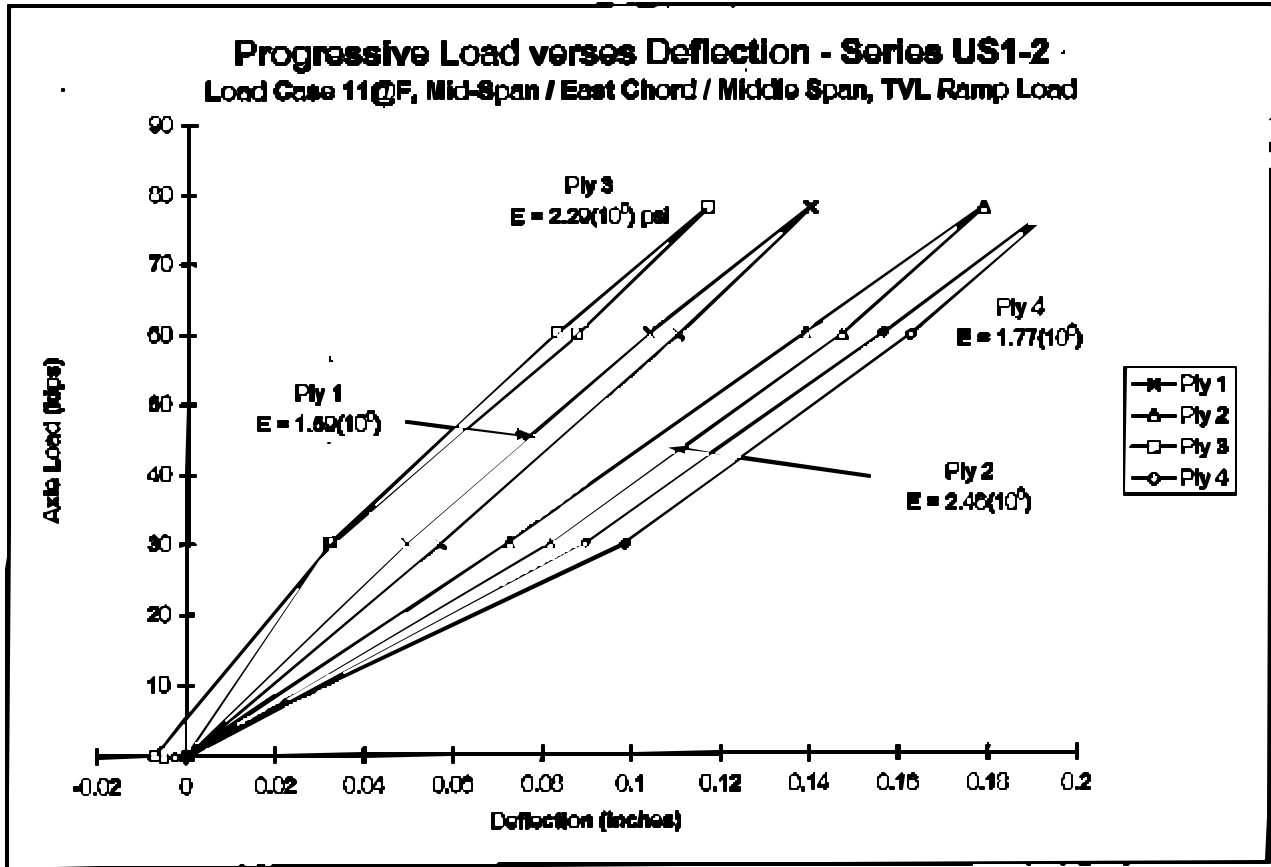


Figure 7-6. Load-deflection relationship for Bridge 101, US1-2, load 11@F, Piles 1 thru 4.

Another observation is that the load deflection relationships of all four piles generally are linear from 30 kips to 78 kips, but the initial load-deflection relationship from zero to 30 kips is somewhat non-linear. This effect is attributed to the initial closing of gaps and lack of initial adequate bearing surfaces supporting a member tested in bending. Residual displacement and recovery from many previous service loads could be a factor, too.

Figure 7-7 shows the load-strain relationship for each of the eight extensometers mounted on the bottom, horizontal surface of piles of the east chord. Extensometers 2, 3, 5, and 8 were mounted on Piles 1, 2, 3, and 4 of the east chord at mid-span of the center span respectively. Extensometers 0 and 1 were mounted on Piles 2 and 4 of that chord on the south span. Extensometers 6 and 7 were mounted on Piles 1 and 3 of that chord on the north span. Positive strain values indicate tensile strain on the bottom surface

of the beams. The plotted results show that the change in strain in the piles essentially was linear from 30 to 78 kips. A small degree of non-linearity occurred from 0 to 30 kips. This effect is very consistent with what was observed in the displacement transducer data. Also, comparing Piles 1 to 4 in Span 2 with the displacement data of Figure 7-6, it is noted that the order of magnitude, increasing from Ply 3 to Ply 1 to Ply 2 and finally Ply 4, is the same. This behavior tends to indicate that the displacement and strain data are recording similar data relationships. Also, the strains were tensile in the middle span and compressive in the outer spans. This indicates a downward curvature in the middle span and upward curvature in the outer spans. As with the deflection data, the level of strains shows a similar consistent behavior between alternate piles.

The preceding results are summarized in Table 7-3 for the 78 kips load level. There appears to be a proportional relationship between increased deflection and increased strain relative to the zero load state. For example, at the 78 kip axle load, Ply 1 had a measured displacement of 0.140 inches and a corresponding strain of 0.000446 inches/inch. Dividing displacement by strain measurement, a ratio of 314 is obtained. The ratios are 314, 252, 273, and 252 for Piles 1, 2, 3, and 4, respectively. There is a reasonable consistency shown between the deflection measurements and the strain measurements.

Table 7-3. Summary of Deflection and Strain measurements on the east chord of Bridge 101 while experiencing a load of 78 kips during 11@F loading. Instrumentation data set US2-1.

Measurements at Mid-span of Center Span	Deflection (inches)	Strain (in/inx10 ⁶)
Chord Ply 1	0.140	446
Chord Ply 2	0.178	707
Chord Ply 3	0.117	429
Chord Ply 4	0.195	774
Average Piles 1 & 3	0.128	438
Average Piles 2 & 4	0.187	740
Measurements at mid-span of north span	Deflection (inches)	Strain (in/inx10 ⁶)
Chord Ply 1	0.0194	-120.0
Chord Ply 3	0.0196	-80.5
Measurements at mid-span of south span	Deflection (inches)	Strain (in/inx10 ⁶)
Chord Ply 2	No measurement	-52.5
Chord Ply 4	No measurement	-160.9

Positive deflection is downward. Positive stress is tensile stress.

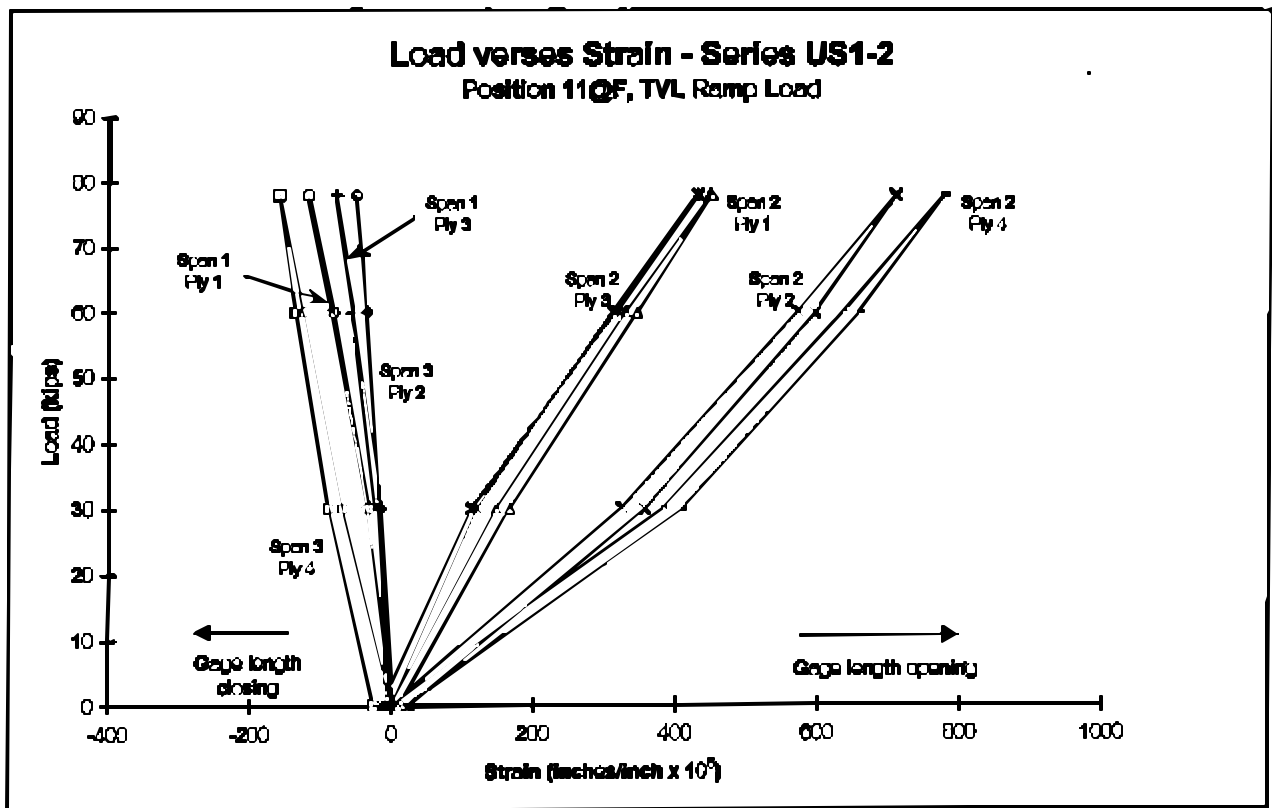


Figure 7-7. Load-Strain relationship for Bridge 101, US1-2, load 11@F, eight extensometers.

Deflections Relative to the Displaced Chord

Test Results

The displaced chord-referenced deflection data associated with load cases [11@I](#), 11@F, and 11@C are presented in Figures 7-8 to 7-10.

A positive (negative) magnitude is downward (upward) movement. As an example, the first displacement recorded for load 11@F for Ply 1 is 0.1423 inches. In this case, the load applied is directly over the point of measurement and the displacement is downward. For the same ply, loadings 11@I and 11@C produced displacement values of -0.0274 and -0.0193 inches. For both values, the displacement was upward, which coincides with the load being applied at mid-span of an adjacent span.

Figure 7-8 presents displacement as the TLV applied load to the north span (Span 1) of Bridge 101. The points in the figure above location F are mid-span displacements of individual piles. The displacements shown for the middle span are measurements relative to the displaced chord.

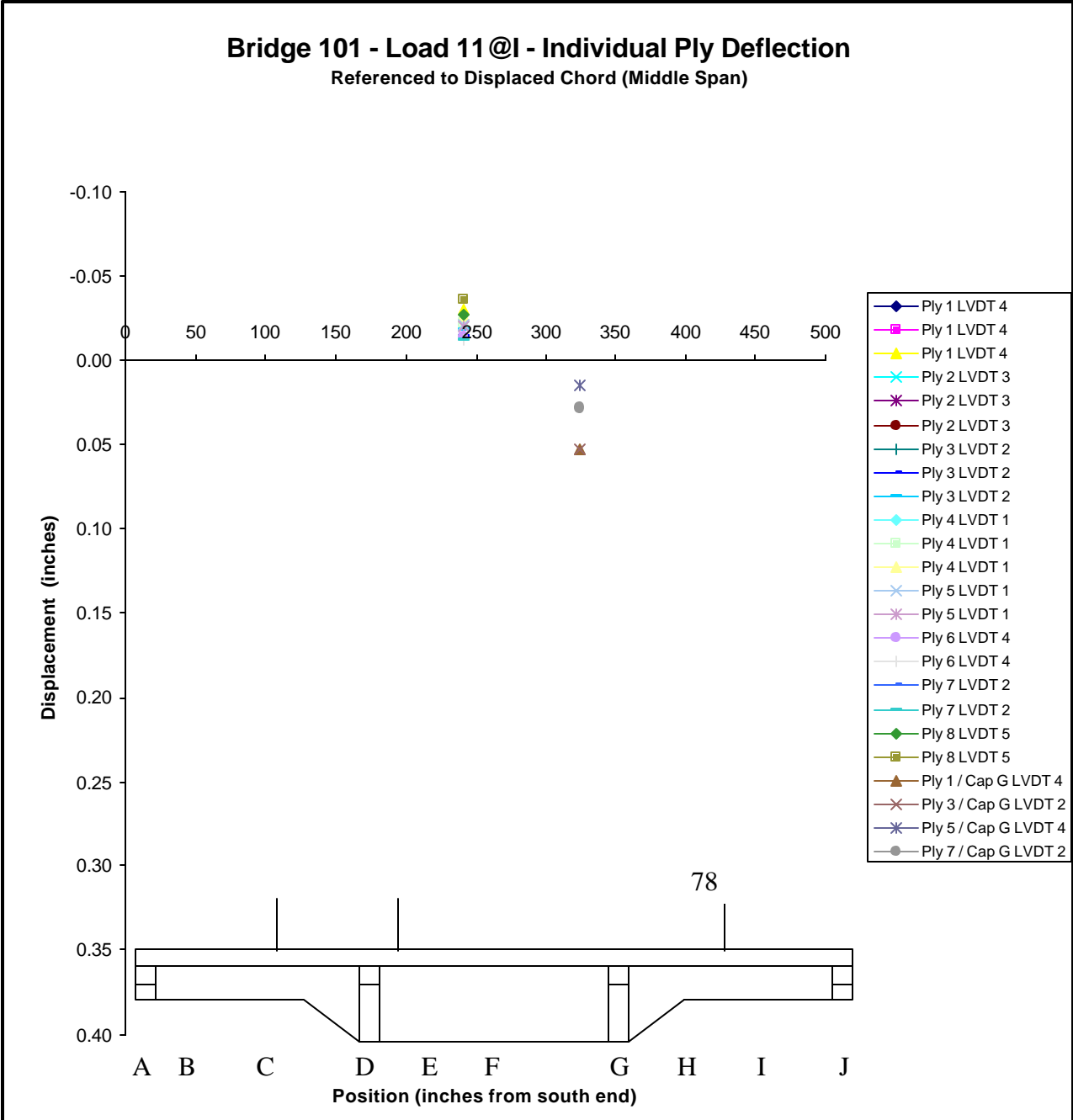


Figure 7-8. Transducer measurements for displacement referenced to the displaced chord and relative ply/cap motion for a 78 Kip load at 11@I on Bridge 101.

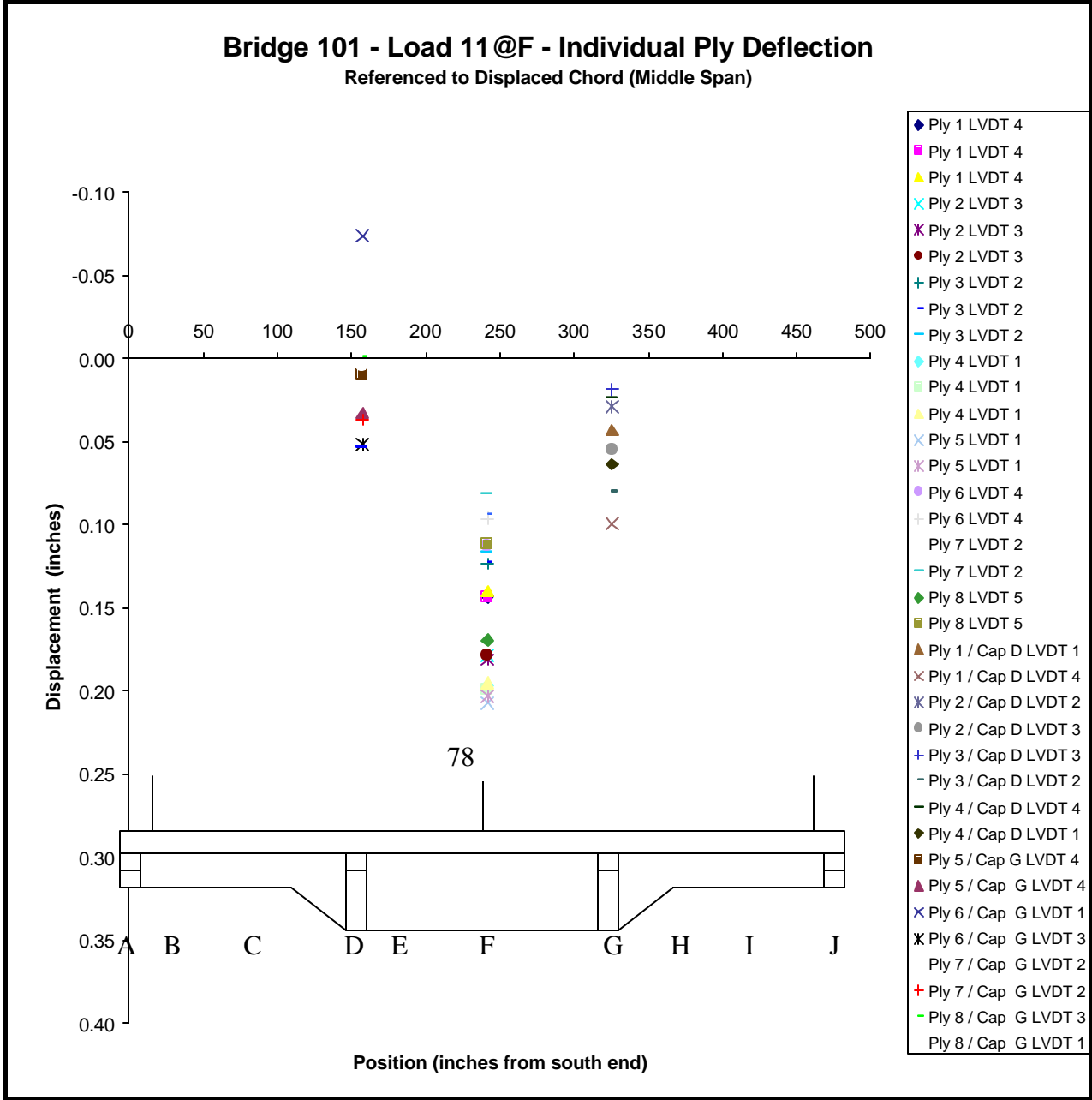


Figure 7-9. Transducer measurements for displacement referenced to the displaced chord and relative ply/cap motion for a 78 Kip load at 11@F on Bridge 101.

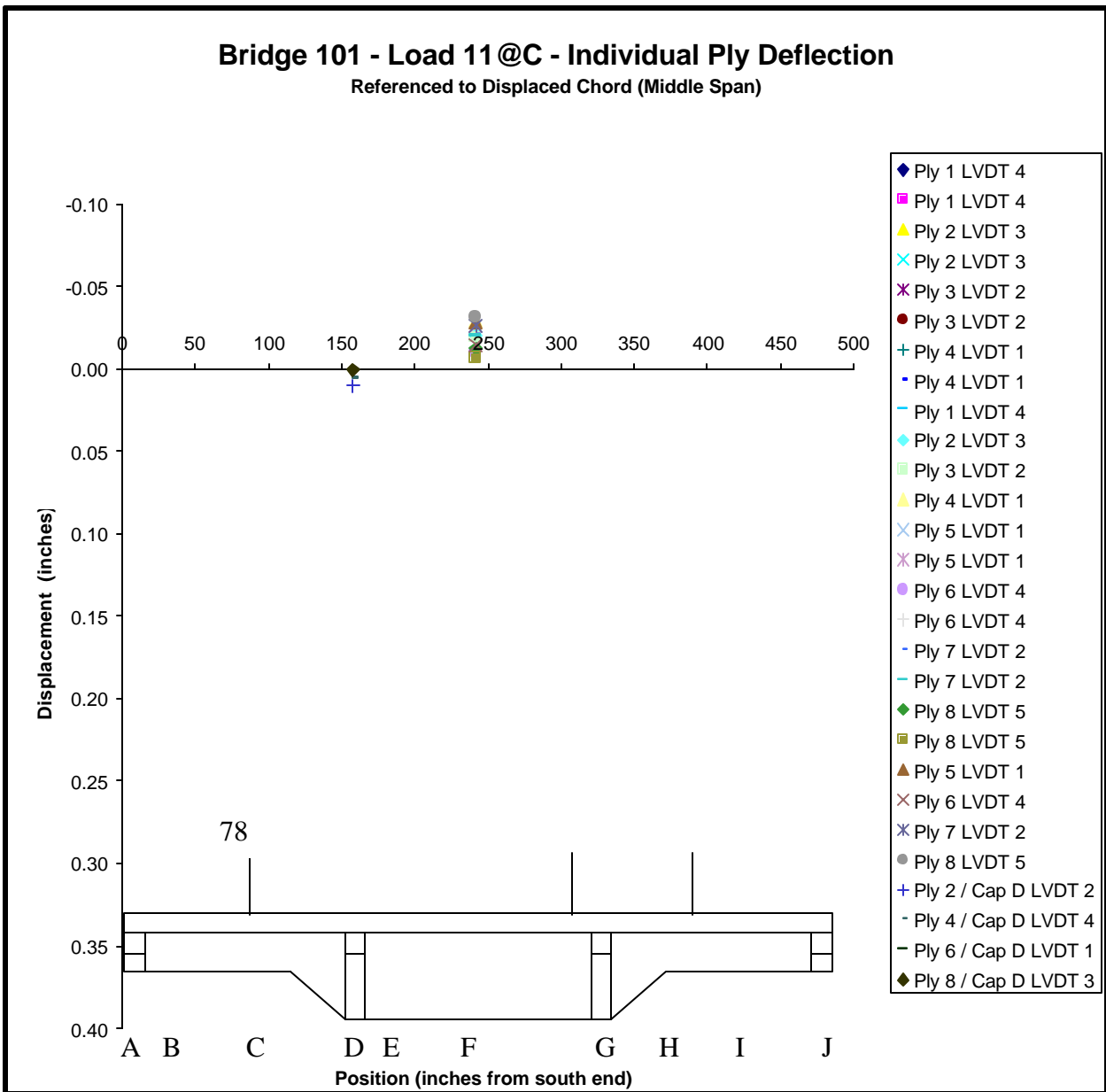


Figure 7-10. Transducer measurements for displacement referenced to the displaced chord and relative ply/cap motion for a 78 Kip load at 11@C on Bridge 101.

All measurements of individual piles indicated a reasonably consistent uplift in the middle span due to the 78 kip load applied at location I. From the actual recorded data (not included herein), the mean values were 0.023 inches for the east piles, 0.019 inches for the west piles, and 0.021 inches for all eight piles.

The relative displacements between Cap G and the chord piles also are presented in Figure 7-8. Measurements indicate that all the piles moved closer to the cap member due to the applied load, i.e. gap closure occurred. Piles 1 and 3 experienced 0.0524 and 0.0528 inches of closure, respectively. Piles 5 and 7 experienced 0.0151 and 0.0289 inches of closure, respectively.

While the closing motion is small, it would have a noticeable effect on ground referenced measurements of the center and north spans. For example, from the actual recorded data, Ply 1 indicated a mean mid-span upward of 0.027 inches for the center span while the support G indicated a closing motion of 0.0524 inches. No data exist for the support D for this load case. Assuming no closing at cap D, the net effect of the motion at G would be obtained by subtracting half the closing motion from the mid-span measured displacement. For this example, subtracting half the measured closing motion, 0.0524 inches, from the 0.027 inches upward motion measured by the displaced chord method would only have net displacement referenced to the ground of 0.0008 inches upward. Although small in magnitude, the effect of the ply-to-cap motion would make the 0.027 inches upward motion appear to be effectively no deflection when observed from the ground.

Figure 7-9 shows results for the load case 11@F, compiled from eight separate load applications. Data were available for both mid-span data referenced to the displaced chord of the center span and for the relative motion between the piles and caps supporting that span. The mean deflection referenced to the displaced chord of the piles was 0.150 inches downward. The east piles deflected 0.160 inches down (mean value, with a range from 0.121 to 0.197 inches), while the west piles deflected by 0.135 inches down (mean value, with a range from 0.088 to 0.205 inches). Downward displacement was expected as the load was applied at mid-span.

The average gap closing between the piles and Cap D was 0.007 inches and for Cap G was 0.059 inches. Except for two measurements, the data at Cap D, show a consistent closure motion for all piles. Ply 8 at Cap D has a small separating motion of 0.0004 inches, which is effectively no motion. On the other extreme, Ply 6 indicated that a gap of 0.074 inches opened between that ply and Cap D. If Ply 6 data were ignored, the gap closing average for Cap D would be about 0.018 inches.

From the actual recorded data, the mean mid-span displacements for Piles 1, 2, 3, and 4 for load 11@F, were 0.142, 0.179, 0.121 and 0.197 inches, respectively, for the east chord. For the west chord, Piles 5, 6, 7 and 8 had mid-span displacements of 0.205, 0.105, 0.088 and 0.141 inches respectively. The gap closure measurements between Piles 1 through 8 and Cap D were 0.0430, 0.0290, 0.0185, 0.0237, 0.0098, -0.0740, 0.0045 and -0.0004 inches, respectively. For Cap G, Piles 1 through 8 had 0.0993, 0.0549, 0.0799, 0.0636, 0.0327, 0.0515, 0.0367 and 0.0533 inches, respectively, of measured gap closure. For each ply, the net effect of the gap closure on the mid-span deflection can be calculated by adding half the sum of the gap closure measurements from Caps D and G.

For Ply 1, the gap closures were 0.0430 and 0.0993 inches. The net effect to the mid-span displacement is 0.071 inches. Adding the net effect to the mean mid-span displacement of 0.142 inches increases the displacement to 0.2134 inches. For Ply 1, gap closure is equivalent to 50 percent of the mid-span deflection. For Piles 2 through 8, the net gap closure effect increased the mid-span deflections to 0.2213, 0.1701, 0.2405, 0.2264, 0.0934, 0.1084 and 0.1670 inches, respectively. Considering these values, if the measurements were taken with a reference that included the gap closure effect, the displacement referenced to the displaced chord would be modified by the following percentages. For Ply 1, a 50 percent increase; for Ply 2, a 23 percent increase; for Ply 3, a 41 percent increase; for Ply 4, a 22 percent increase; for Ply 5, a 10 percent increase; for Ply 6, an 11 percent decrease; for Ply 7, a 24 percent increase; and for Ply 8, a 19 percent increase. This is only the effect of the closing of bearing surfaces, the motion of the caps on the pile supports is examined subsequently.

Figure 7-10 shows the displaced chord and ply-cap relative motion for the load case 11@C. This case is a mirror image of 11@I except that loads of Axles 12 and 13 of the TLV are slightly higher. The mean mid-span displacement of the piles measured relative to the displaced chord was 0.021 inches upward, with the east piles deflecting a mean of 0.023 inches upward while the west piles deflected a mean of 0.019 inches upward. This upward displacement was expected. The relative motion measured at Cap D was a small amount of closure. The mean motion was 0.004 inches. The behavior was similar to that observed in 11@I.

Comparison of Analytical Results to Field Measurements

Deflection predictions from the various analytical beam models were used to evaluate test results of load cases 11@I, 11@F, 11@C. Simply supported single span, continuous, semi-continuous and fixed end single span models were used. The single span (fixed end) model set the bound of greatest (least) expected deflection. For the single span, fixed end and the continuous model, the average E for each span of the bridge was used and the section properties were the sum of all eight piles. For the semi-continuous model, the E values of piles with matching support and continuity conditions were averaged. Support motion was assumed to be zero. Hence, field data used were displacements measured relative to the displaced chord.

The loads used in the modeling included the TLV load axle and the other axles supporting the TLV car (refer to Figs. 7-2 to 7-4 and Tables 5-1 and 5-3). The results presented from the modeling are the differences between the 0 kip displacements subtracted from the 78 kip displacements. As an example, for load case 11@F with no load applied by the TLV load axle, Axle 10 applied a 67.4 kip load and Axle 12 applied a 69.7 kip load. When the TLV load axle reached 78 kips, the loads on the Bridge 101 were 47.9 kips by Axle 10, 78 kips by Axle 11 and 50.2 kips by Axle 12. The modeling was done in one step by applying a 78 kip load downward by Axle 11 and 19.5 kip loads upward by Axles 10 and 12.

Table 7-4 presents the predicted mid-span deflections of four models and three load cases for Bridge 101. The bridge did not have the tie rods connecting the piles at mid-span for each chord. In the semi-continuous mode, low material property values were assigned to the link elements. The removal of the links allowed each system to respond to loads without forcing the systems to have the same mid-span deflections. Consequently, two values of displacement for each mid-span location are tabulated. The two systems are distinguished by the model description. The system noted by "Hinge at D" was half of the model system that had a continuous member over Spans 1 and 2 plus a single span element over Span 3. The point of discontinuity was over Cap D between Spans 2 and 3. The other system, noted "Hinge at G", was modeled with a single span member over Span 1 plus a continuous member over Spans 2 and 3.

Cap G was between Spans 1 and 2. Because of the continuity difference and differing ply E values, the curvature and displacements of the two systems were different. Because of this, two values for each mid-span location were predicted.

The load position of highest interest for this bridge was load 11@F (TLV load axle positioned mid-span in the center span). The displacement predicted is for the change in displacement from a zero to a load of 78 kips. Besides the 78 kip change at mid-span, each end span had an axle from the TLV car on it. The axles were near the outer abutments, but the load change on these axles was approximately 25 percent of that of the load axle and acting in the opposite direction of the TLV load.

The single span model predicted 0.0143 inches upward in Span 1, 0.2295 inches downward in Span 2 and 0.0137 inches upward in Span 3. The fixed end model predicted 0.0012 inches upward in the outer spans and 0.0574 inches downward in the center span. There was a minor difference in the upward displacement values due to differing E values for Spans 1 and 3, but not enough to affect magnitude by 0.0001 inch. The continuous model predicted 0.0588 inches upward, 0.1304 inches downward, and 0.0578 inches upward in Spans 1, 2, and 3, respectively. These fall between the upper and lower bounds.

The semi-continuous model predicted distinct values for two representative chord sub-systems. As presented in the Table 7-4 for position 11@F the first sub-system, (“Hinge at D”) predicted 0.0675 inches upward, 0.1597 inches downward and 0.0136 inches upward for Spans 1, 2 and 3, respectively. For this sub-system, Spans 1 and 2 were fully continuous while Span 3 was a single span, pin-supported member. Span 3 nearly had the same displacement as that predicted by the single span model, the difference is attributed to a slightly different mean E value for that member.

Table 7-4. Predicted deflection of mid-span chord members for Bridge 101 using four analytical models.

Models	Mid-span Deflection *		
	Span 1 (inches)	Span 2 (inches)	Span 3 (inches)
11@I			
Fixed Model	0.0491	-0.0022	-0.0114
Continuous Model	0.1376	-0.0456	-0.0163
Semi-continuous Model Hinge at D**	0.1414	-0.0719	-0.0459
Semi-continuous Model Hinge at G***	0.2032	0.0021	-0.0266
Single Span Model	0.1964	-0.0208	-0.0463
Displaced Chord Field Data		-0.021	
11@F			
Fixed Model	-0.0012	0.0574	-0.0012
Continuous Model	-0.0588	0.1304	-0.0578
Semi-continuous Model Hinge at D**	-0.0675	0.1597	-0.0136
Semi-continuous Model Hinge at G***	-0.0148	0.1748	-0.0710
Single Span Model	-0.0143	0.2295	-0.0137
Displaced Chord Field Data		0.150	
11@C			
Fixed Model	-0.0119	-0.0022	0.0471
Continuous Model	-0.0126	-0.0449	0.1332
Semi-continuous Model Hinge at D**	-0.0263	0.0022	0.1869
Semi-continuous Model Hinge at G***	-0.0499	-0.0766	0.1448
Single Span Model	-0.0483	-0.0208	0.1886
Displaced Chord Field Data		-0.021	

* Predicted by models or measured relative to the displaced chord.

** Hinge at D is for piles discontinuous over Cap D.

*** Hinge at G is for piles discontinuous over Cap G.

Note that the displacement of Span 1 (0.0675 inches upward) is significantly larger than the displacement of Span 3 (0.0136 inches upward). This is an effect of the continuity of the member between spans 1 and 2. The continuity reduced the predicted downward displacement mid-span from 0.2295 inches when modeled as a single span member to 0.1597 inches when modeled as a member continuous over Spans 1 and 2. The effect on Span 1 is an additional amount of upward motion as a

result of the load in Span 2. The deflection effect to Span 1 from the load applied to that span would be less than the simple span model deflection, 0.0143 inches upward. Most of the upward motion observed in Span 1, 0.0675 inches, was an effect of the load on Span 2.

The second sub-system presented (“Hinge at G”) predicted 0.0148 inches upward 0.1748 inches downward and 0.0710 inches upward for Spans 1, 2, and 3, respectively. For this system, Spans 2 and 3 were fully continuous while Span 1 was a single span, pin-supported member. Similar to the first system, Span 1 predicted a similar value to the deflection predicted by the single span model. Span 3 included the effects from the load in Span 2, thus the displacement was much higher than with the single span model.

Table 7-4 also presents mean measured displacement of piles in the rows headed by “Mean Field Data.” For load position 11@F, the mean field measurement was 0.150 inches of displacement downward for Span 2, the middle span of the bridge. The fixed (single span) model prediction was 0.0574 inches downward (0.2295 inches downward). The field measurement falls in this range. The continuous model predicted 0.1304 inches. The semi-continuous model with a hinge at D, meaning those piles discontinuous at Cap D between Spans 2 and 3, predicted a downward displacement of 0.1597 inches downward, which is close to the measured value. The semi-continuous model with a hinge at G, for the piles discontinuous over Cap G, predicted 0.1748 inches downward.

For load cases of 11@I and 11@C, the TLV load was applied mid-span of one of the outer spans. The other spans were loaded by the regular axles of the TLV, each reduced in load by 25 percent of the load applied by the TLV load axle. For load case 11@I, where the load was applied mid-span of Span 1, the deflection predictions for Span 1 ranged from 0.0491 inches to 0.2032 inches downward. In Span 3, an upward motion was predicted and ranged from 0.0463 inches by the single span model to 0.0114 inches by the fixed end model. In Span 2, the predictions were predominantly upward, 0.0022 inches to 0.0719 inches with one downward displacement of 0.0021 inches given by the semi-continuous model with a hinge at G.

For load case 11@C, where the load was applied mid-span of Span 3, the deflection predictions for Span 3 ranged from 0.0471 inches to 0.1886 inches downward. In Span 1, an upward motion was

predicted and ranged from 0.0119 inches for the fixed model to 0.0499 inches for one of the semi-continuous model systems. In Span 2, the predictions predominantly were upward, 0.0022 inches to 0.0766 inches (with one downward displacement of 0.0022 inches), given by the semi-continuous model with a hinge at D. The predicted results of 11@I and 11@C were consistent with each other, reflecting that the load arrangement of 11@I was the mirror image of 11@C. Slight variations in displacement predictions are due to differences in ply E values in each span. The mean measured deflections of the mid-span piles of Span 2 were 0.021 inches downward for both load positions 11@I and 11@C. For these two load positions, the measured data were within the bounds expected and the single span model gave the closest prediction.

Based on comparing the displacement predictions for Span 2 to the corresponding measured displacements, Bridge 101 performed within the range of the models, thus the data appears reasonable.

Displacements Relative to the Ground

Ground referenced transducer data for load conditions 11@I, 11@F and 11@C are presented graphically in Figures 7-11 to 7-13. The data in the columns headed “Span 1” and “Span 3” are mid-span displacements of individual piles referenced to the ground. A downward displacement is positive. The additional data are the ground-referenced displacements of the supporting caps. These data are presented in the columns headed “Cap D” or “Cap G.” Positive magnitude of a measurement indicates downward displacement of the bottom horizontal surface of the supporting caps. The figures also present both types of data. The ply displacement measurements always are presented mid-span of the center span while the relative motion between caps and piles always are presented over the caps.

For each load case, there exists ground referenced transducer data for Spans 1 and 3, but no measurement of displacement relative to the ground was made in the middle span. The displacement of the caps was measured at four positions on each cap, two locations under each stringer.

In Load case 11@I a 78 kip load was applied mid-span in Span 1. Spans 2 and 3 had loads applied from Axles 9 and 10 of the TLV, which were reducing as the load was applied. The recorded

tabulated ground reference data (not included here) and Figure 7-11 show this behavior. Span 1 has a downward deflection due to the 78 kip load applied at mid-span.

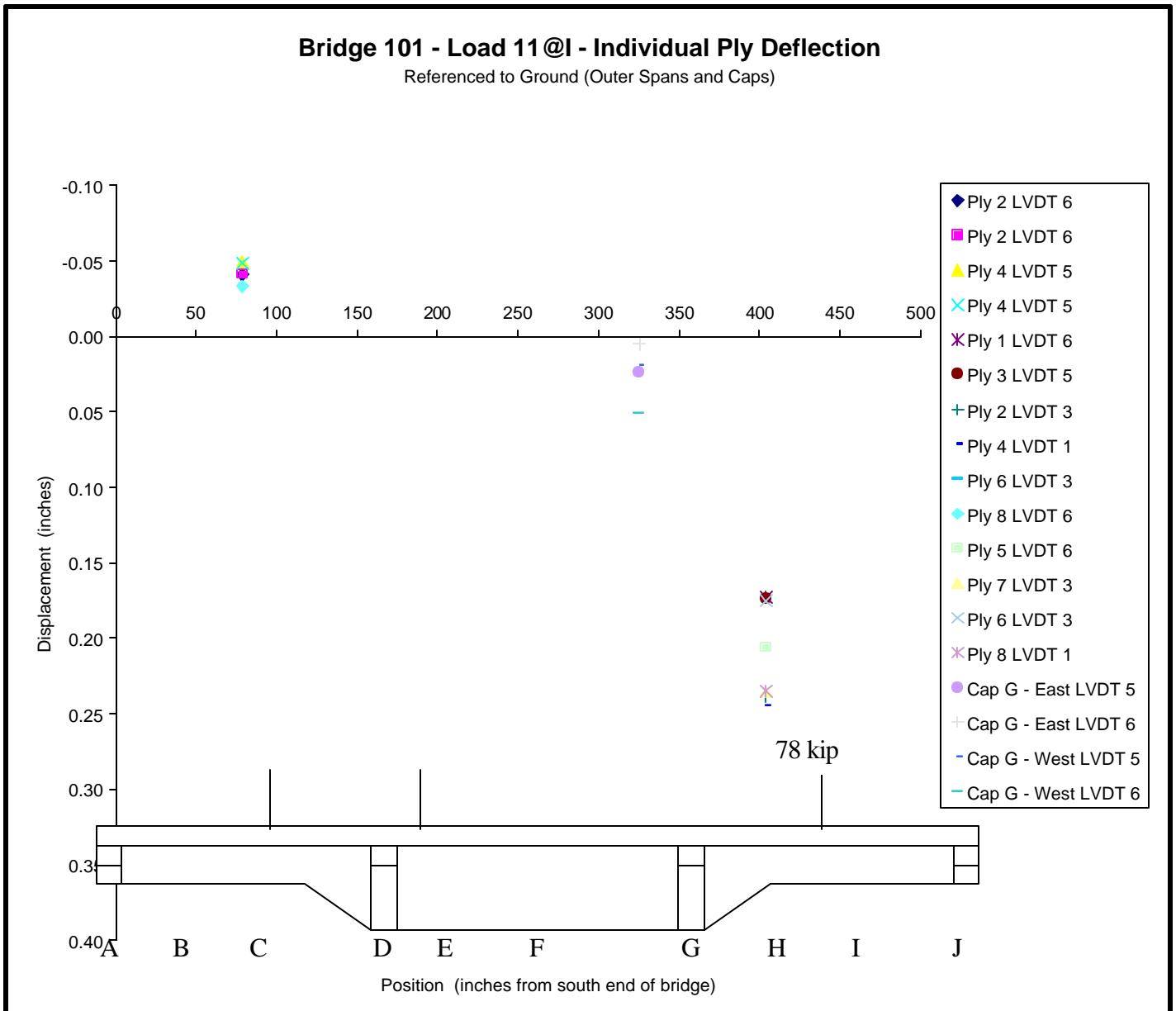


Figure 7-11. All electronic ground referenced data for Bridge 101, for 78 kip load at 11@I.

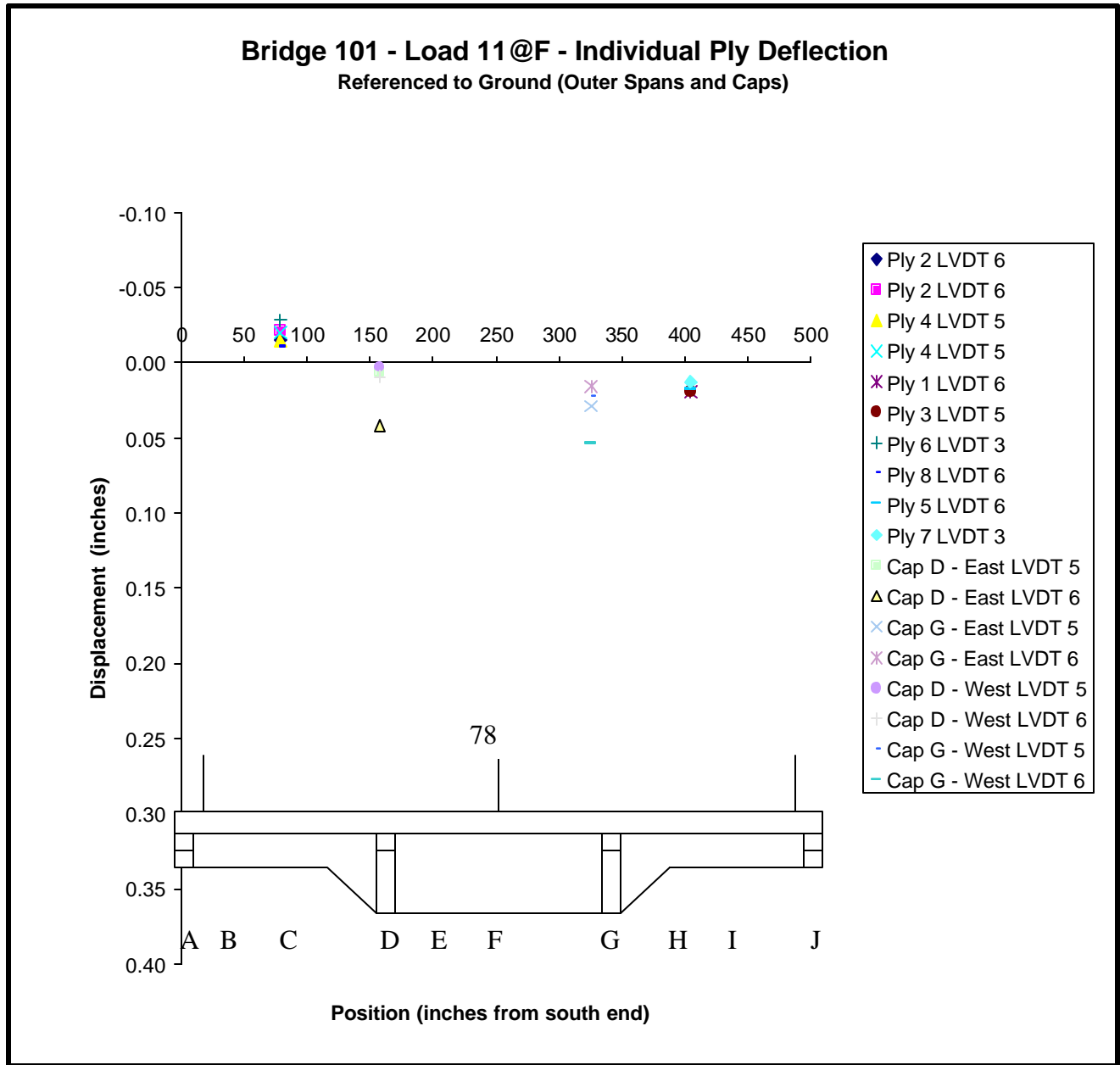


Figure 7-12. All electronic ground referenced data for Bridge 101, for 78 kip load at 11@F.

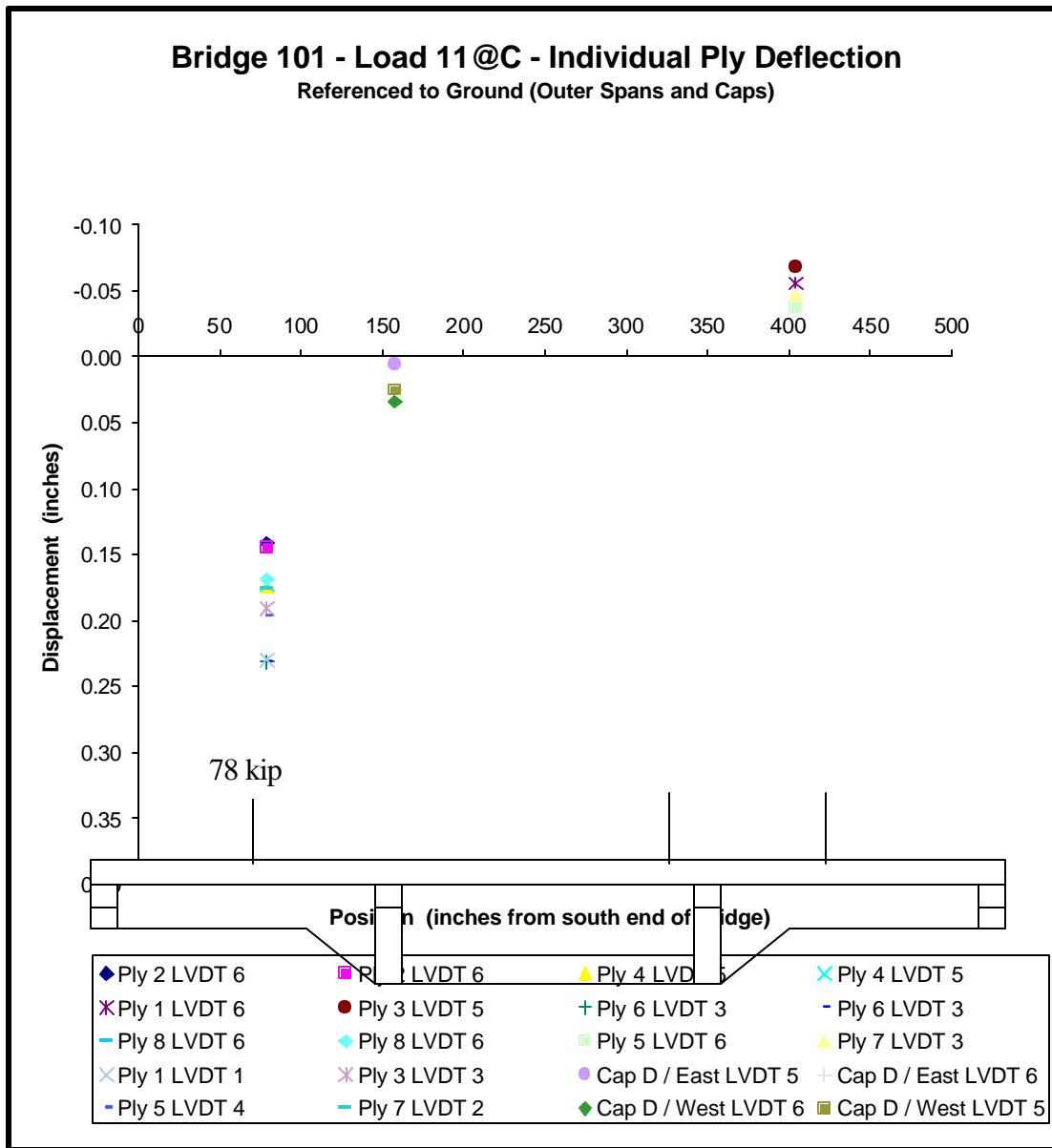


Figure 7-13. All electronic ground referenced data for Bridge 101, for 78 kip load at 11@C.

The two chords displaced similarly. The east (west) chord had a mean ply displacement of 0.208 inches downward (0.213 inches downward). The mean value was 0.210 inches. Span 3 experienced upward motion. The mean displacement values for the east chord, west chord and all piles combined, were 0.045, 0.035 and 0.042 inches, respectively. The upward displacement is deemed a result of reducing the loads on Axles 9 and 10. For this load case, cap G displaced downward. The mean

displacement value was 0.025 inches, but the individual measurements ranged from 0.0194 to 0.0512 inches.

Piles of the same lap configuration behaved similarly. From Figure 4-4, Piles 2, 4, 5, and 7 in Span 1 are single span with no continuity to Span 2 and Piles 1, 3, 6, and 8 in Span 1 are continuous across Span 2. Piles 2, 4, 5, and 7 displaced 0.239, 0.245, 0.206 and 0.236 inches downward, respectively, all similar in magnitude. Piles 1, 3, 6, and 8 displaced 0.173, 0.174, 0.175 and 0.235 inches downward, respectively, all but one behaving similarly. In general, the single span piles displaced more than the continuous piles.

Some general observations concerning results shown in Figure 7-11 can be made. The piles of Span 1 displaced due to the 78 kip load applied to that span, and the reduction in load on Axles 9 and 10 resulted in a degree of upward displacement in Span 3. This behavior was expected. Behavior of Span 2 is unknown. Cap G displaced downward, ranging from 0.0052 to 0.0512 inches downward at four locations along the cap. The mid-span data load case 11@F are provided in Table 7-6 and Figure 7-12 show the main response. Span 1 deflected slightly upward, 0.018 inches, while Span 2 shows a slight deflection downward, 0.017 inches. Although opposite in magnitude, the deflections are relatively small compared to the 0.210 inch mean ply displacement from the previous load position of 11@I. Cap D had a mean displacement of 0.015 inches and Cap G had a mean of 0.030 inches, both downward. Both caps had one measurement quite large in comparison to the others, but the absolute magnitude was still quite small and believable.

For load case 11@F, that the deflection measurements of Span 2 (referenced to the displaced chord) can be added to the relative cap-ply motion plus the cap motion to estimate displacement referenced to the ground. From Table 7-6, Cap D had a mean ply to cap closing motion of 0.007 inches and a cap motion of 0.0152 inches, resulting in a total of 0.0222 inches of downward support motion. Cap G experienced 0.059 inches closing for relative ply to cap motion and 0.0303 inches of cap motion, totaling 0.0893 inches downward. The combined effect (the average of the sums of the gap closing and cap motion) is an additional 0.0557 inches of displacement at mid-span of Span 2. This additional

deflection alters displacement of the mid-span to 0.2057 inches downward if measured from the ground reference. This leaves a 37 percent difference between the deflection referenced to displaced chord and the estimated measurement from the ground. In other words, for this case, the mid-span deflection referenced to the displaced chord may be less than 75 percent of the ground-referenced deflection.

The ground reference data for load case 11@C are shown in Figure 7-13. For Span 3, subject to the 78 kip load, the east (west) chord had a mean ply displacement of 0.175 inches (0.195 inches) downward. The overall mean was 0.185 inches downwards. For Span 1 the east (west) chord displaced 0.062 inches (0.043 inches) upward. The overall mean was 0.052 inches upward. The upward displacement is attributed to reducing loads on Axles 12 and 13. For this load case, cap D displaced downward. The cap displacements ranged from 0.006 to 0.0339 inches at various locations and had a mean value of 0.023 inches. In mirror image, the response is similar the response observed for load case 11@I.

From Figure 4-4, Piles 1, 3, 6, and 8 in Span 3 all are single span with no continuity to Span 2 and Piles 2, 4, 5 and 7 in Span 3 are continuous across Span 2. In Span 3, Piles 1, 3, 6, and 8 displaced 0.230, 0.190, 0.231 and 0.168 inches downward, respectively. For the same span, Piles 2, 4, 5, and 7 displaced 0.143, 0.173, 0.197, and 0.176 inches downward, respectively. The single span piles generally displaced more than the continuous piles.

Investigation of Support Motion and Gap Closing

Following tests of the bridges in Fort Collins, it was realized that the bridges had some degree of support motion, but the source of the motion was unknown, as no instrumentation was set up for that purpose. The ramp load tests on Bridge 101 allowed a quantification of support motion and the gap closing motion between the piles and caps. For load case 11@F, both motion of the caps and motion between the caps and piles were measured. Typical measurements of cap motion were 0.01 to 0.03 inches at the 78 kips load level. Relative motion between the piles and caps was as high as 0.03 to 0.05 inches for a 78 kip load. The combination of the cap motion and relative motion between the caps and piles

does add a measurable component to measurements of the chord system from a ground reference. While the motion was measurable, determining the mechanism of that motion was not possible due to limited access to those bearing surfaces.

An investigation was made to determine whether cap deformation was either a rigid body displacement or flexural bending. Bridge 101 was instrumented to monitor this motion during loading. The interior displacements were obtained by displacement transducers between the bottom of the cap and the ground. Displacements at the ends of the cap, 0" and 168" from the east end of the cap, were taken from optical data (thus are less accurate than the transducer data). Also the optical data was at the center of the cap width, and the interior data was at the outside, adjacent to the ply ends.

Figures 7-14 and 7-15 show the cap displacements for the 0, 30, and 78 kips TLV axle load levels. The measurements as presented were zeroed to the initial no-load condition. The curvature suggests the caps did not rotate as a rigid body, but more like a multi-span beam. Figures 7-16 and 7-17 present the cap displacements due to the full range of the ramp load. Each value is the net displacement from 0 to 78 kips, i.e. the difference in magnitude between the 78 kips value and the original 0 kip value. This removes the initial deflected shape due to train weight and dead load. Cap D deflected most beneath the east chord (0.0416 inches) and cap G deflected most beneath the west chord (0.0536").

The relative motion between chord piles and the cap also was monitored in Bridge 101 for loading 11@F. Figures 7-18 and 7-19 illustrate the results for Cap D and Cap G. The deflections shown are the changes in distance between the member and each of the piles, measured directly with transducers. Values shown were adjusted by setting the zero kip load values to zero.

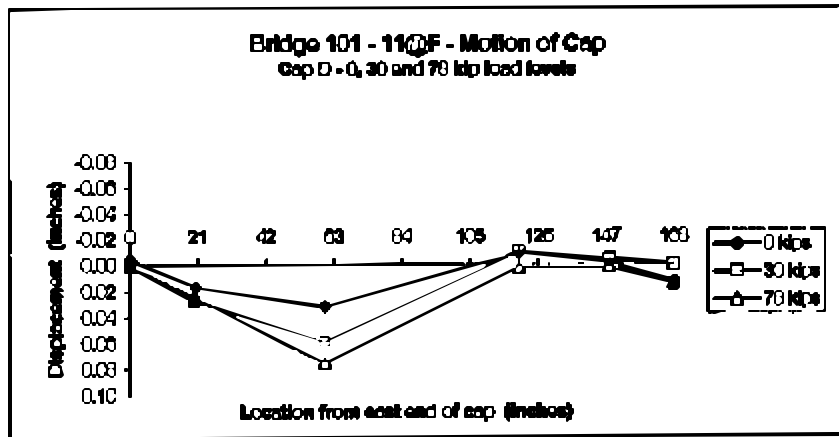


Figure 7-14. Deflection measurements of Cap D referenced to the ground for 0, 30, and 78 kip loads applied by the TLV for load 11@F.

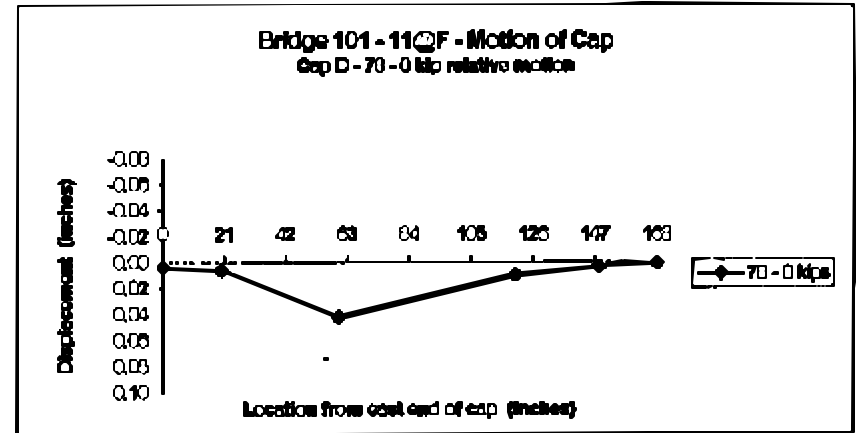


Figure 7-16. Differential motion of Cap D from 0 to 78 kips by the TLV for load 11@F.

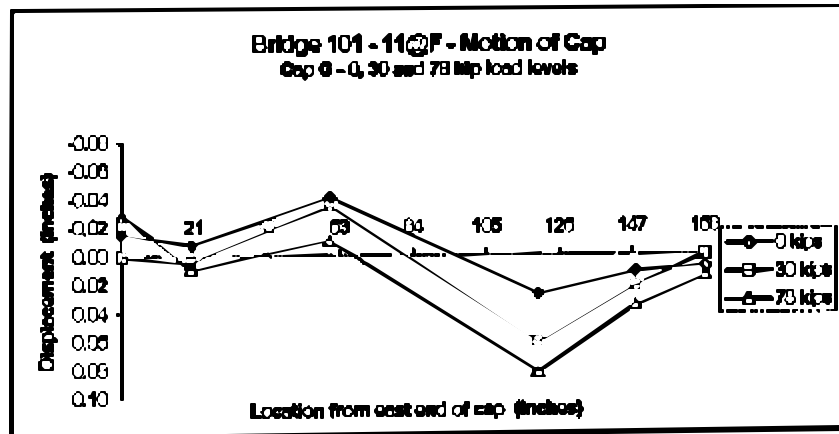


Figure 7-15. Deflection measurements of Cap G referenced to the ground for 0, 30, and 78 kip loads applied by the TLV for load 11@F.

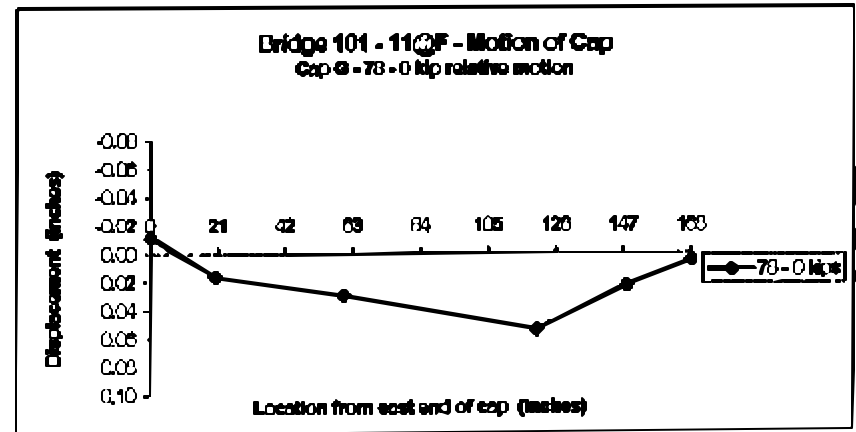


Figure 7-17. Differential motion of Cap G from 0 to 78 kips by the TLV for load 11@F.

In these plots, positive motion (shown downward) indicates the cap and ply are getting closer together (either by gap closing or bearing deformation). A negative value (shown upward) indicates a separation occurred.

The results show that most of the piles moved closer to the supporting cps, as expected. The motion between 0 to 30 kips was about one-half the motion between 0 to 78 kips. The magnitude of the motions varied greatly. For example, (from Fig. 7-19) Ply 1 moved 0.0933 inches closer to the cap, while (from Fig. 7-18) Ply 8 on Cap D actually separated 0.0004 inches. The largest closing motion was recorded for Ply 2, 0.043 inches on Cap D and 0.0993 inches on Cap G. Because of the size of the caps and the inaccessible nature of the interior surfaces, it was not possible to assess whether the members had physical gaps or not. Piles 6, 7 and 8 on Cap D showed separation. The largest magnitude was 0.099 inches for Ply 1 on Cap G. Ply 6 separated 0.166 inches between 0 and 30 kips, but reduced to 0.074 inches at the 78 kip level. This may have been as a result of tie rod contact changing. The motions observed contribute to the displacements measured relative to the ground for the piles themselves.

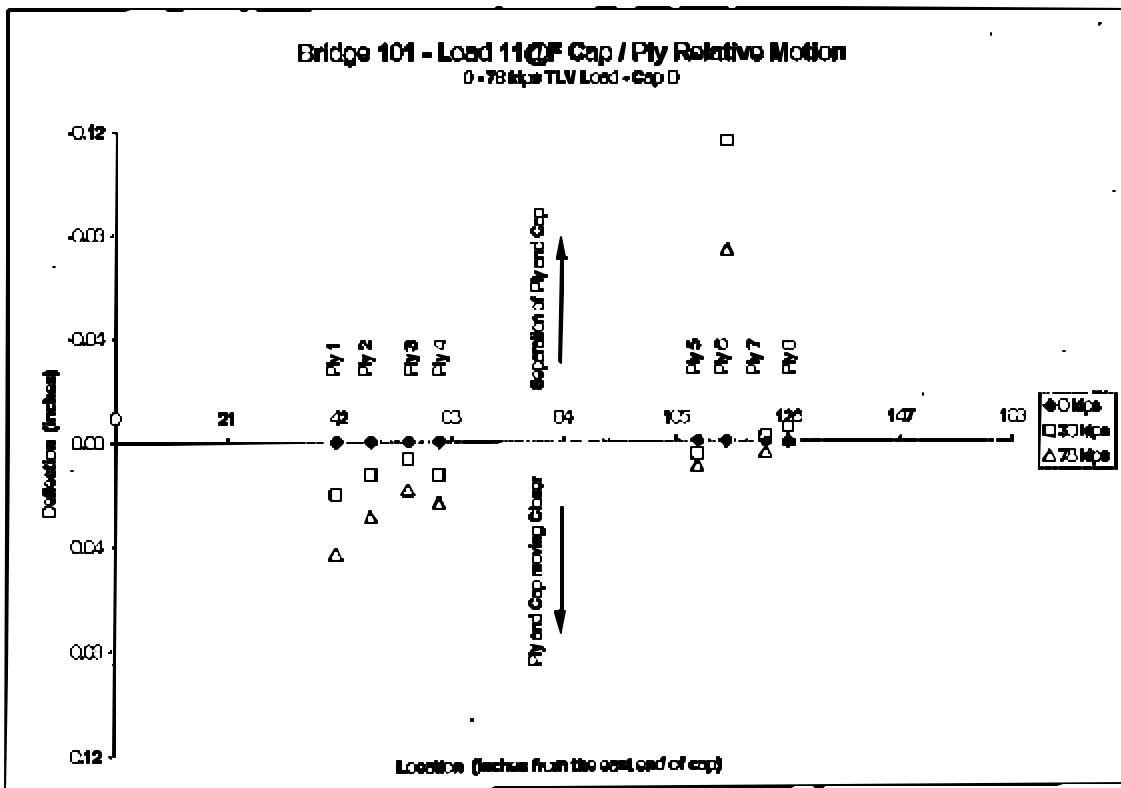


Figure 7-18. Relative motion between Cap D and piles 1 to 8 for 0, 30, and 78 kip loads by 11@F.

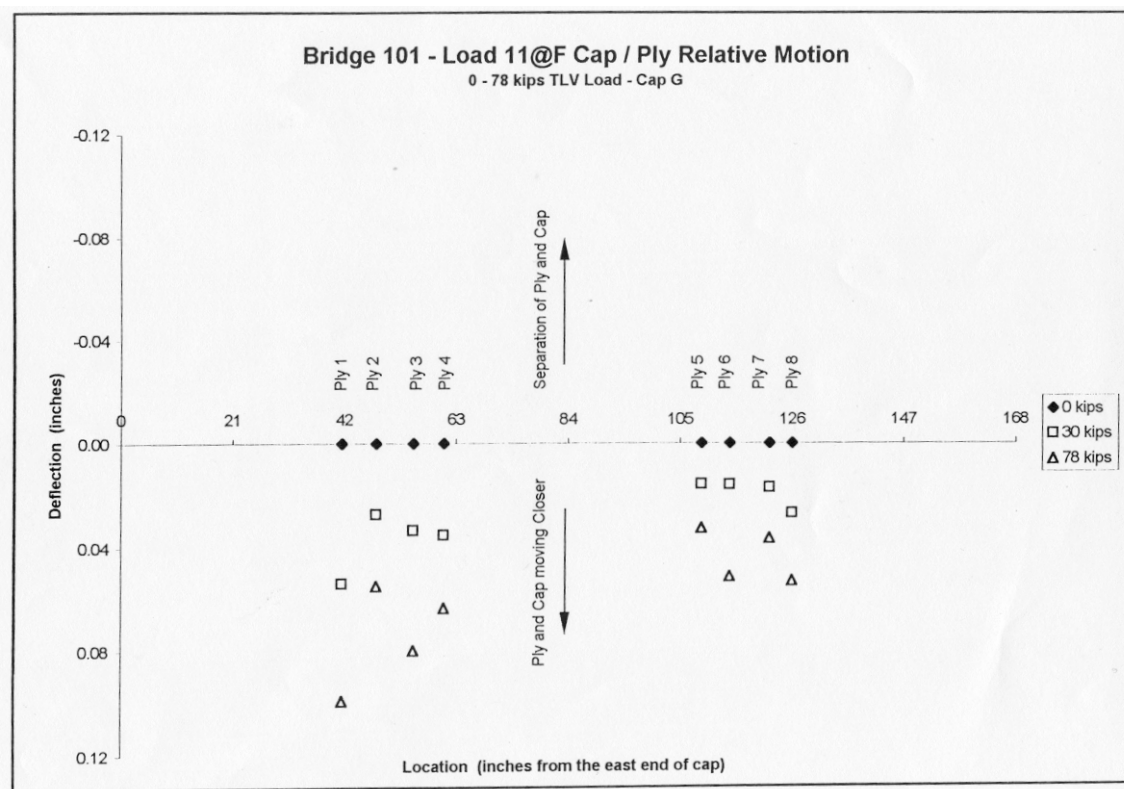


Figure 7-19. Relative motion between Cap G and Piles 1 to 8 for 0, 30, and 78 kip loads by 11@F.

CHAPTER 8

LOAD DISTRIBUTION BETWEEN PILES

Empirical Formulation

Load sharing among the piles was studied empirically on two bases, measured deflection and measured strain.

Consider the equation for deflection of a simply supported, single-span member with a point load at mid-span. If rewritten to solve for the load resisted, the relationship can be expressed as:

$$\text{Estimated Load Resisted} = C \frac{\Delta EI}{l^3} \quad (5)$$

where C is a constant defined by the load position and support conditions of a beam at each end of its span, Δ is deflection at the mid-point of the span, E is the modulus of elasticity for the material, I is the moment of inertia of the beam and l is the length of the span.

For strain, the relationship is:

$$\text{Estimated Load Resisted} = C \frac{\epsilon ES}{l} \quad (6)$$

where C is a constant defined by the load position and support conditions of the beam at each end of its span, ϵ is strain at the mid-point of the span, E is the modulus of elasticity for the material, S is the section modulus of the beam and l is the length of the span.

For this study, it is assumed that each ply is supported and loaded in the same manner. Thus C is the same for every ply and is assigned a relative value of 1. All the other quantities are known for each ply considered. Whether based on deflection or strain, an indicator of load share can be obtained by summing the individual resisting loads and dividing by each by the total.

Load shares were examined for Span 6 of Bridge 32.35. Table 8-1 presents the variables and predicted percentages of load carried by each ply. Figure 8-1 schematically illustrates the percentage of load carried by each individual ply. In this case, deflection data were available only for Piles 1, 2 and 3. Strain information was available only for Piles 1 to 4 and 7.

Table 8-1. Comparison of percentage of load determined by deflection or strain. Variables for each ply used in computation have been included.

Young's Modulus	(psi)	2.09E+06	2.28E+06	1.97E+06	2.09E+06	2.18E+06
Moment of Inertia	(in ⁴)	3035	3035	3035	3035	3035
Section Modulus	(in ³)	362	362	362	362	362
Span Length	(in)	180	180	180	180	180
Measure Deflection	(in)	0.126	0.161	0.117	NR	NR
Measured Strain	(in/in x 10 ⁻⁶)	331	442	399	638	512
Load Estimate						
Based on Deflection	lbs*	137	191	120		
Based on Strain	lbs*	1393	2033	1584	2684	2243
Normalized percentage load predictions						
Based on deflection	%	11.5	16	10		
Based on strain	%	8.8	12.8	10	16.9	14.1

Since deflection was known for only three piles, an adjustment was made. Assuming each chord supports 50 percent of an axle load, three out of four piles were assumed to support 75 percent of the 50 percent, or 37.5 percent of the total load. Estimated load values were calculated for the other two piles. A load of 191.2 lbs was calculated for Piles 2 and 120.0 lbs for Ply 3. The sum of the three piles was 448.1 lbs. If this value was 37.5 percent of the total axle load, that value would then be 1,195 lbs. Using this estimate, 136.9 lbs is 11.5 percent of 1,195 lbs. Using this process, Piles 1, 2 and 3 were estimated to carry 11.5 percent, 16.0 percent and 10.0 percent, respectively, of the total load applied to Span 6. The load values themselves have no real meaning because C is unknown.

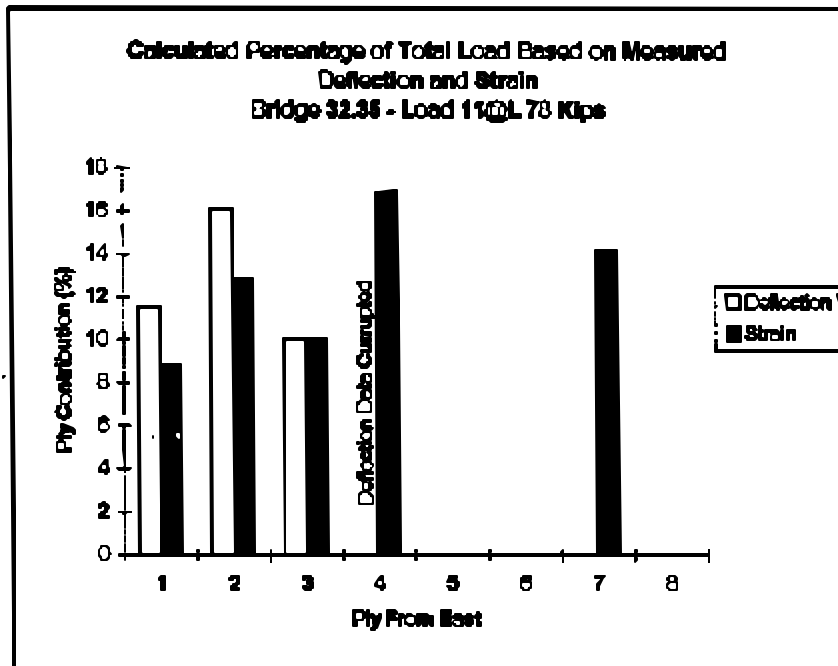


Figure 8-1. Estimated percentages of load carried by each ply based on deflection or strain measured at mid-span, Span 6, Bridge 32.35.

For Ply 1, using strain data with C assigned a value of 1, an estimated load value of 1,393 lbs was calculated. Assuming that the 5 piles with known strain support 62.5 percent of the total load, percentages were calculated for each ply with known strain. Piles 1, 2, 3, 4, and 5 were estimated to carry 8.8 percent, 12.8 percent, 10.0 percent, 16.9 percent, and 14.1 percent of the total load applied to Span 6.

In a report to the AAR (Gutkowski et al. 1998), a similar empirical computation was done for the static load and deflection data. The results for Span 6 of Bridge 32.35 were that Piles 2, 4, and 7 carried 11.5 percent, 14.7 percent, and 11.3 percent of the total axle loads applied, respectively. Herein, for the TLV ramp load, the deflection based data estimated Ply 2 to carry 16.0 percent (no estimates available for Piles 4 and 7) and the extensometer based data estimated Piles 2, 4, and 7 to carry 12.8 percent, 16.9 percent, and 14.1 percent of the 78 kip axle load, respectively.

Strain measurements also were available for Bridge 101. Data were available for seven piles with respect to strain and all eight piles with respect to deflection for ramp load 11@F. Table 8-2 presents the variables and predicted percentages of load carried by each ply. Figure 8-2 presents those percentages graphically. No strain measurement was successfully recorded for Ply 6.

Table 8-2. Comparison of percentage of load determined by deflection or strain for Span 2, Bridge 101. Variables for each ply used in computation have been included.

Variables		Ply 1	Ply 2	Ply 3	Ply 4	Ply 5	Ply 6	Ply 7	Ply 8
Young's Modulus	(psi)	1.77E+06	2.29E+06	2.46E+06	1.59E+06	1.60E+06	2.21E+06	2.37E+06	2.34E+06
Moment of Inertia	(in ⁴)	2017	2017	2017	2017	2017	2017	2017	2017
Section Modulus	(in ³)	260	260	260	260	260	260	260	260
Span Length	(in)	168	168	168	168	168	168	168	168
Measure Deflection	(in)	0.142	0.179	0.120	0.196	0.205	0.105	0.088	0.141
Measured Strain	(in/in x 10 ⁶)	446	707	429	774	822	NR	318	454
Normalized percentage load predictions									
Based on deflection	%	10.6%	17.4%	12.5%	13.2%	13.9%	9.8%	8.8%	13.9%
Based on strain	%	8.9%	18.3%	11.9%	13.9%	14.8%		8.5%	12.0%
Sum of chords:		East Chord				West Chord			
Based on deflection	%	53.6%				46.4%			
Based on strain	%	52.9%				35.3% - one ply not predicted			

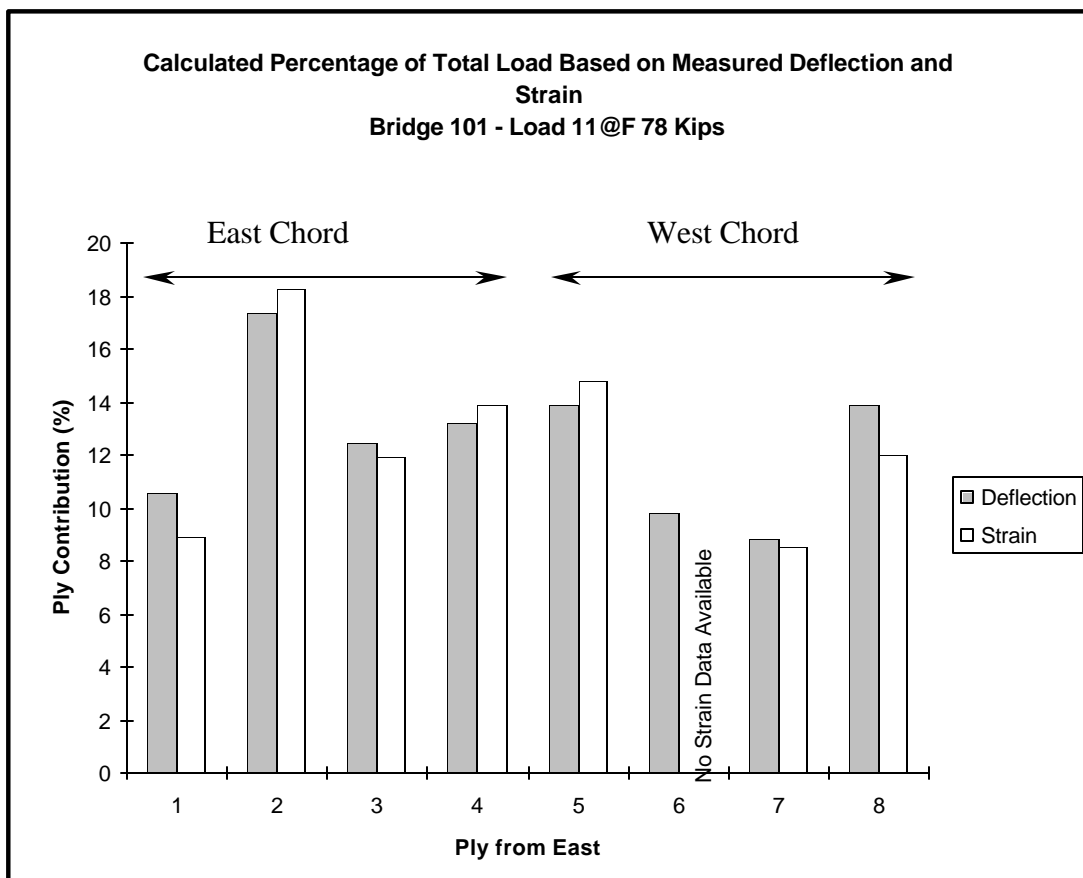


Figure 8-2. Estimated percentage of load carried by each ply based on deflection or strain measured at mid-span, Span 2, load 11@F for 78 kips, Bridge 101.

The bar graph presents load percentage estimates for each ply side by side. Similarity between the deflection based and strain based estimates is apparent in the figure. That two independent types of data produce such similar results supports their reliability. This is encouraging since the extensometer data from the static testing was thought to be suspect because of possible drift. However, it appears that reasonable data was collected for this case.

It appears that Ply 2 carries a much higher load percentage of the total axle load than any of the others, 17.4 percent based on deflection and 18.1 percent based on strain. The lowest load percentage carried was carried by Ply 7, 8.8 percent based on deflection and 8.4 percent based on strain

This data can also be compared to load sharing estimates from the AAR reports (Gutkowski et al. 1998 and Gutkowski et al. 1999) that were based on stiffness and deflections from two static loads. In the AAR reports, the values are normalized to present the load share of a single ply as a percentage of the four piles of one chord. (100 percent per chord, 200 percent for all eight piles.) To bring these values to a form comparable the load share estimates from the AAR report have been divided by 2 to represent a percentage share of the total load applied. Two load cases were evaluated. From the AAR report, for Span 2 of Bridge 101, Piles 1 to 8 carried 10.1 percent, 13.2 percent, 11.6 percent, 15.2 percent, 17.0 percent, 9.0 percent, 8.6 percent and 15.4 percent of the total axle loads for one load case and 11.4 percent, 18.0 percent, 12.3 percent, 16.4 percent, 17.4 percent, 9.3 percent, 9.4 percent, and 18.2 percent of the total axle loads for the other. From Table 8-2, the deflection based data estimated Piles 1 to 8 to carry 10.6 percent, 17.4 percent, 12.5 percent, 13.2 percent, 13.9 percent, 9.8 percent, 8.8 percent, and 13.9 percent and the extensometer based data estimated Piles 1 to 5, 7 and 8 to carry 8.8 percent, 18.1 percent, 11.8 percent, 13.8 percent, 14.7 percent, 8.4 percent, and 11.9 percent of the 78 kip axle load. There is a clear consistency in the pattern.

CHAPTER 9

ROLLING LOAD TESTS – BRIDGE 101

The pilot rolling load tests were accomplished by collecting data while various trains crossed the bridge as well as by use of the test train itself. For the purpose of this report, some of the data collected from the tests on Bridge 101 are presented and compared to static load data.

Conduct of the Tests

Bridge 101 was monitored for deflection as the locomotive, instrumentation car, and TLV car moved over the bridge. The train was rolling from the North to the South and (from Span 3 to Span 1) at a minimum unassisted acceleration rate. Specifically, the drive axles of the locomotive were engaged, and the train was allowed to accelerate from fully stopped at a minimal acceleration. The velocity of the train was estimated by timing a marker on the train as it moved across the length of the bridge. In this case the average locomotive velocity was approximately 4-7 mph. Table 9-1 and Figures 9-1 and 9-2 present deflection data collected.

Test Results

Figure 9-1 illustrates the displaced chord mid-span deflection data for Piles 5, 6, 7, and 8 in Span 2. Figure 9-2 illustrates ground reference response of mid-span deflection in Piles 6 and 8 in Span 3. Both figures present the displacements from Table 9-1 on the y-axis and the time referenced to the start of the test on the x-axis. On either of the graphs, when a pair of axles crosses the span instrumented, the deflections measured forms a U-shaped pattern. A reference to the axle pair causing the deflection is provided under each U-shaped pattern. For example, in Figure 9-1, the first U-shaped pattern indicates that loads from Axles 1 and 2 began causing deflection at the monitored location in Span 2 at about 9 seconds. The maximum deflections effects occurred at about 12 seconds. Those deflections were 0.173, 0.079, 0.076, and 0.143 inches for Piles 5, 6, 7, and 8, respectively. The major deflection effects of Axles

1 and 2 were complete by about 15 seconds. This cycle can be identified for each pair of axles of the train as they cross the spans instrumented.

From the digital data used for plotting Figure 9-1, the maximum recorded deflection effect from axles pairs 1 and 2, 3 and 4, 5 and 6, 7 and 8, 9 and 10, and 12 and 13 occurred at 12.07, 18.10, 22.64, 30.20, 33.22, and 37.71 seconds. An exception is that Ply 5 had its maximum deflection at 39.16 seconds, with 12 and 13 on Span 2.

Figures 9-1 and 9-2 illustrate the deflections on the same time scale allowing some comparison between the figures. For example, in Figure 9-1, Axles 1 and 2 created the maximum deflection in Span 2 at 12.07 second while the maximum displacement effect from Axles 1 and 2 occurred in Span 1 at 15.09 seconds, shown in Figure 9-2. This illustrates that Span 2 was crossed prior to Span 1. The offset of these two U-shaped deflection patterns indicated the maximum deflections measured in Span 1 occurred about three seconds after the maximum deflection measurements in Span 2. As the train increased velocity, this offset diminished. For example, the maximum effect of axles 12 and 13 occurred at 37.71 seconds for Span 2 in Figure 9-1 and at 39.16 seconds for Span 1 in Figure 9-2, a difference of 1.45 seconds.

Comparison of the deflection patterns of Figures 9-1 and 9-2 also illustrate the difference between measurements referenced to the displaced chord and those referenced to the ground. In Figure 9-1, the measurements are referenced to the displaced chord in Span 2. The effects on Span 2 from axles 1 and 2 begin at about 9 seconds and end at about 15 seconds, a six second interval. Specifically, from Table 9-1, the maximum effect on Span 2 of Axles 1 and 2, 0.173 inches, occurred at 12.07 seconds. At this point it is estimated that Axles 1 & 2 are approximately centered over Span 2, with no loads on Span 1. In Figure 9-2, the measurements are referenced to the ground in Span 1. The effects from Axles 1 and 2 on Span 1 begin at about 9 seconds and end at about 18 seconds, a nine second interval. (Note that the same loads affect Span 1 about three seconds later than they affect Span 2.) Span 1 began experiencing a displacement effect while the loads from Axles 1 and 2 were on Span 2.

Table 9-1. Record of displacement data for rolling train loads, instrumentation position US2-1, train moving forward slowly.

Time	Displaced Chord Measurements				Ground Referenced	
	LVDT 1	LVDT 4	LVDT 2	LVDT 5	LVDT 3	LVDT 6
	Span 2 Ply 5	Span 2 Ply 6	Span 2 Ply 7	Span 2 Ply 8	Span 3 Ply 6	Span 3 Ply 8
0.00	0.000	0.000	0.000	0.000	0.000	0.000
1.49	0.000	-0.001	-0.001	0.000	0.000	0.000
3.00	-0.001	-0.002	-0.002	0.001	0.000	-0.001
4.51	-0.003	-0.004	-0.004	-0.004	-0.003	-0.003
6.03	-0.004	-0.001	-0.004	-0.010	-0.005	-0.005
7.53	-0.002	0.005	-0.004	-0.006	-0.006	-0.005
9.05	0.017	0.016	0.007	0.022	0.002	0.008
10.56	0.139	0.062	0.060	0.109	0.024	0.034
12.07	0.173	0.079	0.076	0.143	0.045	0.051
13.58	0.163	0.063	0.048	0.097	0.171	0.127
15.09	0.009	-0.001	-0.007	-0.015	0.237	0.185
16.60	0.015	0.015	0.001	0.034	0.223	0.157
18.10	0.175	0.082	0.065	0.132	0.083	0.071
19.62	0.171	0.069	0.057	0.106	0.156	0.127
21.14	0.014	0.006	-0.002	0.017	0.247	0.179
22.64	0.109	0.038	0.026	0.086	0.139	0.095
24.15	0.094	0.016	0.019	0.055	0.148	0.104
25.67	0.005	-0.001	0.005	0.013	0.172	0.100
27.17	-0.003	-0.004	0.002	0.013	0.033	0.009
28.69	0.000	0.000	0.003	0.009	0.006	0.001
30.20	0.088	0.034	0.028	0.090	0.030	0.037
31.71	0.094	0.012	0.013	0.036	0.133	0.098
33.22	0.163	0.091	0.072	0.132	0.126	0.080
34.73	0.110	0.010	0.015	0.042	0.249	0.208
36.24	-0.001	-0.002	0.001	-0.010	0.110	0.051
37.71	0.113	0.064	0.058	0.120	0.036	0.042
39.16	0.139	0.022	0.024	0.041	0.247	0.202
40.67	-0.001	0.004	0.004	0.015	0.072	0.029
42.18	0.007	0.006	0.007	0.017	0.012	0.005
43.69	0.007	0.005	0.007	0.016	0.010	0.003
Maximum	0.175	0.091	0.076	0.143	0.249	0.208

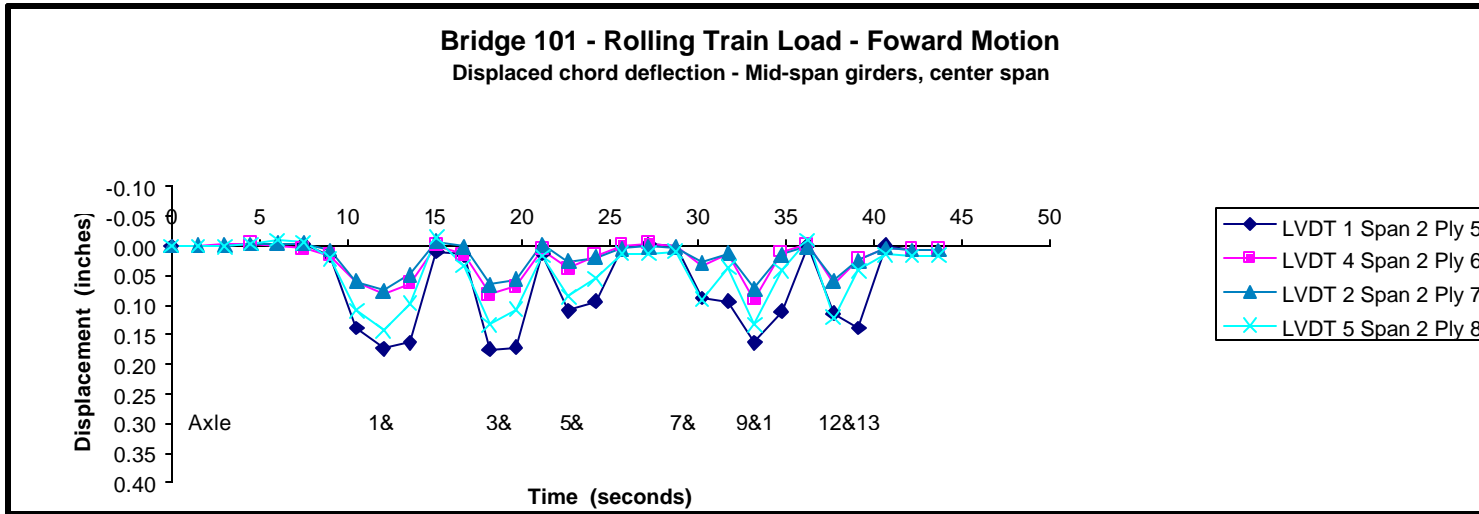


Figure 9-1. Displaced chord referenced displacement record, Bridge 101, instrumentation position US2-1, train rolling forward slowly.

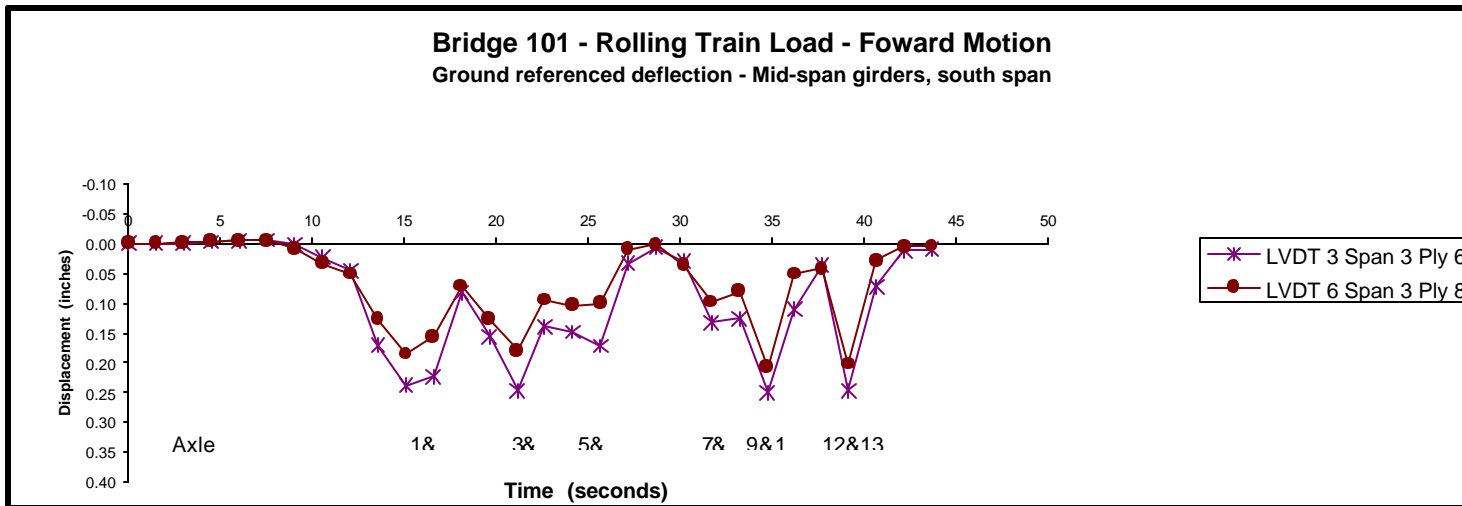


Figure 9-2. Ground referenced displacement record, Bridge 101, instrumentation position US2-1, train rolling forward slowly.

For example, from Table 9-1, the downward displacement effect on Span 1 due to the load on Span 2 at 12.07 seconds was 0.045 and 0.051 inches, in transducers 3 and 6, respectively. As no loads had yet been applied to Span 1, the effect of downward displacement in Span 1 due to loads applied to Span 2 indicate ground referenced effect to measurements in Span 1 of support motion to the magnitude of about 0.05 inches. This was consistent with static and ramp load measurements.

Note that in Figure 9-1, at the beginning and end of each U-shaped set of deflections, the measured deflection returns to the zero value of the Y-axis. This indicates that the piles recover almost completely whenever the axle loads are removed from the span instrumented relative to the displaced chord. Observe that in Figure 9-2, that the beginning and end of the U-shape patterns from axles 1 and 2, 3 and 4, and 5 and 6 or axles 7 and 8, 9 and 10 and 12 and 13 do not return to near zero, as in Figure 9-1, but rather remain displaced between 0.05 and 0.10 inches. This appears to be the effect of loads in Span 2 causing ground-referenced measurements in Span 1 due to support motion of some form. Between the effects of axles 5 and 6 and 7 and 8 in Figure 9-2, the displacement measurements almost return to zero at about 29 seconds. The axles noted are those of the instrumentation car. Recall from Table 6-4 that the dimension between Axles 6 and 7 was 610 inches. The bridge was only 483 inches long. As this car crossed the bridge, there was a brief period in which no load was on the bridge. During this no load condition, the ground referenced piles returned to a position close to the initial position of the test. The only time the measurements referenced to the ground were effectively on the zero axis were when no loads were on the bridge.

The maximum displacements recorded in the Figure 9-1 and 9-2 were caused by different sets of axles. In Figure 9-1, the maximum recorded effect was of 0.175 inches, referenced to the displaced chord in Ply 5 of Span 2 as caused by Axles 3 and 4. In Figure 9-2, the maximum recorded effect was 0.249 inches, in Ply 6 of Span 1 as caused by Axles 9 and 10. While not directly comparable, it is interesting that the maximum effects came from different load sources. The rolling load data acquisition was performed at the maximum data collection rate as the unit was set up for the static and ramp load tests. While the unit is capable of much faster acquisition, it was not modified for faster acquisition at the

time. Because the time intervals between measurements are about 1.5 seconds, the possibility of recording the absolute maximum deflection in a span is unrealistic.

Table 9-2 presents the deflection measurements, referenced to the displaced chord, recorded for Piles 5, 6, 7, and 8 in Span 2 during static load testing. The deflections are plotted for each static load position in Figure 9-3. Initially, Axles 1 and 2 dominated the response. The static load positions 1@G through 2@D, in Figure 9-3, represent data equivalent to the first U-shaped pattern, in Figure 9-1, i.e. from the time period from about 8 seconds to about 15 seconds. The deflections of the two groups of data can be compared, but with the realization that Figure 9-3 presents only a portion of the load positions presented in Figure 9-1. To aid in comparison, axle identification has been added under the static data in Figure 9-3 to clarify comparable loads to those shown in Figure 9-1.

Comparing the data from Table 9-1 and Figure 9-1, representing the rolling load measurements, to Table 9-2 and Figure 9-3, there are clear similarities. The displacements of Piles 5, 6, 7, and 8, whether rolling load deflections or static, each displace in similar patterns due to the loads from Axles 1 and 2 over Span 1. For example, the maximum displacements from the rolling loads were 0.173, 0.079, 0.076, and 0.143 inches downward for Piles 5, 6, 7, and 8, respectively. This compares to maximum static displacements of 0.166, 0.078, 0.070, and 0.131 inches for Piles 5, 6, 7, and 8, respectively. The magnitudes are similar, and the order of least to highest deflection remains constant. The only difference is that the maximum displacements from the static tests did not come from the same load case.

Table 9-3 presents the maximum displacements of each ply recorded due to the rolling loads over Span 2 and three static load positions that may be close to corresponding to the load positions when the rolling data was measured. The static load positions are 1@F, 2@G and 1@E. The load position 1@F is the first axle positioned at mid-span of Span 2. The position 2@G places the second axle over Cap G with axle 1 just past mid-span of Span 2. The position 1@E centers Axles 1 and 2 in Span 2. Deflections from any of the three static load cases compare reasonably well with the maximum deflections measured due to the rolling load.

Table 9-2. Displaced chord deflection of piles for Span 2, Bridge 101, west chord.

Position	LVDT 1 Ply 5	LVDT 4 Ply 6	LVDT 2 Ply 7	LVDT 5 Ply 8
1@J	-0.012	-0.011	-0.011	-0.015
1@I	-0.017	-0.018	-0.020	-0.056
2@J	-0.013	-0.012	-0.022	-0.053
1@H	-0.012	-0.012	-0.020	-0.054
1@G-	0.020	0.010	0.003	0.016
1-2@G-	0.115	0.028	0.039	0.056
1@F	0.157	0.061	0.052	0.089
1@F	0.159	0.064	0.054	0.099
2@G	0.166	0.078	0.056	0.116
1@E	0.165	0.073	0.063	0.131
1@E	0.163	0.070	0.062	0.126
1@D+	0.165	0.061	0.069	0.097
1@D+	0.165	0.063	0.070	0.103
1-2@D	0.134	0.044	0.022	0.060
1-2@D	0.134	0.044	0.022	0.063
1@C	0.081	0.008	-0.002	0.016
1@C	0.068	-0.007	-0.011	-0.014
2@D-	-0.004	-0.029	-0.028	-0.065
2@D-	-0.004	-0.028	-0.029	-0.055
1@B	-0.017	-0.027	-0.031	-0.073
1@B	-0.017	-0.026	-0.029	-0.083
1@A+	-0.023	-0.024	-0.031	-0.077
1@A+	-0.021	-0.022	-0.029	-0.069
9@J-	0.109	0.016	0.023	0.058
9@J-	0.109	0.016	0.022	0.055
10@J-	0.015	-0.006	-0.016	-0.025
9@I	0.064	-0.004	-0.008	-0.012
9@H	0.004	-0.017	-0.025	-0.050
9@H	0.003	-0.015	-0.024	-0.042
9@G-	0.021	-0.003	-0.012	-0.009
9-10@G	0.111	0.027	0.039	0.075
9@F	0.162	0.068	0.055	0.096
9@E	0.165	0.065	0.059	0.107
9@E	0.164	0.064	0.059	0.111
9@D+	0.175	0.069	0.076	0.118

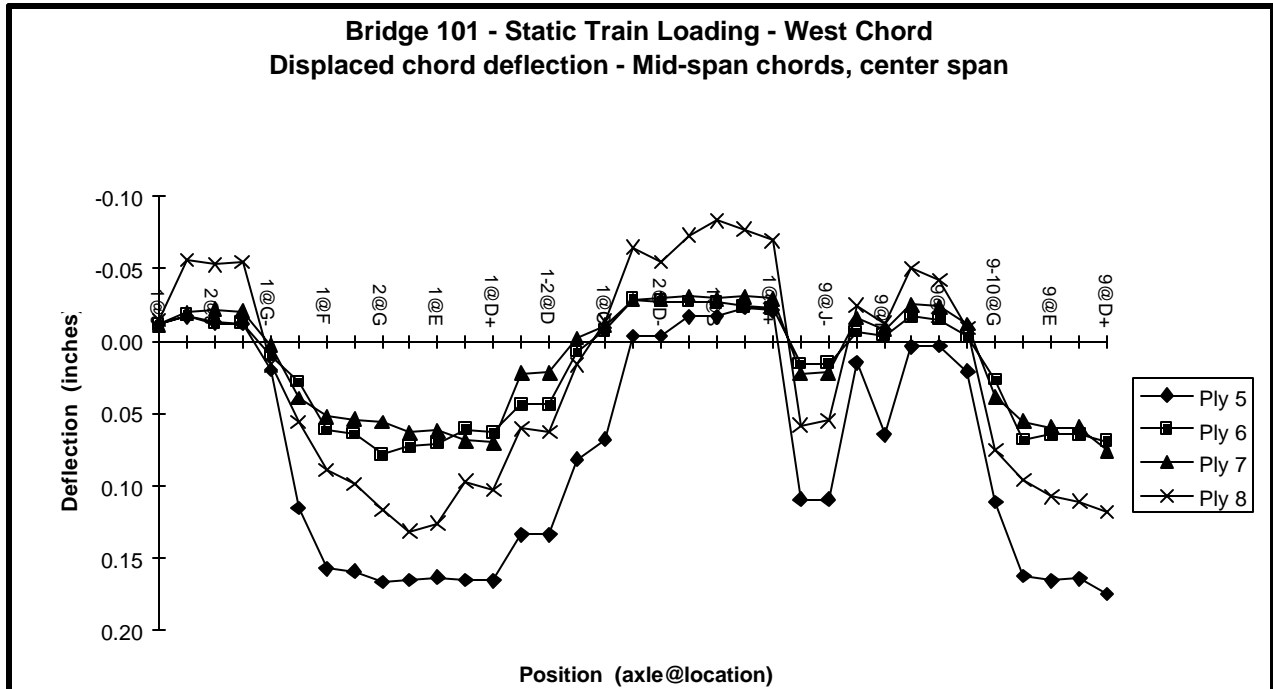


Figure 9-3. Deflections of chord piles of the west chord, mid-span of Span 2, Bridge 101 due to static train loads.

Table 9-3. Deflection of west chord piles at mid-span of the center span of Bridge 101 for moving and similar static loads.

	Moving Train	Static Load 1@F	Static Load 2@G	Static Load 1@E
West Chord Piles	Maximum Deflection (inches)	Deflection (inches)	Deflection (inches)	Deflection (inches)
5th Chord Ply	0.173	0.158	0.166	0.164
6th Chord Ply	0.079	0.063	0.078	0.071
7th Chord Ply	0.076	0.053	0.056	0.063
8th Chord Ply	0.143	0.094	0.116	0.129
Average	0.118	0.092	0.104	0.107

Load case 1@E appears to produce results closest to the maximum deflections measured due to the rolling load. From Table 9-3, the rolling train measurements for Piles 5 to 8 in Span 2 were 0.173, 0.079, 0.076, and 0.143 inches downward, respectively, or a mean displacement of 0.118 inches downward. For load position 1@F, measurements of 0.164, 0.071, 0.063, and 0.129 inch downward for

Piles 5, 6, 7, and 8 were taken, producing a mean displacement of 0.107 inches. For this comparison, the displacements caused by the moving loads were slightly greater than those of the static loads. On average, the moving loads increased the deflection from 0.107 to 0.118 inches, or a 10 percent increase (dynamic impact effect). However, the inaccuracy of identifying the train positions for the moving train is a factor to consider when interpreting these results. The rolling load tests were performed as brief pilot study to complement the static load tests results. In a subsequent study (apart from this project) extensive rolling train tests were to be conducted for Bridge 101 (Gutkowski 2000). Use of electronic triggers to capture train positions at the time of data acquisition was planned for train speeds up to 20 mph.

CHAPTER 10

CONCLUSIONS AND RECOMMENDATIONS

The following conclusions are made from the results of the research project present in this report.

- At some pile bents support motion was evident in the range of .05-.10" to downward.
- Relative displacement between piles and caps was typically, below .06"
- Few cases of upward displacement were observed, support motion was a likely factor.
- Cap displacement influences the relative displacement and load share of chord piles.
- Strain and deflection data for the piles of stringers produced similar empirical load share values.
- Empirical calculation reflecting MOE and span type showed a ply takes between 17 percent and 35 percent of chord loading. This changed moderately if support motion was removed.
- The MOE data indicated that the wood material was stiffer and stronger than anticipated and this is partially attributed to long term drying effects.
- There was no evident pattern of load sharing among piles of a chord. This is attributed to variability in MOE value, cap displacement, differential bearing conditions of individual piles and possible relative (track to tie, tie to chord, chord to cap) motion.
- Differences in deflection response of spaced stringers versus packed stringers was small.
- Relative motions due to gaps and incomplete bearing appear to have had a significant effect on response.
- Response was linear from 30-78 kips. From 0-30 kips, some non-linearity occurred and is attributed to closure or opening of gaps at connectors and bearing surfaces.
- A semi-continuous beam model provided reasonable predictions of the deflection response of the bridges.

Some recommended future work resulted from the study.

- The AAR plans to strengthen Bridge 101 and retest it under moving train loads.
- Rigorous modeling to account for interconnection of the piles and likely relative motions

involved throughout the bridge is necessary to provide accurate predictions of field behavior.

- More extensive instrumentation of all piles simultaneously is helpful in conducting more extensive assessment of load sharing.

REFERENCES

- American Railway Engineering Association, 1995 Manual for Railway Engineering, AREA, Washington, D.C., 1995.
- Byers, William G. "Service life of timber trestles", Probabilistic Mechanics and Structural and Geotechnical Reliability, Proceedings of the Specialty Conference Proceedings of the 1996 7th Specialty Conference on Probabilistic Mechanics and Structural Reliability Aug 7-9, Worcester, MA. 1996.
- Gutkowski, R. M., Robinson, G. C. and Peterson, M. L., "Field Load Testing of Old Timber Railroad Bridges," Proceedings - Structural Faults and Repair-97, 7th International Conference and Exhibition, Edinburgh, Scotland, E.C.S. Publications, Edinburgh. 1997.
- Gutkowski, R.M., Peterson, M. and Robinson, G.C., "Field Studies of Timber Railroad Bridges, Contract No. TRAC-95-445," Association of American Railroads, Transportation Technology Center, Pueblo, Colorado 81001. 1998.
- Gutkowski, R. M., Peterson, M., Robinson, G. C., "Field Load Tests of Timber Railroad Bridges under Static and Ramp Loads." Proceedings of the 5th World Conference on Timber Engineering, Montreux, Switzerland, Vol. 2, pp. 108-115, Presses Polytechniques et Universitaires Romandes, Lausanne, Switzerland. 1998.
- Gutkowski, R.M., Peterson, M., Robinson, G.C., Oliva-Maal, D., Otter, D. and Uppal, S., "Field Studies of Timber Railroad Bridges, R-933," Association of American Railroads, Transportation Technology Center, Inc., Pueblo, Colorado. August 1999.
- Gutkowski, R.M., Robinson, G. and Peterson, M., "Field load testing of existing timber railroad bridges." Proceedings of "1999 RILEM Symposium on Timber Engineering." Stockholm, Sweden. 1999.
- Gutkowski, R.M., Peterson, M. and Doyle, K., "Laboratory Load Testing and Modeling of Timber Trestle Railroad Bridges." Proceedings of "1999 RILEM Symposium on Timber Engineering." Stockholm, Sweden. 1999.
- Gutkowski, R.M., Peterson, M., Brown, K. and Shigidi, A., "Field Load Testing and Modeling of a Strengthened Timber Trestle Railroad Bridge." Proceedings of "CMEM 99 - 9th International Conference on Computational Methods and Experimental Measurements, Sorrento, Italy. 1999.
- Gutkowski, R.M., Peterson, M. and Robinson, G.C., "Field Studies of Timber Railroad Bridges-II, Contract No. TRAC-95-445", Association of American Railroads, Transportation Technology Center, Pueblo, Colorado 81001. August 2000.
- Gutkowski, R.M., Doyle, K.R. and Balogh, J., "Laboratory Tests of a Timber Trestle Bridge Chord." Proceedings of the World Conference on Timber Engineering – 2000, Whistler Resort, B.C., Canada. Department of Civil Engineering, Department of Wood Science; School of Architecture, University of British Columbia, Vancouver, Canada. 2000.
- Gutkowski, R.M., Shigidi, A.M.T., and Peterson, M.L. "Field Tests of a Strengthened Timber Trestle Railroad Bridge," World Conference on Timber Engineering – 2000, Whistler Resort, B.C.,

- Canada; Department of Civil Engineering, Department of Wood Science; School of Architecture, University of British Columbia, Vancouver, Canada. 2000.
- Gutkowski, R.M., Balogh, J., and Shigidi, A., "Load Testing of a Rehabilitated Timber Trestle Railroad Bridge." Proceedings of "STRUCTURAL FAULTS + REPAIR – 99, 10th International Conference And Exhibition, London, England. 2001
- Gutkowski, R.M., Shigidi, A.M.T., Tran, A.V. and Peterson, M. (accepted for publication in 2001). Field studies of a Strengthened Timber Railway Bridge, Transportation Research Record, Transportation Research Board, National Research Council, Washington, D.C. 2001.
- McCormac, Jack C. Structural Analysis, Fourth Edition. Harper and Row, Publishers Inc., New York, 1984.
- Oommen, G and R A P Sweeney. "Application of Modern Technologies in Railway Bridge Infrastructure Management and Decision Making. Transportation Infrastructure," Environmental Challenges in Poland and Neighboring Countries, 2. Environment –Vol. 5, NATO Advanced Research Workshops, Poland 1996.
- Peterson, M. L. and R. M. Gutkowski, Evaluation of the Structural Integrity of Timber Bridge Structures", NDT&E International. 1998.
- Robinson, G.C., Gutkowski, R.M., Peterson, M.L. and Criswell, M.E., "Field Testing of Open-Deck Timber Trestle Railroad Bridges," Structural Research Report No. 80. Colorado State University, Fort Collins, Colorado, 80523. December 1998.
- Robinson, G.C. "Field Load Testing of Open-Deck Timber Trestle Railroad Bridges," M.S. Thesis, Department of Civil Engineering, Colorado State University. Fort Collins, Colorado 80523. 1998.
- Rajan, S.D., GS-USA Frame Program, Version 4.4, Department of Civil Engineering, Arizona State University, Tempe, Arizona 85287-5306, 1991-1994.
- Sandoz, J.L., Ultrasonic solid wood evaluation in industrial applications. Xth Int. Symposium on Nondestructive Testing of Wood. Ed. Presses Polytechniques et Universitaires Romandes, CH-Lausanne. 1996.